

**STABILITY AND TEXTURE OF CO<sub>2</sub>/N<sub>2</sub> FOAM IN SANDSTONE**

BY

**Mohammed Abdul Qadeer Siddiqui**

A Thesis Presented to the  
DEANSHIP OF GRADUATE STUDIES

**KING FAHD UNIVERSITY OF PETROLEUM & MINERALS**

DHAHRAN, SAUDI ARABIA

In Partial Fulfillment of the  
Requirements for the Degree of

**MASTER OF SCIENCE**

In

**PETROLEUM ENGINEERING**

**February, 2016**

KING FAHD UNIVERSITY OF PETROLEUM & MINERALS

DHAHRAN- 31261, SAUDI ARABIA

**DEANSHIP OF GRADUATE STUDIES**

This thesis, written by **MOHAMMED ABDUL QADEER SIDDIQUI** under the direction of his thesis advisor and approved by his thesis committee, has been presented and accepted by the Dean of Graduate Studies, in partial fulfillment of the requirements for the degree of **MASTER OF SCIENCE IN PETROLEUM ENGINEERING**.

Dr. Rahul Narayanrao Gajbhiye  
(Advisor)

Dr. Abdullah S. Sultan  
Department Chairman

Dr. Sidqi M Abu-Khamsin  
(Member)

Dr. Salam A. Zummo  
Dean of Graduate Studies



Dr. Abdullah S. Sultan  
(Member)

19/5/16

Date

© Mohammed Abdul Qadeer Siddiqui

2016

*To my beloved parents, brothers and little sister who stood by me with their love, support and encouragement during this journey at King Fahd University of Petroleum & Minerals.*

## ACKNOWLEDGMENTS

First and foremost I thank Allah Almighty for His unlimited mercy and countless blessings. Without His decree nothing is possible including my successful completion of studies at King Fahd University of Petroleum & Minerals (KFUPM).

I would like to extend my gratitude to the prestigious King Fahd University of Petroleum & Minerals (KFUPM) and the Petroleum Engineering Department for providing me the opportunity to complete my higher studies here and for all the help and support throughout my thesis work at KFUPM. I am really grateful to have gained knowledge from such experienced and high caliber faculty and researchers. The knowledge, experience and skills that I have acquired during my stay at KFUPM have played an important role in my life and I am sure it will bear me great rewards and fruits in my future endeavors as well.

I would like to acknowledge the financial support provided by the Deanship of Scientific Research (DSR) at KFUPM for this research through the startup research grant (Project # 131025). Laboratory facilities provided by the Petroleum Engineering Department and the Centre of Integrated Petroleum Research are also acknowledged.

I am deeply grateful to my thesis advisor Dr. Rahul N. Gajbhiye for his guidance and support throughout my research. All of my meetings, interactions and discussions with him have always taught me something new. I have acquired under his supervision and guidance not only knowledge required for the completion of my thesis but also knowledge that would help me enhance my overall personality throughout my life. I would also like to extend gratitude to my thesis committee members Dr. Sidqi M Abu-

Khamsin and Dr. Abdullah S. Sultan for their guidance and support. I also express my gratitude for all the resources provided to me by the department for my research work.

I would like to thank Mr. Aziz Arshad (now retired) and Mr. Zaid Zaffar Jangda, researchers at the Centre of Integrated Petroleum Research, for helping me on the complex core-flooding equipment whenever required. They extended their help even during off-duty hours and also during vacations. I owe my technical know-how of the complicated equipment to these two highly qualified and experienced researchers. I would also like to thank Mr. Abdulraheem Mohammadain and Mr. Abdul Samad Idrisu from the Petroleum Engineering Department for their constant support and logistics whenever required.

I cannot conclude without acknowledging the love, support and encouragement given to me by my family who has been a great source of inspiration and comfort for me throughout my thesis. Without their love and prayers this journey would have been a lot difficult. I especially thank my parents for instilling in me through their upbringing qualities that have helped me stand out among my peers in my academic career up to now. I also thank all my friends at the university who made my stay here at KFUPM an enjoyable and memorable one. I will never forget the friends I made here during my Masters degree and I wish all of them great success in their lives.

# TABLE OF CONTENTS

<b>ACKNOWLEDGMENTS .....</b>	<b>V</b>
<b>TABLE OF CONTENTS .....</b>	<b>VII</b>
<b>LIST OF TABLES .....</b>	<b>IX</b>
<b>LIST OF FIGURES .....</b>	<b>X</b>
<b>LIST OF ABBREVIATIONS .....</b>	<b>XIV</b>
<b>ABSTRACT.....</b>	<b>XV</b>
<b>ARABIC ABSTRACT .....</b>	<b>XVII</b>
<b>CHAPTER 1 INTRODUCTION.....</b>	<b>19</b>
<b>CHAPTER 2 LITERATURE REVIEW.....</b>	<b>22</b>
<b>2.1 Basic Concepts of Foam .....</b>	<b>22</b>
2.1.1 Definition.....	22
2.1.2 Classification of Foam.....	22
2.1.3 Main Foam Properties .....	24
2.1.4 Mechanisms of Foam Generation in Porous Media.....	26
2.1.5 Effect of Foam on Gas Mobility .....	28
<b>2.2 Studies on Foam Flow in Porous Media .....</b>	<b>29</b>
<b>2.3 Problems with sc-CO<sub>2</sub>-Foam .....</b>	<b>35</b>
<b>2.4 Potential of Mixed CO<sub>2</sub>/N<sub>2</sub>-Foam.....</b>	<b>37</b>
<b>CHAPTER 3 PROBLEM STATEMENT AND RESEARCH OBJECTIVES .....</b>	<b>39</b>
<b>CHAPTER 4 EXPERIMENTAL PROCEDURE AND METHODOLOGY .....</b>	<b>41</b>
<b>4.1 Materials .....</b>	<b>41</b>
<b>4.2 Equipment.....</b>	<b>42</b>

<b>4.3 Methodology .....</b>	<b>47</b>
<b>CHAPTER 5 RESULTS AND DISCUSSION.....</b>	<b>57</b>
<b>5.1 IFT Results and Discussion.....</b>	<b>57</b>
5.1.1 IFT Results and Discussion of Fluorosurfactant FS-51 .....	57
5.1.2 IFT Results and Discussion of Alpha-olefin-sulfonate (AOS) .....	59
5.1.3 IFT Results and Discussion of Witcolate Surfactant .....	61
<b>5.2 Measurement of Core Properties .....</b>	<b>63</b>
<b>5.3 Foam-flooding Experiment Results and Discussion .....</b>	<b>65</b>
5.3.1 Foam-flooding Experiment Results and Discussion for Fluorosurfactant FS-51 .....	66
5.3.2 Foam-flooding Experiment Results and Discussion for Alpha-olefin-sulfonate (AOS).....	68
5.3.3 Foam-flooding Experiment Results and Discussion for Witcolate Surfactant.....	71
<b>5.4 Foam Texture Analysis Results and Discussion.....</b>	<b>73</b>
5.4.1 Image Analysis Results and Discussion for Fluorosurfactant FS-51 .....	74
5.4.2 Image Analysis Results and Discussion for Alpha-olefin-sulfonate (AOS).....	77
<b>CHAPTER 6 CONCLUSIONS AND RECOMMENDATIONS .....</b>	<b>80</b>
<b>REFERENCES.....</b>	<b>83</b>
<b>APPENDIX-A.....</b>	<b>87</b>
<b>APPENDIX-B.....</b>	<b>90</b>
<b>VITAE.....</b>	<b>119</b>



## LIST OF TABLES

Table 4-1 Injection scenarios for CO <sub>2</sub> /N <sub>2</sub> -surfactant flooding .....	50
Table 5-1 Measured core properties .....	64
Table A-1 Fluorosurfactant FS-51 concentration and corresponding measured IFT .....	87
Table A-2 AOS surfactant concentration and corresponding measured IFT .....	87
Table A-3 Witcolate surfactant concentration and corresponding measured IFT .....	87
Table A-4 Average steady-state $\Delta P$ values (in psi) for foam-flooding of fluorosurfactant FS-51 .....	88
Table A-5 Average steady-state $\Delta P$ values (in psi) for foam-flooding of AOS .....	88
Table A-6 Average steady-state $\Delta P$ values (in psi) for foam-flooding of witcolate.....	88
Table A-7 Average circularity of foam bubbles with fluorosurfactant FS-51 .....	89
Table A-8 Average circularity of foam bubbles with AOS .....	89

## LIST OF FIGURES

Figure 2.1: Generalized foam system [32].....	22
Figure 2.2: Schematic of gas flow in porous media in presence of foam [34]. .....	23
Figure 2.3: Foam viscosity vs. foam quality [6] .....	25
Figure 2.4: Schematic of neck snap – off mechanism [7].....	27
Figure 2.5: Schematic of lamella division mechanism [7] .....	27
Figure 2.6: Schematic of leave – behind mechanism [7].....	28
Figure 2.7: Effect of liquid rate and gas saturation in gas permeability with and without surfactant [4].....	29
Figure 2.8: Pressure temperature phase diagram for CO <sub>2</sub> .....	36
Figure 4.1: Schematic of the core-flooding experimental setup .....	43
Figure 4.2: Vinci Technologies IFT 700.....	46
Figure 5.1: IFT vs. fluorosurfactant FS-51 surfactant concentration.....	58
Figure 5.2: Shapes of drops of (a) 0 vol% (b) 0.05 vol% (c) 0.10 vol% (d) 0.15 vol% (e) 0.20 vol% and (f) 0.30 vol% fluorosurfactant in sc-CO <sub>2</sub> at 1500 psi and 50°C. .....	59
Figure 5.3: IFT vs. AOS surfactant concentration .....	60
Figure 5.4: Shapes of drops of (a) 0 vol% (b) 0.15 vol% (c) 0.30 vol% (d) 0.50 vol% (e) 0.75 vol% and (f) 1.0 vol% AOS in sc-CO <sub>2</sub> at 1500 psi and 50°C. ....	61
Figure 5.5: IFT vs. witcolate surfactant concentration .....	62
Figure 5.6: Shapes of drops of (a) 0 vol% (b) 0.0125 vol% (c) 0.025 vol% (d) 0.05 vol% and (e) 0.075 vol% witcolate in sc-CO <sub>2</sub> at 1500 psi and 50°C.....	63
Figure 5.7: Flow rate vs. pressure drop to calculate permeability (before and after foam flooding) .....	64
Figure 5.8: Average steady-state $\Delta P$ vs. foam quality (fluorosurfactant FS-51).....	67
Figure 5.9: Average steady-state $\Delta P$ vs. foam quality (AOS) .....	70
Figure 5.10: Average steady-state $\Delta P$ vs. foam quality (Witcolate).....	72
Figure 5.11: 8-bit Analyzed Foam Images for Fluorosurfactant FS-51.....	74
Figure 5.12: Average circularity vs. foam quality for fluorosurfactant FS-51 .....	76
Figure 5.13: 8-bit Analyzed Foam Images for AOS.....	77
Figure 5.14: Average circularity vs. foam quality for AOS .....	79
Figure B.1: Shape of distilled water drop in CO <sub>2</sub> (0% surfactant) at 1500 psi and 50°C. 90	90
Figure B.2: Shape of 0.05 vol% fluorosurfactant FS-51 in CO <sub>2</sub> at 1500 psi and 50°C ....	90
Figure B.3: Shape of 0.10 vol% fluorosurfactant FS-51 in CO <sub>2</sub> at 1500 psi and 50°C ....	91
Figure B.4: Shape of 0.15 vol% fluorosurfactant FS-51 in CO <sub>2</sub> at 1500 psi and 50°C ....	91
Figure B.5: Shape of 0.20 vol% fluorosurfactant FS-51 in CO <sub>2</sub> at 1500 psi and 50°C ....	92
Figure B.6: Shape of 0.30 vol% fluorosurfactant FS-51 in CO <sub>2</sub> at 1500 psi and 50°C ....	92
Figure B.7: Shape of distilled water drop in CO <sub>2</sub> (0% surfactant) at 1500 psi and 50°C. 93	93
Figure B.8: Shape of 0.15 vol% AOS in CO <sub>2</sub> at 1500 psi and 50°C .....	93

Figure B.9: Shape of 0.30 vol% AOS in CO <sub>2</sub> at 1500 psi and 50°C .....	94
Figure B.10: Shape of 0.50 vol% AOS in CO <sub>2</sub> at 1500 psi and 50°C .....	94
Figure B.11: Shape of 0.75 vol% AOS in CO <sub>2</sub> at 1500 psi and 50°C .....	95
Figure B.12: Shape of 1.0 vol% AOS in CO <sub>2</sub> at 1500 psi and 50°C .....	95
Figure B.13: Shape of distilled water drop in CO <sub>2</sub> (0% surfactant) at 1500 psi and 50°C	96
Figure B.14: Shape of 0.0125 vol% witcolate in CO <sub>2</sub> at 1500 psi and 50°C.....	96
Figure B.15: Shape of 0.025 vol% witcolate in CO <sub>2</sub> at 1500 psi and 50°C.....	97
Figure B.16: Shape of 0.05 vol% witcolate in CO <sub>2</sub> at 1500 psi and 50°C.....	97
Figure B.17: Shape of 0.075 vol% witcolate in CO <sub>2</sub> at 1500 psi and 50°C.....	98
Figure B.18: 8-bit analyzed foam image using fluorosurfactant FS-51 for foam quality 0.70 and 0% N <sub>2</sub> .....	99
Figure B.19: 8-bit analyzed foam image using fluorosurfactant FS-51 for foam quality 0.70 and 5% N <sub>2</sub> .....	99
Figure B.20: 8-bit analyzed foam image using fluorosurfactant FS-51 for foam quality 0.70 and 10% N <sub>2</sub> .....	100
Figure B.21: 8-bit analyzed foam image using fluorosurfactant FS-51 for foam quality 0.70 and 15% N <sub>2</sub> .....	100
Figure B.22: 8-bit analyzed foam image using fluorosurfactant FS-51 for foam quality 0.70 and 20% N <sub>2</sub> .....	101
Figure B.23: 8-bit analyzed foam image using fluorosurfactant FS-51 for foam quality 0.80 and 0% N <sub>2</sub> .....	101
Figure B.24: 8-bit analyzed foam image using fluorosurfactant FS-51 for foam quality 0.80 and 5% N <sub>2</sub> .....	102
Figure B.25: 8-bit analyzed foam image using fluorosurfactant FS-51 for foam quality 0.80 and 10% N <sub>2</sub> .....	102
Figure B.26: 8-bit analyzed foam image using fluorosurfactant FS-51 for foam quality 0.80 and 15% N <sub>2</sub> .....	103
Figure B.27: 8-bit analyzed foam image using fluorosurfactant FS-51 for foam quality 0.80 and 20% N <sub>2</sub> .....	103
Figure B.28: 8-bit analyzed foam image using fluorosurfactant FS-51 for foam quality 0.90 and 0% N <sub>2</sub> .....	104
Figure B.29: 8-bit analyzed foam image using fluorosurfactant FS-51 for foam quality 0.90 and 5% N <sub>2</sub> .....	104
Figure B.30: 8-bit analyzed foam image using fluorosurfactant FS-51 for foam quality 0.90 and 10% N <sub>2</sub> .....	105
Figure B.31: 8-bit analyzed foam image using fluorosurfactant FS-51 for foam quality 0.90 and 15% N <sub>2</sub> .....	105
Figure B.32: 8-bit analyzed foam image using fluorosurfactant FS-51 for foam quality 0.90 and 20% N <sub>2</sub> .....	106

Figure B.33: 8-bit analyzed foam image using fluorosurfactant FS-51 for foam quality 0.95 and 0% N <sub>2</sub> .....	106
Figure B.34: 8-bit analyzed foam image using fluorosurfactant FS-51 for foam quality 0.95 and 5% N <sub>2</sub> .....	107
Figure B.35: 8-bit analyzed foam image using fluorosurfactant FS-51 for foam quality 0.95 and 10% N <sub>2</sub> .....	107
Figure B.36: 8-bit analyzed foam image using fluorosurfactant FS-51 for foam quality 0.95 and 15% N <sub>2</sub> .....	108
Figure B.37: 8-bit analyzed foam image using fluorosurfactant FS-51 for foam quality 0.95 and 20% N <sub>2</sub> .....	108
Figure B.38: 8-bit analyzed foam image using AOS surfactant for foam quality 0.70 and 0% N <sub>2</sub> .....	109
Figure B.39: 8-bit analyzed foam image using AOS surfactant for foam quality 0.70 and 5% N <sub>2</sub> .....	109
Figure B.40: 8-bit analyzed foam image using AOS surfactant for foam quality 0.70 and 10% N <sub>2</sub> .....	110
Figure B.41: 8-bit analyzed foam image using AOS surfactant for foam quality 0.70 and 15% N <sub>2</sub> .....	110
Figure B.42: 8-bit analyzed foam image using AOS surfactant for foam quality 0.70 and 20% N <sub>2</sub> .....	111
Figure B.43: 8-bit analyzed foam image using AOS surfactant for foam quality 0.80 and 0% N <sub>2</sub> .....	111
Figure B.44: 8-bit analyzed foam image using AOS surfactant for foam quality 0.80 and 5% N <sub>2</sub> .....	112
Figure B.45: 8-bit analyzed foam image using AOS surfactant for foam quality 0.80 and 10% N <sub>2</sub> .....	112
Figure B.46: 8-bit analyzed foam image using AOS surfactant for foam quality 0.80 and 15% N <sub>2</sub> .....	113
Figure B.47: 8-bit analyzed foam image using AOS surfactant for foam quality 0.80 and 20% N <sub>2</sub> .....	113
Figure B.48: 8-bit analyzed foam image using AOS surfactant for foam quality 0.90 and 0% N <sub>2</sub> .....	114
Figure B.49: 8-bit analyzed foam image using AOS surfactant for foam quality 0.90 and 5% N <sub>2</sub> .....	114
Figure B.50: 8-bit analyzed foam image using AOS surfactant for foam quality 0.90 and 10% N <sub>2</sub> .....	115
Figure B.51: 8-bit analyzed foam image using AOS surfactant for foam quality 0.90 and 15% N <sub>2</sub> .....	115
Figure B.52: 8-bit analyzed foam image using AOS surfactant for foam quality 0.90 and 20% N <sub>2</sub> .....	116

Figure B.53: 8-bit analyzed foam image using AOS surfactant for foam quality 0.95 and 0% N <sub>2</sub> .....	116
Figure B.54: 8-bit analyzed foam image using AOS surfactant for foam quality 0.95 and 5% N <sub>2</sub> .....	117
Figure B.55: 8-bit analyzed foam image using AOS surfactant for foam quality 0.95 and 10% N <sub>2</sub> .....	117
Figure B.56: 8-bit analyzed foam image using AOS surfactant for foam quality 0.95 and 15% N <sub>2</sub> .....	118
Figure B.57: 8-bit analyzed foam image using AOS surfactant for foam quality 0.95 and 20% N <sub>2</sub> .....	118

## **LIST OF ABBREVIATIONS**

<b>EOR</b>	Enhanced Oil Recovery
<b>AOS</b>	Alpha-olefin-sulfonate
<b>PV</b>	Pore Volume
<b>IFT</b>	Interfacial Tension
<b>SAG</b>	Surfactant Alternating Gas
<b>WAG</b>	Water Alternating Gas

## ABSTRACT

Full Name : Mohammed Abdul Qadeer Siddiqui  
Thesis Title : Stability and Texture of CO<sub>2</sub>/N<sub>2</sub> Foam in Sandstone  
Major Field : Petroleum Engineering  
Date of Degree : [February 2016]

Foam formed when gas and surfactant are injected in porous media can overcome problems associated with gas injection enhanced oil recovery (EOR) techniques like viscous fingering, gravity override and high gas mobility. The reduced recovery efficiency of the reservoir due to these problems can be overcome by means of foam. Foam is a dispersion of gas in liquid phase. Gases most commonly used in foam EOR techniques are CO<sub>2</sub> and N<sub>2</sub>. Foams with these two gases have been extensively studied and compared. A common problem with CO<sub>2</sub>-foam is that it becomes weaker above supercritical conditions of CO<sub>2</sub> of 1100 psi and 31°C. At same high pressure and temperature conditions N<sub>2</sub> forms stronger foam than CO<sub>2</sub>. Due to weakening of CO<sub>2</sub>-foam above supercritical pressure and temperature of CO<sub>2</sub>, gas mobility is not effectively reduced which leads to poor sweep efficiencies. Few studies have shown potential of mixed CO<sub>2</sub>/N<sub>2</sub>-foam in bulk media. However, foam stability and texture of mixed CO<sub>2</sub>/N<sub>2</sub>-foam have not been yet investigated in porous media.

In this study, oil-free steady-state foam flooding experiments were performed in a sandstone core above the supercritical conditions of CO<sub>2</sub> using three different surfactants- fluorosurfactant FS-51, alpha-olefin-sulfonate (AOS) and witcolate. Effect of addition of

N<sub>2</sub> to sc-CO<sub>2</sub>-foam in different proportions was studied with the three different surfactants. Co-injection of all three fluids – surfactant, CO<sub>2</sub> and N<sub>2</sub> was performed and pressure drop ( $\Delta P$ ) data across the core was recorded and foam images were captured through a visual cell and analyzed using ‘ImageJ’ image analysis software. Interfacial tension experiments were also performed at same pressure and temperature conditions as foam-flooding experiments to determine the critical micelle concentration (CMC) of the three surfactants. The surfactants were injected at their CMC’s during foam-flooding experiments.

Results from the foam-flooding experiments showed improvement in foam strength as N<sub>2</sub> is added to CO<sub>2</sub> above its supercritical conditions. The improvement in foam strength was evident by increase in steady-state pressure drop ( $\Delta P$ ) across the core. Analysis of captured foam images also provided evidence of increasing foam strength as the circularity of foam bubbles was significantly enhanced with addition of N<sub>2</sub>.

This study aims to provide a solution to the problem of weakening of sc-CO<sub>2</sub>-foam. With the increasing number of CO<sub>2</sub>-EOR projects around the world in lieu with the need of CO<sub>2</sub> sequestration, the results from this study provide a safe and effective method to improve CO<sub>2</sub>-foam at high pressure and temperature reservoir conditions which could develop CO<sub>2</sub>-foam EOR potential and help in keeping as much as CO<sub>2</sub> below the ground.



## ملخص الرسالة

### ARABIC ABSTRACT

الاسم الكامل: محمد عبد القدير صديقي

عنوان الرسالة: الاستقرار و البنية التركيبية لرغوة ثاني أكسيد الكربون / النيتروجين في الصخر الرملي

التخصص: هندسة البترول

تاريخ الدرجة العلمية: فبراير 2016

تتكون الرغوة عندما يتم حقن الغاز و مزيلات التوتر السطحي في الوسط المسامي مما يمكن من تجاوز المشاكل المتعلقة بحقن الغاز في تقنيات تعزيز الزيت المستخلص مثل التصعب اللزج، تجاوز تحكم الجاذبية و الحركية العالية للغاز. بسبب هذه المشاكل تنقل كفاءة الاستخلاص من الممكن والتي يمكن تجاوزها عن طريق الرغوة. الرغوة هي عبارة عن انتشار الغاز في طور سائل. من أكثر الغازات استخداما في التقنيات الرغوية لتعزيز النفط المستخلص غاز ثاني أكسيد الكربون ( $CO_2$ ) و النيتروجين ( $N_2$ ). تم دراسة و مقارنة الرغوات المكونة بهذين الغازين على نطاق واسع. من المشاكل الشائعة عند استخدام رغوة مكونة من ثاني أكسيد الكربون أنها تصبح أضعف عند ظروف أعلى من الظروف فوق الحرجة لثاني أكسيد الكربون عند ضغط 1100 psi ودرجة حرارة  $31^\circ$  مئوية. عند نفس ظروف الضغط العالي و درجة الحرارة يكون غاز النيتروجين رغوات أقوى من التي يشكلها ثاني أكسيد الكربون. بسبب ضعف رغوات ثاني أكسيد الكربون عند ظروف أعلى من الضغط و درجة الحرارة الفوق حرجة لا يتم تقليل حركية الغاز مما يؤدي إلى ضعف كفاءة الإزاحة. أوضحت القليل من الدراسات مقدرات الرغوات المكونة عن طريق مزج ثاني أكسيد الكربون و النيتروجين في الوسط الكلي. مع ذلك، لم يتم دراسة الاستقرار و البنية التركيبية للرغوة المكونة من خليط ثاني أكسيد الكربون و النيتروجين في الوسط المسامي.

في هذه الدراسة، أجريت تجارب الحقن الرغوي المستقرة الخالية من الزيت على عينات اسطوانية من الصخور الرملية عند ظروف أعلى من الظروف فوق الحرجة لثاني أكسيد الكربون باستخدام ثلاثة أنواع مختلفة من مزيلات التوتر السطحي fluorosurfactant FS-51، alpha-olefin-sulfonate (AOS) و witcolate. تم دراسة تأثير إضافة نسب مختلفة من النيتروجين على الرغوة المكونة من ثاني أكسيد الكربون و مزيل التوتر السطحي. تم حقن الموائع الثلاثة مزيل التوتر السطحي، ثاني أكسيد الكربون و النيتروجين وتم رصد تغير الضغط عبر العينة الاسطوانية كما تم التقاط صور للرغوة من خلال وحدة شفافة وتم تحليل الصور عن طريق برنامج ImageJ. أجريت تجارب التوتر السطحي عند نفس ظروف الضغط ودرجة الحرارة التي أجريت عندها تجارب الحقن الرغوي. لتحديد تركيز المذيلات الحرج (CMC) لمزيلات التوتر السطحي. تم حقن مزيلات التوتر السطحي عند تركيز السيرفاكتانت الحرج (CMC) خلال تجارب الحقن الرغوي.

أوضحت نتائج الحقن الرغوي تحسنا في قوة الرغوة عند إضافة النيتروجين إلى ثاني أكسيد الكربون عند ظروف أعلى من الظروف فوق الحرجة. برهنت زيادة تغير الضغط المستقر عبر العينة الاسطوانية على تحسن قوة الرغوة. تحليل الصور الملتقطة للرغوة أيضا أعطى دليلا على زيادة قوة الرغوة عن طريق زيادة استدارة فقاعات الرغوة عند إضافة النيتروجين.

تهدف هذه الدراسة لتقديم حل لمشكلة ضعف الرغوة المكونة من ثاني أكسيد الكربون و مزيلات التوتر السطحي. مع ازدياد عدد مشروعات تعزيز النفط المستخلص عن طريق ثاني أكسيد الكربون حول العالم على الرغم من الحاجة لحجز ثاني أكسيد الكربون، نتاج هذه الدراسة تقدم طريقة آمنة و فعالة لتحسين الرغوة المكونة من ثاني أكسيد الكربون عند ظروف ضغط و درجة حرارة عالية للمكمن و التي يمكن أن تطور إمكانية تقنيات تعزيز النفط المستخلص عن طريق الرغوة المكونة من ثاني أكسيد الكربون كما تساعد في حفظ أكبر كمية ممكنة من ثاني أكسيد الكربون تحت الأرض.

# CHAPTER 1

## INTRODUCTION

Foam is formed when surfactant and gas are injected in a porous medium due to dispersion of gas into the liquid phase. Foam is essential in enhanced oil recovery (EOR) projects where the main aim is to recover trapped oil from the reservoirs. Foam formed by using surfactant and gas has proved to significantly increase the oil recovery because foam increases the apparent viscosity of the system and thus enhances the sweep efficiency [20, 1, 30, 38, 36]

High mobility ratio, gravity segregation, and reservoir heterogeneity are the most common problems faced during gas injection enhanced oil recovery (EOR) processes. This has a detrimental effect on the recovery efficiency of the EOR process due to low microscopic and macroscopic sweep efficiencies. Methods like surfactant alternating gas (SAG) and water alternating gas (WAG) were proposed to increase the macroscopic sweep efficiency. In SAG processes foam is generated when gas moves through the surfactant-invaded zone of the formation which improves the macroscopic sweep efficiency by reducing the gas mobility. In WAG processes, due to absence of surfactant in the water, foam is not generated and gas mobility is still considerably high making SAG processes more advantageous.

Most commonly used gases in surfactant alternating gas (SAG) processes are CO<sub>2</sub> and N<sub>2</sub>. The CO<sub>2</sub> and N<sub>2</sub> foam behaves differently depending on the pressure and temperature condition [18-20]. CO<sub>2</sub> foam and N<sub>2</sub> foam have their own strengths and weaknesses. It has been observed in some studies that ultimate recovery obtained by N<sub>2</sub> foam is greater than CO<sub>2</sub> foam while some studies show that the pressure requirement for CO<sub>2</sub> foam injection is less compared to N<sub>2</sub> foam. CO<sub>2</sub> is more soluble in oil as compared to N<sub>2</sub> which is advantageous for swelling of oil thereby

reducing the viscosity of oil and making it flow easily towards the production wells. However, the solubility of CO<sub>2</sub> in aqueous phase is detrimental for foam generation. Carbonic acid which is corrosive could be formed if CO<sub>2</sub> dissolves in water while N<sub>2</sub> being an inert gas does not react with water making it safer for field applications.

Due to awareness of global warming and need for sequestration CO<sub>2</sub> foam gained popularity over N<sub>2</sub>. Some of the advantages of CO<sub>2</sub> make it a favorable choice for EOR processes like its higher solubility in oil and higher miscibility. CO<sub>2</sub> at supercritical condition is unable to generate strong foam especially during co-injection of surfactant and gas in spite of the aforementioned advantages. CO<sub>2</sub> foam gets weaker with increasing pressure which increases mobility of CO<sub>2</sub> and hence resulting in poor sweep efficiency. Moreover, when CO<sub>2</sub> comes in contact with oil in the reservoir, it hardly forms foam most likely due to its higher solubility in oil or due to the detrimental effects of oil on foam.

Replacing part of CO<sub>2</sub> by N<sub>2</sub> could possibly overcome these drawbacks associated with the CO<sub>2</sub> foam. N<sub>2</sub> remains in subcritical state for most of the reservoir and operating conditions unlike CO<sub>2</sub>. Addition of N<sub>2</sub> to CO<sub>2</sub> can generate foam at supercritical conditions of CO<sub>2</sub> and open pathway for the successful application CO<sub>2</sub>-foam EOR at high pressure and temperature reservoir conditions.

The purpose of this study was to study the properties of mixed CO<sub>2</sub>/N<sub>2</sub> foam generated by replacing part of CO<sub>2</sub> by N<sub>2</sub> gas. By maintaining pressure above supercritical pressure of CO<sub>2</sub> the experiments were carried out by co-injecting surfactant and CO<sub>2</sub>/N<sub>2</sub> gas mixture at different proportions through the core. By varying individual gas and liquid injection rates, foam quality and CO<sub>2</sub>/N<sub>2</sub> ratio a series of experiments were performed to incorporate the effect of these

parameters on foam stability and texture. The results obtained in terms of pressure response (high/low) and foam texture at different individual gas and liquid injection rates, foam quality and  $\text{CO}_2/\text{N}_2$  ratio are important for deciding injection strategy and design parameters (gas/liquid injection rates, foam quality and  $\text{N}_2/\text{CO}_2$  ratio) for foam EOR processes. It could strengthen  $\text{CO}_2$ -foam EOR potential and open pathway to successfully utilize sc- $\text{CO}_2$ -foam at actual reservoir conditions.

This report has been divided into six chapters. Chapter 2 comprises of a literature review of basic foam concepts and foam flow in porous media in general and specifically problems associated with sc- $\text{CO}_2$ -foam and potential of mixed  $\text{CO}_2/\text{N}_2$ -foam. Chapter 3 mentions the problem statement and the research objectives. Chapter 4 includes the details of the equipment and materials used in the experiments and the detailed procedure of the experiments. Chapter 5 consists of all the results, where they are discussed and compared on the basis of pressure drop response and foam texture analysis. Chapter 6 gives the conclusions and future recommendations for this research.

## CHAPTER 2

### LITERATURE REVIEW

#### 2.1 Basic Concepts of Foam

##### 2.1.1 Definition

Foam is generally defined as a dispersion of gas bubbles in aqueous phase. The dispersed phase (gas) exists as discontinuous phase whereas liquid phase is continuous phase. The contact between bubbles of gas occurs through several thin liquid films called “lamellae” (singular “lamella”). The stability of these films is usually strengthened by surfactants (Figure 2.1). Foam stability is governed by lamellae in the absence of oil. If these films are stable, foam is stable and vice versa. The stability of lamellae can be improved by adding surfactant in aqueous phase. [18]

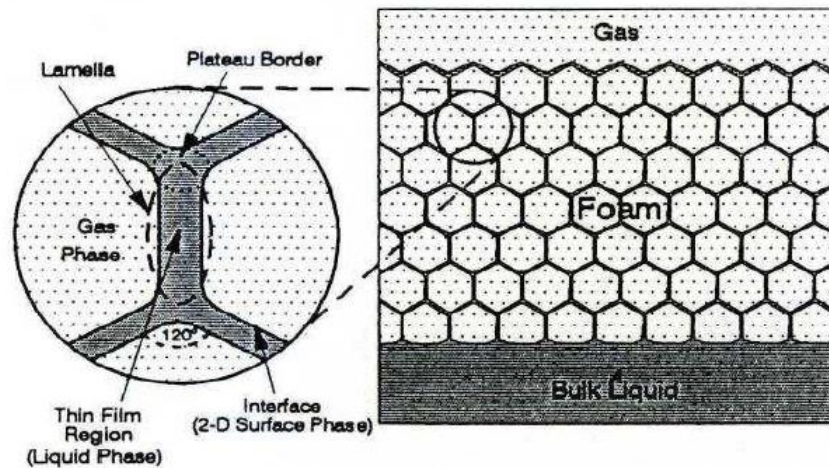


Figure 2.1: Generalized foam system [32]

##### 2.1.2 Classification of Foam

Generally, foams can be divided into two broad groups: bulk foams and foams in porous media.

### 2.1.2.1 Bulk Foam

Bulk foam refers to the volume in which foam resides which is much larger than individual bubble sizes. Bulk foam can be considered to be one homogeneous phase where gas and liquid phase velocities are considered similar since bubbles in bulk foam are relatively small compared to flow channel [31]. In oil industry, bulk foams are used in drilling, cementing and fracturing. The half-life time of bulk foams is often used to evaluate the foaming ability of surfactants.

### 2.1.2.2 Foam in Porous Media

Foam in porous media, on the other hand, is dependent on the distribution of pore size and pore throat [37]. A single bubble occupies one or more pore bodies in porous media, meaning that foam behaves as a discontinuous and non-homogeneous phase within porous media [11].

When foam flows in porous media very often it results in gas trapping or gas flowing as a continuous or discontinuous phase. Trapped gas occurs when all gas-flow paths are blocked by foam. If the gas-flow is continuous, some flow-channels might exist that are not disrupted by lamellae. Conversely, if gas-flow is discontinuous, lamellae interrupt all flow channels and foam flows as train of bubbles (Figure 2.2). [34]

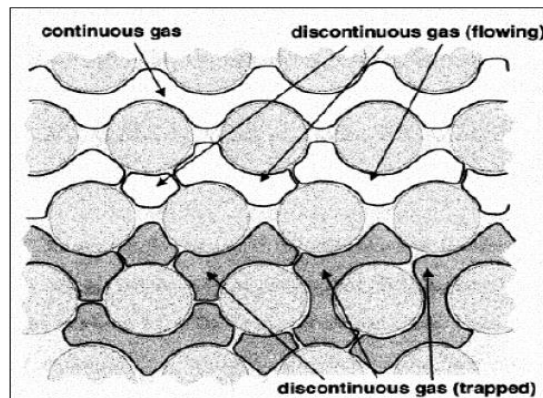


Figure 2.2: Schematic of gas flow in porous media in presence of foam [34].

## 2.1.3 Main Foam Properties

### 2.1.3.1 Foam Texture

Bubble size distribution characterizes the foam texture. Foam is said to be of 'fine texture' when the bubble size distribution is narrow. On the other hand, foam is said to have a 'coarse texture' when the bubble size distribution is wide. Foam stability was compared on the basis of bubble size distribution, and it was concluded that for a narrow bubble size distribution foam was more stable when compared to foam with a wide size distribution. Fine textured stable foam has a low mobility as a result of reduced relative permeability of gas and increased effective viscosity. Foam texture is a function of surfactant concentration, surfactant type, pore structure, pressure, and injection rates. In general, for a constant volume of fluid, foam with smaller bubble size is more viscous. [14]

### 2.1.3.2 Foam Quality

Foam quality is the volume fraction of the foam which contains gas. It is defined as:

$$\text{Foam Quality} = \frac{\text{gas volume}}{\text{gas volume} + \text{liquid volume}} \times 100\%$$

In core-flooding experiments, injection (or in-situ) foam quality is often used and is defined as:

$$\text{Injection foam quality} = \frac{\text{gas injection rate}}{\text{gas injection rate} + \text{liquid injection rate}} \times 100\%$$

Several studies have tried to relate foam quality to foam mobility [5, 26]. These studies show that a certain range of foam quality exists within which foam is able to reduce mobility and this range depends on chemical and fluid properties, rock properties, as well as injection methodology and



rates. Several authors have reported the mobility reducing range to be between 40 to 95% foam qualities [9, 21].

The effect of foam quality on viscosity was described using experimental results by dividing the range of foam qualities into regions of distinct bubble interactions. The first region exists between 0 to 52% foam qualities, characterized by spherical bubbles uniformly dispersed throughout the foam volume. The flow is Newtonian and the bubbles do not contact each other. Above 53% foam quality, spherical bubbles are packed loosely in a cubic arrangement and contact one another during flow which results in an increase in viscosity. Above foam quality of 74% the bubbles change their shapes from spheres to parallelepipeds while flowing. This third range exhibits maximum foam viscosities [5]. Figure 2.3 shows foam quality versus foam viscosity [6]. Describing the curve, above 95% foam quality, foams are unstable; liquid becomes the dispersed phase, like a mist. On the lower scale of the curve, at foam qualities below 40%, gas exists as dispersed pockets (of gas) in the liquid. Foam is very unstable at such qualities.

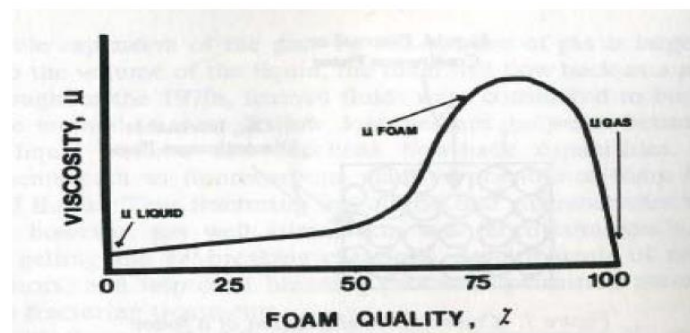


Figure 2.3: Foam viscosity vs. foam quality [6]

## 2.1.4 Mechanisms of Foam Generation in Porous Media

At the pore-level, there are three basic mechanisms in which foam is generated: snap – off, leave – behind, and lamellae division. Understanding of these mechanisms is important to reach to physically meaningful conclusions for foam generation and coalescence in porous media.

### 2.1.4.1 Snap-off

Snap – off occurs repeatedly during flow of more than one phase in porous media irrespective of the absence or presence of surfactant. In the presence of surfactant, three types of snap – off exist [7].

*Pre-neck snap – off* occurs when a bubble blocks a given pore throat. Depending on the geometry of pore throat, snap – off occurs when there is sufficient amount of liquid just upstream that accumulates and squeezes the initial bubble to smaller one.

*Rectilinear snap – off* occurs mostly further downstream in long pores with sharp corners [7].

During *Neck snap – off* (Figure 2.4), a bubble first approaches a pore throat and blocks it at the upstream. At this point, capillary pressure starts increasing and must exceed the entry pressure to let the bubble pass through the pore throat. Upon entering the downstream body, the capillary pressure at bubble front falls with expansion at the interface. This negative gradient in capillary pressure initiates a gradient in liquid pressure that drives the liquid from the pore body into the pore throat where it accumulates as a collar [7].

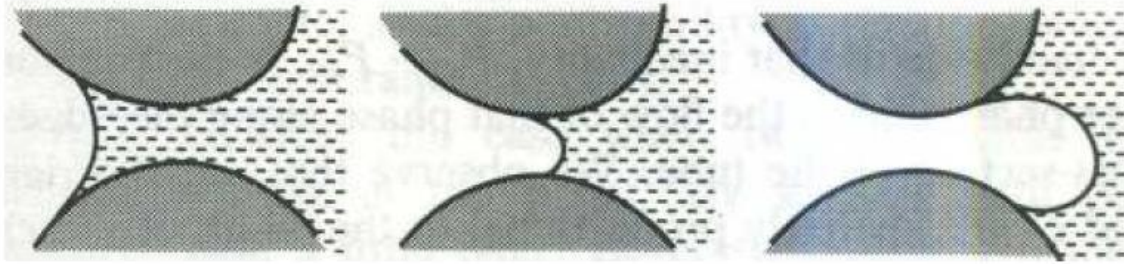


Figure 2.4: Schematic of neck snap – off mechanism [7].

#### 2.1.4.2 Lamella Division

In lamella division mechanism, the breaking-up of a bubble into two smaller ones occurs when stretching around a branch point of a flow channel [7] as shown Figure 2.5.

Figure 2.5: Schematic of lamella division mechanism [7]

This division of a lamella depends on several factors. The main factor is the bubble size. It has been found that foam bubble does not divide when approaching a branch point if its size is smaller than that of the pore-body. So, it can be said that the division generally occurs if bubble size is greater than size of the pore-body [7]. However, that statement has remained controversial since the lamella may be drained of liquid and coalescence might occur in the process [16].

### **2.1.4.3 Leave-behind**

As described in Figure 2.6, two gas menisci invade pore bodies. First, a lens is left behind as two menisci converge downstream and the lens may drain to a lamella later [29].

Lamellae created by snap – off and lamella – division mechanisms are generally perpendicular to local flow direction. Whereas, lamellae created by leave – behind are parallel to flow direction and thus do not make gas phase discontinuous.

Figure 2.6: Schematic of leave – behind mechanism [7]

### **2.1.5 Effect of Foam on Gas Mobility**

Gas mobility can be reduced significantly in porous media in the presence of foam. The lamellae in foam can be stationary or in motion. Stationary lamellae make the gas immobilized by trapping it whereas moving lamellae cause a resistance to flow of gas due to the surface tension on individual lamellae and drag forces acting on them when they slide along the pore bodies. In both cases gas mobility is lowered but with different mechanisms. In the first case, gas relative permeability is decreased with increasing gas saturation trapped by stationary lamellae. In the second case gas apparent viscosity is increased, not actual viscosity, since a portion of gas flow experiences the “flow-resistance” caused by moving lamellae. Therefore, effect of foam on gas mobility can be interpreted as an increase in gas apparent viscosity or as a decrease in gas relative permeability. [14]

Figure 2.7 shows the results from an experimental study [4] in which it was concluded that gas permeability was reduced significantly since lamellae were stabilized in the presence of surfactant (the top and bottom curves). However, the middle curve does not show an increase in gas saturation due to trapping in both cases. This lead to a conclusion that the effect of increasing trapped gas saturation is not comparable to that of pore throat blocking.

Figure 2.7: Effect of liquid rate and gas saturation in gas permeability with and without surfactant [4]

## **2.2 Studies on Foam Flow in Porous Media**

Isaacs et al. (1988) investigated steam-foam stability in porous media at elevated temperatures using different surfactants mainly to observe the influence of these surfactants on heavy oil recovery. In this study, non-condensable gas foams were generated in a sand-pack by injection of

hot water (or steam), gas (Nitrogen) and surfactant. Experiments were also carried out in the absence of non-condensable gases to determine the effect of steam velocity, permeability, salinity and surfactant concentration on mobility reduction. It was concluded that formation of steam-foam required a critical steam velocity that was roughly proportional to the inverse of permeability. Also, there was an optimum surfactant concentration beyond which no additional mobility reduction could be achieved. This optimum concentration shifts to higher levels in presence of oil. Non-condensable gas foams were stable provided gas and foaming agent injection rate was maintained. A rapid decline in pressure drop  $\Delta P$  occurred when surfactant injection was stopped. At high temperatures and pressures, high-salinity environments had no detrimental effects on foam stability with a surfactant known to be intolerant to brine at ambient conditions. Increased oil recovery was observed with and without non-condensable gas along with surfactant. [22]

Suffridge et al. (1989) studied foam performance at typical reservoir conditions using bulk foam experiments, screening core flooding experiments and actual core flooding experiments. Most core tests were performed on foot long Berea sandstone. Some tests were also performed on 4 ft cores. Screening core tests were performed at constant pressure drop conditions of 10 psi/ft and some tests at 200 psi/ft while actual core flooding experiments were performed at constant velocity conditions ranging from 0.5 ft/day to 20 ft/day. Incremental pressure drops were recorded at selected distances from the injection face. According to Suffridge et al., during bulk foam experiments lower molecular weight alkanes were more detrimental to foam volume. It was concluded that presence of oil is usually deleterious to foam stability but it may not be a serious problem in miscible processes mainly because when foam injection is initiated after water-flooding, oil saturations are much lower and would be comprising of higher molecular weight

alkanes/aromatic residues. Basically, lower oil saturations and higher carbon number residues would not be expected to show severe adversity to many surfactant systems. In this study, all foams were generated at unsteady-state conditions and it was found that under such conditions foam texture would be dynamic and constantly changing with gas throughput. It was found that after about 9.5 PV of CO<sub>2</sub> injection in the presence of foam, CO<sub>2</sub> permeability was reduced approximately by a factor of 10 compared to CO<sub>2</sub> permeability in the absence of foam. It was also concluded that effective foam can be generated in an oil-wet environment provided appropriate foaming agents are selected. [33]

Osterloh and Jante (1992) studied the effects of gas and liquid velocities on steady-state foam flow in porous media at high temperatures. Experiments were performed at 150°C using nitrogen gas along with C<sub>16-18</sub> alpha-olefin-sulfonate (AOS) and pressure gradients were measured in a 6.2 mD sand pack over a wide range of fractional flows and gas and liquid velocities. It was found that during the transient surfactant displacement by foam, propagation of foam was piston-like. Also, the rate of propagation was almost equal to the gas injection rate. Steady-state pressure gradients, and hence foam rheology, were characterized by the value of fractional flow of gas ( $f_g$  or foam quality) and were divided into two distinctive flow environments. One environment was gas-rate dependent and the other was liquid-rate dependent. In one environment, the response of pressure gradients to gas and liquid velocity was exactly opposite than that in the other environment. In the gas-rate dependent environment ( $f_g < 0.94$ ), the pressure gradient was practically independent on liquid velocity and mainly dependent on gas velocity. In the liquid-rate dependent flow environment ( $f_g > 0.94$ ), the pressure gradient was practically independent on gas velocity and mainly dependent on liquid velocity. The transition point of  $f_g$  equal to 0.94 possibly corresponds to that at which limiting capillary pressure was reached. It was also found

that at very high liquid velocity ( $f_g > 0.998$ ), a chaotic like flow existed in which pressure drop ( $\Delta P$ ) fluctuated and dropped to very low levels and steady-state could not be attained. [28]

Liu et al. (1992) studied displacement by foam in porous media utilizing C<sub>16-18</sub> AOS surfactant and nitrogen in a sandpack. It was concluded that foam flow is not a piston-like process neither does it follow Buckley-Leverett theory. It was found that the breakthrough time, final gas saturation and apparent viscosity of foam can all be correlated to the surfactant concentration and be used for prediction of foam flow. One important conclusion they made was that surfactant adsorption had only a minor effect on the foam flow behavior. It retards the foam front velocity, however, the effect is not very significant for the bulk of the displacement. They also concluded that the apparent foam viscosity can become very high at high surfactant concentration. It can be much greater than that of either of its components: gas or water. [24]

Chang et al. (1994) performed laboratory foam flow tests to determine reservoir simulator foam parameters for a particular CO<sub>2</sub>-foam pilot. Oil-free core tests were performed at 101°F and 2100 psig. Foam was generated by co-injection of CO<sub>2</sub> and surfactant into a brine-saturated core. Foam qualities of 66.7%, 80.0% and 85.7% were examined. Flow rates were varied in terms of superficial velocities ranging from 0.36 to 34.38 ft/day and the pressure drop across the core  $\Delta P$  was measured. It was concluded that for each of the tests performed, resistance factor ranged from 3-63 indicating foam was generated at all the conditions tested and a minimum velocity or pressure was not required as confirmed in a previous study by Chou. The resistance factor decreased and the mobility increases with increasing superficial velocity. It was found that in general higher surfactant concentrations have higher resistance factors (lower mobility). It was also concluded that effect of foam quality on resistance factor (or mobility) is not very significant. [8]



Holt et al. (1996) studied the effect of system pressure on foam stability in porous media both in the presence and absence of oil with pressures ranging from 10 to 300 bar. Two surfactants, C<sub>16</sub> AOS and a betaine surfactant were used. Pressure drop  $\Delta P$  across the cores was measured for investigating foam stability. It was concluded that in the absence of oil  $\Delta P$  increases with increasing system pressure for both surfactants used. For the fluorinated betaine,  $\Delta P$  increased threefold between system pressures 10 and 290 bar, while a 30 fold increase was found for C<sub>16</sub> AOS. However, in the presence of oil, C<sub>16</sub> AOS formed stronger foam at reservoir conditions and rather weak foam at relaxed conditions in both the Oseberg and Snorre cores. Almost opposite trend is seen for the betaine surfactant in the presence of oil where strongest foam was generated at relaxed conditions in the Oseberg core whereas in the Snorrecore equivalent strong foam was generated at both relaxed and reservoir conditions. The observations in this study show that both the foam stability in absence of oil and the oil-foam interactions varies differently with pressure for different surfactants implying that flooding experiments at reservoir conditions (especially pressure) are required for a proper screening of foamers. [19]

Tsau et al. (1997) evaluated foam properties in porous media and in the bulk phase for possible correlation. They studied effectiveness of CO<sub>2</sub>-foam in reducing mobility. Oil-free foam flooding was performed in dual permeability setup comprising of composite cores arranged in series and in contact with each other during flooding. Several surfactants were tested with dense CO<sub>2</sub> for foaming ability. Critical Micelle Concentrations (CMC) for all surfactants used were determined through interfacial tension (IFT) measurements. First, base-line experiments were performed using CO<sub>2</sub> and brine followed by foam flooding using CO<sub>2</sub> and surfactant. Mobility was calculated using Darcy law to compare between foam and base-line experiments. All mobility measurements were carried out at 77°F and 2000 psig. During co-injection of CO<sub>2</sub>-brine or CO<sub>2</sub>-

surfactant foam quality was maintained at 80%. However, total injection rate was varied from 5 cc/hr to 15 cc/hr. It was concluded that stability of foam in the bulk phase can be correlated with the performance of foam flowing in porous media and that greater foam stability gives more mobility reduction in foam displacement. The mobility reduction factor increases as the IFT between CO<sub>2</sub> and aqueous phase decreases but there exists an optimum concentration at which the most stable foam in the bulk phase is formed and it is close to the CMC of each surfactant. [35]

Chang et al. (1999) performed a series of oil-free steady state CO<sub>2</sub>-foam flow experiments at reservoir conditions of 101°F and 2100 psig to study the effects of foam quality and flow rate on CO<sub>2</sub>-foam behavior. Three total injection rates 4.2, 8.4 and 16.8 cc/hr and five foam qualities 20%, 33.3%, 50%, 66.7% and 80% were used to determine the effects on foam mobility. Co-injection of CO<sub>2</sub>-brine was preceded by CO<sub>2</sub>-surfactant to compare between the calculated mobilities. The pressure drop  $\Delta P$  across the core was also recorded for each experiment. It was concluded that total mobility of CO<sub>2</sub>/brine increases as the CO<sub>2</sub> fraction is increased from 0.333 to 0.8. Foam mobility for CO<sub>2</sub>/surfactant decreases as the foam quality is increased. Also, as the total injection rate is increased foam mobility increases and hence foam resistance factor decreases with increasing flow rate. It was also observed cyclic pressure response with high fluctuation for low foam qualities (no steady-state) but for foam qualities of 66.7% and 80% the  $\Delta P$  was stable with very little fluctuation. [9]

Apaydin and Kavscek (2000) conducted transient oil-free nitrogen-foam flow experiments in homogenous porous media (7 mD sandpack) to study foam generation and propagation as a function of aqueous surfactant concentration. A C<sub>14-16</sub> AOS surfactant was used. The in-situ phase saturation and pressure distribution were measured during the experiments. It was found

that displacement efficiency decreases and gas mobility increases with decreasing surfactant concentration. [3]

Gauglitz et al. (2002) performed oil-free foam flooding experiments in sand packs using different surfactants utilizing both nitrogen and carbon dioxide separately. It was found that foams made with N<sub>2</sub> and CO<sub>2</sub> for all surfactants require a minimum pressure gradient ( $\Delta P_{\min}$ ) for foam generation. This minimum pressure gradient seemed to vary with permeability but a direct relation could not be established. It was also observed that dense CO<sub>2</sub> required lower  $\Delta P_{\min}$  for foam generation when compared to N<sub>2</sub>. This was attributed possibly to the lower IFT of dense CO<sub>2</sub> with the aqueous surfactant phase. [15]

Liu et al. (2006) performed oil-free foam flooding experiments to study foam mobility and adsorption in carbonate cores. Nitrogen gas was used along with a commercial surfactant. Experiments were performed at 40°C and 1500 psi. Flow rate, foam quality and surfactant concentration were varied to see their effects on foam mobility. It was found that at a constant flow rate, gas mobility slightly decreases with increasing foam quality until a critical foam quality  $f_g^*$  above which it increases with foam quality. Also, low gas mobility was found over a wide range of foam qualities. Long times to reach steady state during foam flooding was also reported. [25]

### **2.3 Problems with sc-CO<sub>2</sub>-Foam**

CO<sub>2</sub> can quite easily become a supercritical fluid owing to its relatively lower critical temperature (32°C) and pressure (1070 psi) as can be seen if figure 2.8 below. It is obvious that at most, if not all, reservoir conditions CO<sub>2</sub> would be in a supercritical state.

Figure 2.8: Pressure temperature phase diagram for CO<sub>2</sub>

Du et al. (2008) performed foam flooding experiments comparing CO<sub>2</sub>-foam and N<sub>2</sub>-foam using SDS (sodium dodecyl sulfate) surfactant. A visual analysis of foam propagation was done using CT-scan. Pressure drop across the core ( $\Delta P$ ) was measured for testing the foam stability. It was observed that  $\Delta P$  for CO<sub>2</sub>-foam was lower than that for N<sub>2</sub>-foam signifying lower apparent viscosity for CO<sub>2</sub>-foam. N<sub>2</sub>-foam propagation was found to be piston like through CT-scan analysis but similar conclusion could not be reached for CO<sub>2</sub>-foam. When the system pressure was increased even lower  $\Delta P$  was recorded for CO<sub>2</sub>-foam showing that foam became weaker at high pressure conditions whereas no change was observed in  $\Delta P$  for N<sub>2</sub>-foam. [10]

Farajzadeh et al. (2009) also compared CO<sub>2</sub> and N<sub>2</sub> foams at both low and high pressure and temperature conditions using AOS surfactant. It was observed that CO<sub>2</sub>-foam gave lower pressure drop ( $\Delta P$ ) than N<sub>2</sub>-foam at all pressure and temperature conditions. It was concluded that CO<sub>2</sub>-foam was always weaker than N<sub>2</sub>-foam and CO<sub>2</sub>-foam became weaker with increase in

pressure and temperature but no change was observed in the strength of N<sub>2</sub>-foam. Also, through CT-scan it was observed that N<sub>2</sub>-foam had better frontal displacement than CO<sub>2</sub>-foam. [13]

Solbakken et al. (2013) performed oil-free foam flooding experiments in sandstone core at pressures ranging from 30 bar to 280 bar and at temperatures of 50°C and 90°C. A C<sub>14-16</sub> AOS was used. Supercritical CO<sub>2</sub>-foam was compared to N<sub>2</sub>-foam in this study. It was found that strong CO<sub>2</sub>-foams can be generated even at supercritical conditions and low density CO<sub>2</sub> gives stronger foam. Higher density of CO<sub>2</sub> was found to give reduced foam strengths. Visual observations of foam texture showed that all CO<sub>2</sub>-foams were coarser in contrast to denser N<sub>2</sub>-foams which means that CO<sub>2</sub>-foams were weaker as fine textured foams are stronger than coarse textured foams. Also, it was observed that variation in CO<sub>2</sub>-foam texture did not necessarily change the mobility reduction capability. [2]

## **2.4 Potential of Mixed CO<sub>2</sub>/N<sub>2</sub>-Foam**

Falls et al. (1988) investigated the effect of addition of non-condensable gases like air, methane and N<sub>2</sub> to steam foams through field tests. Alpha-olefin-sulfonate (AOS) was used as the foaming agent. It was concluded that foams formulated with 0.5 mol% N<sub>2</sub> reduced steam mobility, raised reservoir temperature and increased vertical sweep efficiency. It was also concluded that when non-condensable gas is incorporated in steam foam more oil is recovered. Also, the benefits of adding non-condensable gas to steam foam decrease with increase in temperature. [12]

Harris (1995) investigated rheological properties of mixed-gas foams to be used for fracturing fluids. Both anionic and amphoteric foaming agents were used without describing their details. It was concluded that adding small amounts of (even 5%) N<sub>2</sub> to CO<sub>2</sub> foams gave increased

viscosities at low shear rates. It was also concluded that replacement of CO<sub>2</sub> by N<sub>2</sub> in 70% quality foam decreased the half-life of the foam. There was no evidence that addition of N<sub>2</sub> to CO<sub>2</sub> foam improved its static stability. [17]

Nguyen and Ali (1998) studied the effect of addition of N<sub>2</sub> on CO<sub>2</sub> solubility in oil. However, foam was not considered in their study which means no surfactant was used. It was found that addition of N<sub>2</sub> content in CO<sub>2</sub> reduces CO<sub>2</sub> oil solubility and reduced the displacement efficiency. Also, lower oil recovery was reported when N<sub>2</sub> was added to CO<sub>2</sub>. Maximum recovery loss of 10% was reported for 30 mol% addition of N<sub>2</sub>. It is important to note that mixed CO<sub>2</sub>/N<sub>2</sub>-foam flooding was not performed to see if sweep efficiency (or recovery) could be improved with the use of surfactant along with gases (or equivalently by the use of foam). [27]

## CHAPTER 3

### PROBLEM STATEMENT AND RESEARCH OBJECTIVES

As evident from the literature, a determined effort has been carried out worldwide since several decades to develop a foam system consisting of gases like CO<sub>2</sub>, N<sub>2</sub> etc. and different surfactants that is stable under actual reservoir conditions and supercritical gaseous condition like that of CO<sub>2</sub>. However, most of the work done till now has not been able to reach to a conclusion of the most suitable CO<sub>2</sub>-surfactant or N<sub>2</sub>-surfactant system that would form longer-lasting stable foam along with its capability to reduce IFT which is an important factor to be considered in enhanced residual oil recovery studies. Also, inability of foam generation and instability of generated foam means that the problem of high mobility of CO<sub>2</sub> is not tackled, ceasing all the benefits thought to be associated with a quality foam system. To date, formulations of CO<sub>2</sub>-surfactant and N<sub>2</sub>-surfactant systems have been separately studied and compared, but, very few investigations have been performed to determine foamability of mixed CO<sub>2</sub>/N<sub>2</sub>-surfactant system. Also, based on literature review, it has been found that very few attempts have been made so far to visually characterize foam in porous media based on foam texture and bubble size distribution making use of a high-pressure and high temperature (HPHT) visual cell and an image analysis software. Only pressure drop response across the porous media was used to support the hypothesis of foam generation. Moreover, very limited foam experiments have been conducted on sandstone rocks and even less so on long cores. Thus, a systematic investigation into the synergistic properties of a mixed CO<sub>2</sub>/N<sub>2</sub>-surfactant formulation is proposed as a possible solution to foamability and foam stability problems based on pressure response and visual characterization of foam.

In this work, three surfactants were used with sc-CO<sub>2</sub> and N<sub>2</sub>. One foot long sandstone core was used in this study to see the full effect of the injected fluids on foam generation as it generates and propagates through the core. Also, a high-pressure and high temperature (HPHT) visual cell was used to capture the texture of the foam being injected. The texture was then analyzed using 'ImageJ' image analysis software. All the experiments were conducted at a back-pressure range of 1300-1500 psi and a fixed temperature of 50°C. The pressure and temperature conditions were chosen to ensure the supercritical condition CO<sub>2</sub> during foam flooding experiments.

The main objective of this thesis is to evaluate mixture of sc-CO<sub>2</sub>/N<sub>2</sub>-surfactant as a foam EOR solution. The objective here is to carry out steady-state foam flooding experiments to study stability and texture of foam being injected in the sandstone rock using mixture of sc-CO<sub>2</sub> and N<sub>2</sub> with three different surfactant systems and determine the optimum injection strategy based on optimum individual gas/liquid injection rates, CO<sub>2</sub>/N<sub>2</sub> ratio and foam quality.



## **CHAPTER 4**

### **EXPERIMENTAL PROCEDURE AND METHODOLOGY**

For this research, an experimental core-flood setup was used to conduct flow through the prepared sandstone core. The set-up is composed of fluid injection pumps, fluid accumulators, absolute and differential pressure transducers, temperature transducer, core holder, back pressure regulator, overburden pressure pump, pressure multiplier, data acquisition system and an oven. Control and safety valves, tubing, and fittings form an integral part of the setup. This equipment was used to conduct tests to determine the efficiency of the mixed CO<sub>2</sub>/N<sub>2</sub>-surfactant system in forming foam. The flooding system was integrated with a data acquisition system to record all data generated during the flooding test.

Different experiments were carried out by varying different parameters (individual gas and liquid injection rates, foam quality, CO<sub>2</sub>/N<sub>2</sub> ratio etc.) to optimally accommodate effect of different parameters on formation of stable foam.

Foam stability and texture were studied and supported by measuring the pressure drop across the core sample and through visualization of the injected foam through a HPHT visual cell which was placed before the inlet of core in the core-flooding equipment.

#### **4.1 Materials**

##### **4.1.1 Core Sample**

Berea Grey Sandstone cores of 12” length and 1.5” diameter was used in all the experiments. The core samples were procured from Kocurek Industries (USA).

### **4.1.2 Surfactants**

Three types of surfactants were used in this study:

1. Fluorosurfactant FS-51
2. Alpha-olefin-sulfonate (AOS)
3. Witcolate

The amphoteric amine oxide-based fluoro-surfactant was supplied by DuPont. Alpha olefin sulfonate was provided by Al Biariq Petrochemical Industries Company and Witcolate is an anionic surfactant provided by AkzoNobel. All surfactants were provided in sufficient quantities to be used in the experiments. The surfactant solutions were prepared by adding surfactant at its critical micelle concentration in distilled water.

### **4.1.3 CO<sub>2</sub>**

Industrial Grade CO<sub>2</sub> was obtained in sufficient quantity in the form of gas cylinders. The CO<sub>2</sub> was then transferred into the accumulators in the core flooding system.

### **4.1.4 Distilled Water**

Distilled water was used to flush all the lines before changing the surfactant in the system. Also, distilled water was used to flush the core sample before starting flooding of another surfactant into the core.

## **4.2 Equipment**

### **4.2.1 Core-flooding experimental setup**

The core-flooding system used in this study is basically a reservoir condition condensate depletion system that was modified to suit the required specifications. The schematic of the core-

flooding experimental system is shown in Figure 4.1. The system consists of an oven, five floating piston fluid cylinders of various volumes, Quizix pumping system, back pressure regulator and the core holder. The components of the flow, control and measurement systems are installed on the ends of the oven, on its roof, as well as within the oven itself. The system includes 72 air operated solenoid valves that are controlled by software on a dedicated computer. The flow control system components are all inside the oven. All the pressure transducers and Quizix pump controllers are external to the oven. The system is attached to an automatic data logging system which works with the software to record all the data during the experiments in a Microsoft Excel© workbook.

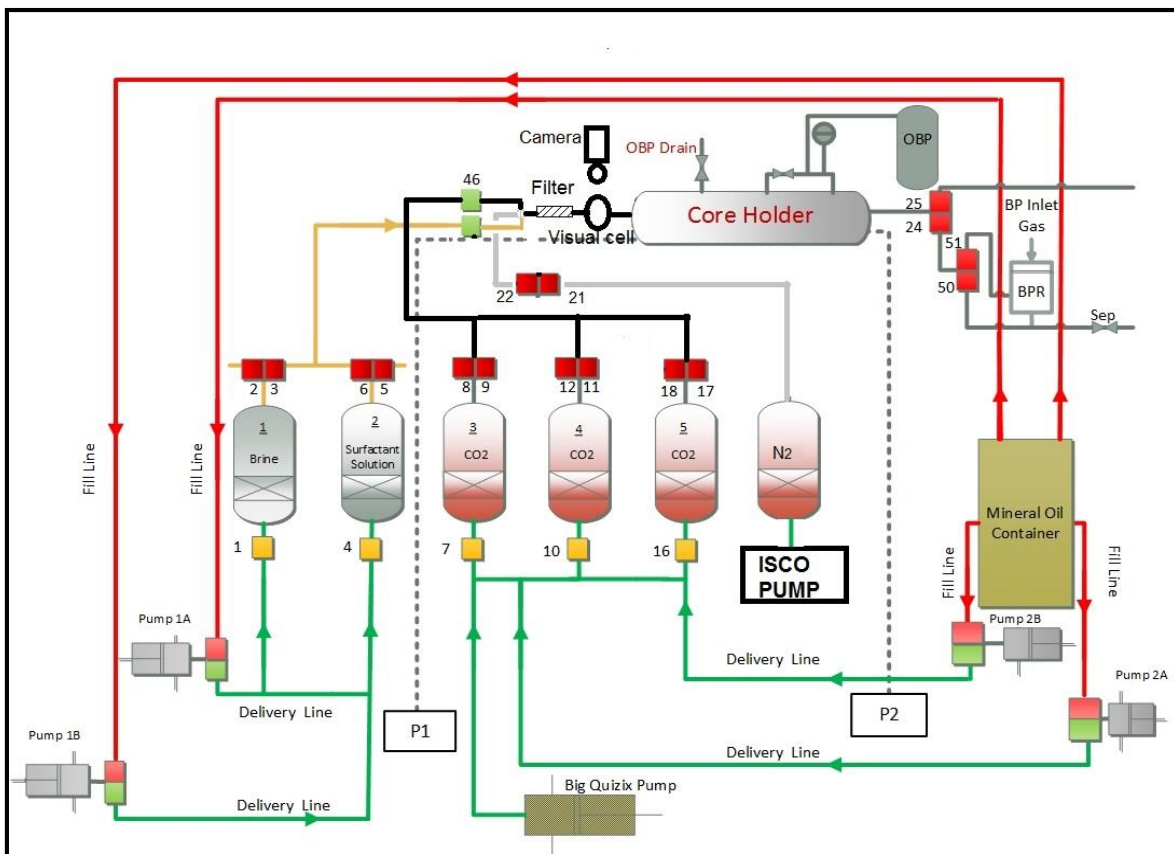


Figure 4.1: Schematic of the core-flooding experimental setup

A brief description of the main components of the system is given below:

## **4.2.2 Pumps**

### **4.2.2.1 Quizix Pumping System**

The pumping system is comprised of six computer controlled positive displacement Quizix pumps. These pumps are very robust and precise which are capable of injecting fluids at high pressure and temperature into the core at very specific flow rates. For continuous flow, each pump has a separate cylinder where if one is being extended the other retracts and prepares for injection as soon as the other reaches the maximum extended position. These cylinders are controlled by a controller for automatic operation. The pumping system can be used in 3 or 5 pump recirculation modes. In a 3 pump mode, fluids are delivered into the core using two pumps (for liquid and gas) and the third pump acts as a servo pump or back pressure regulator to maintain desired pressure in the system. On the other hand, fluids are delivered into the core using four pumps and the fifth pump acts as a servo pump in a 5-pump recirculation mode. In case of the failure of the fifth pump, the sixth pump can be used as a standby pump. The pumping system is placed in the oven to maintain the desired pressure and temperature conditions. The Quizix pumping system window displays all the pumps with operating parameters such as flow rates and pressures which can be changed by the user whenever required.

### **4.2.2.2 Overburden Pressure (OBP) Pump**

A high-pressure syringe pump (ISCO 100D) was used to apply and maintain required overburden pressure (OBP) on the core holder.

#### **4.2.2.3 External Pumps**

Two pumps were used externally before and during the experiments. An Eldex pump was used before starting the foam flooding experiments to fill surfactant solutions in the respective accumulators inside the system and a positive displacement ISCO pump to inject N<sub>2</sub> into the core during foam flooding.

#### **4.2.3 Auxiliary Accessories**

Five high-pressure transfer cells of various volumes were incorporated in the experimental setup to store and inject the fluids. Two of them were one liter cells to contain the surfactant solutions, while the other three cells (two 2 liter cells and one 3 liter cell) all contained CO<sub>2</sub>. All the cells were located inside the oven to maintain desired temperature of fluids. Another high pressure titanium cell acquired through Vinci Technologies was connected to the system by an external valve. This cell contained N<sub>2</sub> to be injected into the core through the ISCO pump. The differential pressure across the core was measured using two differential pressure transducers, one was low range (50 psig) and the other was high range (500 psig). These transducers have high resolution and automatically switch from low to high during the experiment depending on the differential pressure developed in the core. The inlet and outlet core pressures are monitored by precision Quartz dyne pressure transducers that give accurate absolute pressure. During the experiment the core was fitted in to a stainless steel hassler type core holder manufactured by Core Laboratories. It could accommodate up to 2 feet long core and the maximum working pressure of the core holder was 7500 psig.

#### **4.2.4 Back Pressure Regulator**

A dome shaped back pressure regulator was employed to apply and control the back pressure. Nitrogen was used as a medium for back pressure application.

#### 4.2.5 IFT Equipment

The interfacial tension between the injected surfactant solution and CO<sub>2</sub> was measured using IFT 700 equipment manufactured by Vinci Technologies (Figure 4.2). This machine was designed to perform experiments at high pressure (up to 10000 psi) and high temperature (up to 200°C) and could measure IFT values ranging from 0.1 to 72 mN/m. A drop of surfactant solution was created from a calibrated capillary into the bulk fluid (CO<sub>2</sub>) at 1500 psi and 50°C, in a viewing chamber which had a capacity of 20 cc. Then pendant drop method was used since the density of surfactant solution was more than the bulk fluid, i.e. CO<sub>2</sub>. A camera connected to the computer recorded the shape of the drop and solved the Laplace equation to provide the interfacial tension values. The accessories equipped with the main equipment were two manual pumps for the sample fluids (bulk and drop fluids), Peltier Thermostat (PT100) temperature sensor, electric heater, a control panel with a temperature regulator, which enables to set the temperature of the system and one pressure indicator. The video system to view the drop and display it on the computer screen consisted of a CCD color camera 1.4MPixel, a macro zoom lens and an LED for lighting. A computer with the software installed was connected to the system to display and save the results.

Figure 4.2: Vinci Technologies IFT 700

## 4.3 Methodology

### 4.3.1 Experimental Plan

A number of experiments were planned in which the parameters were varied to accommodate the effect of various factors on foam texture and stability. Two injection scenarios were considered:

1. CO<sub>2</sub>-surfactant flooding – base case: sc-CO<sub>2</sub> was co-injected with surfactant solution at total flow rate of 1 cc/min and at four foam qualities (0.70, 0.80, 0.90 and 0.95).
2. Mixed CO<sub>2</sub>/N<sub>2</sub>-surfactant flooding: Mixed sc-CO<sub>2</sub> and N<sub>2</sub> was co-injected with surfactant solution at total flow rate of 1 cc/min and at the same four foam qualities. N<sub>2</sub> was mixed with CO<sub>2</sub> in four proportions 5%, 10%, 15% and 20%.

In both cases above, individual injection rates of CO<sub>2</sub>, N<sub>2</sub> and surfactant solution were varied in such a way that total flow rate of 1 cc/min was maintained and at the same time different foam qualities (0.70, 0.80, 0.90 and 0.95) and N<sub>2</sub>/CO<sub>2</sub> ratios (5%, 10%, 15%, 20%) were achieved.

The parameters that were kept constant during the experiments include:

- x Temperature: 50°C
- x Pressure: 2000 psi (overburden pressure), 1300-1500 psi (backpressure)
- x Core: Berea Sandstone
- x Surfactant Concentration: Fixed above Critical Micelle Concentration (CMC) of each surfactant
- x Total Injection Rate (Gas+Liquid) = 1 cc/min

The parameters that were varied to find the optimum foam forming strategy are:

- x Surfactant Type
  - o Fluoro-Surfactant (FS-51)
  - o Alpha-Olefin-Sulfonate (AOS)
  - o Witcolate
- x Foam Quality
  - o Foam qualities of 0.70, 0.80, 0.90 and 0.95 were used.
- x N<sub>2</sub>/CO<sub>2</sub> Ratio
  - o N<sub>2</sub>/CO<sub>2</sub> ratios of 0.05, 0.10, 0.15 and 0.20 were used.
- x Individual Gas and Liquid Injection Rates
  - o Gas and liquid individual injection rates were varied for each set of experiments in order to vary the injection foam quality and N<sub>2</sub>/CO<sub>2</sub> proportions. However, total injection rate of 1 cc/min was maintained.

### **4.3.2 Core-flooding Experimental Procedure**

To carry out our experiments a methodology was devised and followed which is described below:

#### **4.3.2.1 Measurement of Core Properties**

Firstly, core dimensions were measured, i.e. dry weight, length, diameter and bulk volume.

These measurements were required for the bulk volume, pore volume and porosity calculations.



#### **4.3.2.2 Core Saturation**

Core was then evacuated and saturated with surfactant solution in a high pressure cell at 1800 psi for up to 24 hours.

#### **4.3.2.3 Core Loading**

The core was then loaded in the core-holder and then pressure tested by an external pump by applying an overburden pressure of 1000 psi for up to 24 hours. After making sure that there is no leakage or pressure drop the core holder was fitted into the oven.

#### **4.3.2.4 Pressure Build-up**

Surfactant solution was then injected through the core to build the pressure up to the required back pressure i.e. 1500 psi. Overburden pressure was increased simultaneously to 2000 psi to maintain a net 500 psi pressure differential. Backpressure was applied using nitrogen gas to control the pore pressure.

#### **4.3.2.5 Heating of the system**

The oven was then started to heat the system to 50°C. The fluid accumulator pressures were timely monitored during the heating of the system for safety concerns as the heating could raise the fluid pressures to very high levels depending on the temperature set point.

#### **4.3.2.6 CO<sub>2</sub>/N<sub>2</sub>-surfactant flooding**

For each surfactant, the base case involved co-injection of sc-CO<sub>2</sub> and surfactant solution (0% N<sub>2</sub>) at total flow rate of 1 cc/min and at four foam qualities of 0.70, 0.80, 0.90 and 0.95. Individual CO<sub>2</sub> and surfactant injection rates were varied (Table 4.1) to obtain different foam qualities and N<sub>2</sub>/CO<sub>2</sub> ratios but also maintain the total flow rate of 1 cc/min. After the base case, part of CO<sub>2</sub> was replaced by N<sub>2</sub> in four different proportions 5%, 10%, 15% and 20%. This

replacement of CO<sub>2</sub> was made by adjusting the individual CO<sub>2</sub> and N<sub>2</sub> injection rates. Table 4.1 shows the details of the individual flow rates used where set #1 in each experiment represents the base case (0% N<sub>2</sub>) and subsequent steps represent different N<sub>2</sub>/CO<sub>2</sub> ratios.

Table 4-1 Injection scenarios for CO<sub>2</sub>/N<sub>2</sub>-surfactant flooding

Experiment No.	Foam Quality	Flow Rate Set #	Q <sub>surfactant</sub>	Q <sub>CO2</sub>	N <sub>2</sub> /CO <sub>2</sub> Ratio	Q <sub>N2</sub>	Q <sub>total</sub>
	Fraction		cc/min	cc/min	Fraction	cc/min	cc/min
Experiment-1 (Fluorosurfactant)	0.7	1	0.300	0.700	0.00	0.000	1.000
		2	0.300	0.665	0.05	0.035	1.000
		3	0.300	0.630	0.10	0.070	1.000
		4	0.300	0.595	0.15	0.105	1.000
		5	0.300	0.560	0.20	0.140	1.000
Experiment-2 (Fluorosurfactant)	0.8	1	0.200	0.800	0.00	0.000	1.000
		2	0.200	0.760	0.05	0.040	1.000
		3	0.200	0.720	0.10	0.080	1.000
		4	0.200	0.680	0.15	0.120	1.000
		5	0.200	0.640	0.20	0.160	1.000

Experiment No.	Foam Quality	Flow Rate Set #	Q <sub>surfactant</sub>	Q <sub>CO2</sub>	N <sub>2</sub> /CO <sub>2</sub> Ratio	Q <sub>N2</sub>	Q <sub>total</sub>
	Fraction		cc/min	cc/min	Fraction	cc/min	cc/min
Experiment-3 (Fluorosurfactant)	0.9	1	0.100	0.900	0.00	0.000	1.000
		2	0.100	0.855	0.05	0.045	1.000
		3	0.100	0.810	0.10	0.090	1.000
		4	0.100	0.765	0.15	0.135	1.000
		5	0.100	0.720	0.20	0.180	1.000
Experiment-4 (Fluorosurfactant)	0.95	1	0.050	0.9500	0.00	0.0000	1.000
		2	0.050	0.9025	0.05	0.0475	1.000
		3	0.050	0.8550	0.10	0.0950	1.000
		4	0.050	0.8075	0.15	0.1425	1.000
		5	0.050	0.7600	0.20	0.1900	1.000
<p><i>Same set of above designed experiments were repeated for the other two surfactants as well. Since the total flow rate of 1 cc/min is used for all surfactants, all individual liquid and gas injection rates are therefore same.</i></p>							
Experiment-5 (AOS)	0.7	1	0.300	0.700	0.00	0.000	1.000
		2	0.300	0.665	0.05	0.035	1.000
		3	0.300	0.630	0.10	0.070	1.000
		4	0.300	0.595	0.15	0.105	1.000
		5	0.300	0.560	0.20	0.140	1.000

<b>Experiment No.</b>	<b>Foam Quality</b>	<b>Flow Rate Set #</b>	<b>Q<sub>surfactant</sub></b>	<b>Q<sub>CO2</sub></b>	<b>N<sub>2</sub>/CO<sub>2</sub> Ratio</b>	<b>Q<sub>N2</sub></b>	<b>Q<sub>total</sub></b>
	<b>Fraction</b>		<b>cc/min</b>	<b>cc/min</b>	<b>Fraction</b>	<b>cc/min</b>	<b>cc/min</b>
Experiment-6 (AOS)	0.8	1	0.200	0.800	0.00	0.000	1.000
		2	0.200	0.760	0.05	0.040	1.000
		3	0.200	0.720	0.10	0.080	1.000
		4	0.200	0.680	0.15	0.120	1.000
		5	0.200	0.640	0.20	0.160	1.000
Experiment-7 (AOS)	0.9	1	0.100	0.900	0.00	0.000	1.000
		2	0.100	0.855	0.05	0.045	1.000
		3	0.100	0.810	0.10	0.090	1.000
		4	0.100	0.765	0.15	0.135	1.000
		5	0.100	0.720	0.20	0.180	1.000
Experiment-8 (AOS)	0.95	1	0.050	0.9500	0.00	0.0000	1.000
		2	0.050	0.9025	0.05	0.0475	1.000
		3	0.050	0.8550	0.10	0.0950	1.000
		4	0.050	0.8075	0.15	0.1425	1.000
		5	0.050	0.7600	0.20	0.1900	1.000
<p><i>Same set of above designed experiments were repeated for the other two surfactants as well. Since the total flow rate of 1 cc/min is used for all surfactants, all individual liquid and gas injection rates are therefore same.</i></p>							

<b>Experiment No.</b>	<b>Foam Quality</b>	<b>Flow Rate Set #</b>	<b>Q<sub>surfactant</sub></b>	<b>Q<sub>CO2</sub></b>	<b>N<sub>2</sub>/CO<sub>2</sub> Ratio</b>	<b>Q<sub>N2</sub></b>	<b>Q<sub>total</sub></b>
	<b>Fraction</b>		<b>cc/min</b>	<b>cc/min</b>	<b>Fraction</b>	<b>cc/min</b>	<b>cc/min</b>
Experiment-9 (Witcolate)	0.7	1	0.300	0.700	0.00	0.000	1.000
		2	0.300	0.665	0.05	0.035	1.000
		3	0.300	0.630	0.10	0.070	1.000
		4	0.300	0.595	0.15	0.105	1.000
		5	0.300	0.560	0.20	0.140	1.000
Experiment-10 (Witcolate)	0.8	1	0.200	0.800	0.00	0.000	1.000
		2	0.200	0.760	0.05	0.040	1.000
		3	0.200	0.720	0.10	0.080	1.000
		4	0.200	0.680	0.15	0.120	1.000
		5	0.200	0.640	0.20	0.160	1.000
Experiment-11 (Witcolate)	0.9	1	0.100	0.900	0.00	0.000	1.000
		2	0.100	0.855	0.05	0.045	1.000
		3	0.100	0.810	0.10	0.090	1.000
		4	0.100	0.765	0.15	0.135	1.000
		5	0.100	0.720	0.20	0.180	1.000

<b>Experiment No.</b>	<b>Foam Quality</b>	<b>Flow Rate Set #</b>	<b>Q<sub>surfactant</sub></b>	<b>Q<sub>CO2</sub></b>	<b>N<sub>2</sub>/CO<sub>2</sub> Ratio</b>	<b>Q<sub>N2</sub></b>	<b>Q<sub>total</sub></b>
	<b>Fraction</b>		<b>cc/min</b>	<b>cc/min</b>	<b>Fraction</b>	<b>cc/min</b>	<b>cc/min</b>
Experiment-12 (Witcolate)	0.95	1	0.050	0.9500	0.00	0.0000	1.000
		2	0.050	0.9025	0.05	0.0475	1.000
		3	0.050	0.8550	0.10	0.0950	1.000
		4	0.050	0.8075	0.15	0.1425	1.000
		5	0.050	0.7600	0.20	0.1900	1.000

### 4.3.3 Interfacial Tension Measurements

#### 4.3.3.1 IFT Procedure

1. All the lines, viewing chamber, transfer cells and the capillary were cleaned and dried before being fitted into the main steel base of the equipment.
2. Vacuum was then applied to evacuate the cells, chamber and the lines of any air.
3. The desired working temperature was set.
4. The drop and bulk fluids were then loaded
5. Then the desired pressure was set using the manual pumps.
6. The experiment to be conducted was defined on the software (rising drop for our case).

7. The drop and the bulk fluid density values were entered.
8. Camera focus was then performed to get a clear view of the chamber.
9. Calibration of the needle was done and the detection lines were adjusted.
10. The export parameters were defined to save the results and the images on the computer.
11. The drop of surfactant solution was then created.
12. Depending on the drop, the detection level was adjusted and then the measurements were started and the results and images were saved. In addition to the IFT value, the software also measured the drop diameter, drop volume and the bond number.

Only those results were used and reported where the drop of surfactant was stable for at least 10 minutes. The software developed for this equipment takes into account all the points from the shape of the drop to solve the Laplace equation to calculate the IFT. The software uses at least 80 points on the shape of the drop for the IFT calculation. This enables increased accuracy as earlier software only used two or three main parameters to compute the IFT.

#### **4.3.4 Foam Texture Analysis**

The three injection fluids – surfactant, CO<sub>2</sub> and N<sub>2</sub> simultaneously pass through a porous filter medium which served as a foam generator. Generated foam then passed through a visual cell procured from CoreLab™ before going into the core. Image of this foam was captured using a high definition (HD) 13 MP (Megapixels) Sony camera. The zoomed image of the foam was then analyzed for circularity of the bubbles and bubble-size distribution (area) using ‘ImageJ’ image analysis software. The program uses pixels as the measuring unit.

Circularity of the foam bubble is defined as [23]:

$$Circularity = \frac{4 * \pi * A}{Perimeter^2}$$

Where A is the area of the bubble. When circularity approaches 1, the bubbles are more likely to be perfect circles and when it approaches 0, the bubbles are more likely to be polyhedral in shape.

The procedure for image analysis in ImageJ is as follows:

1. Open the image in ImageJ program.
2. Crop a zoomed version of the foam image in which bubble texture is clear.
3. Convert the image to 8-bit data.
4. Using the shape tools of the ImageJ program identify bubbles' shape from the zoomed image.
5. Get the average circularity and area of the selected foam bubbles and command the program to save the analysis results as excel sheet.



## **CHAPTER 5**

### **RESULTS AND DISCUSSION**

Foam-flooding experiments were performed in this research to help understand the complex phenomena of foam stability and texture in porous media that would occur in a reservoir during foam EOR processes in the harsh subsurface conditions. Flooding experiments involving injection of various fluids in the core provide the nearest actual depiction of an oil-field EOR process achievable on the lab scale. The actual reservoir environment present several thousand feet below the surface is part of a process that has been going on for millions of years which can never be obtained in the laboratory. However, the results of the experiments performed on specialized flooding equipment in this research can be up-scaled and a real field performance can be predicted with the help of proper simulation.

The foam-flooding experiments conducted in this study followed a step-by-step procedure that has been described earlier. The results of each step are described in the following sections.

#### **5.1 IFT Results and Discussion**

##### **5.1.1 IFT Results and Discussion of Fluorosurfactant FS-51**

Interfacial Tension (IFT) was measured between fluorosurfactant solutions prepared in distilled water and CO<sub>2</sub> at 1500 psi and 50°C. It must be noted that 0% surfactant simply represents IFT between distilled water and CO<sub>2</sub>, i.e., no addition of surfactant into distilled water. Table A-1 (Appendix-A) shows the IFT measured for the respective surfactant concentrations and Figure 5.1 shows the behavior of IFT as a function of surfactant concentration.

The critical micelle concentration (CMC) for fluorosurfactant FS-51 was found to be around 0.07 vol% as above this concentration the IFT becomes stable and does not decrease further. For foam-flooding experiments 0.15 vol% surfactant solution was prepared in distilled water which is above the CMC of fluorosurfactant FS-51.

The shapes of drops of surfactant solutions at various concentrations are shown below in Figure 5.2. Enlarged images are presented in Appendix B.

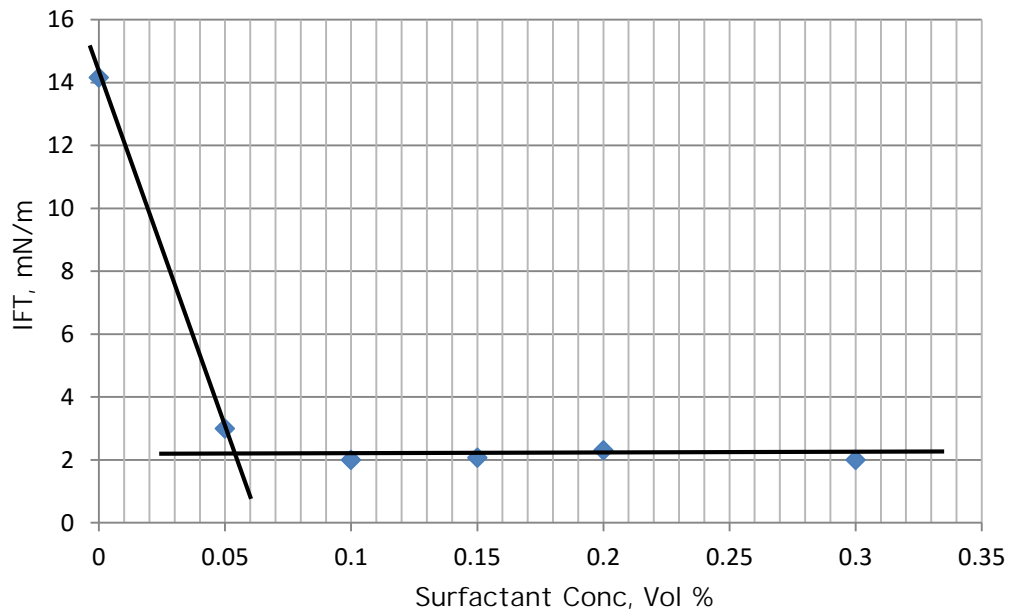


Figure 5.1: IFT vs. fluorosurfactant FS-51 surfactant concentration

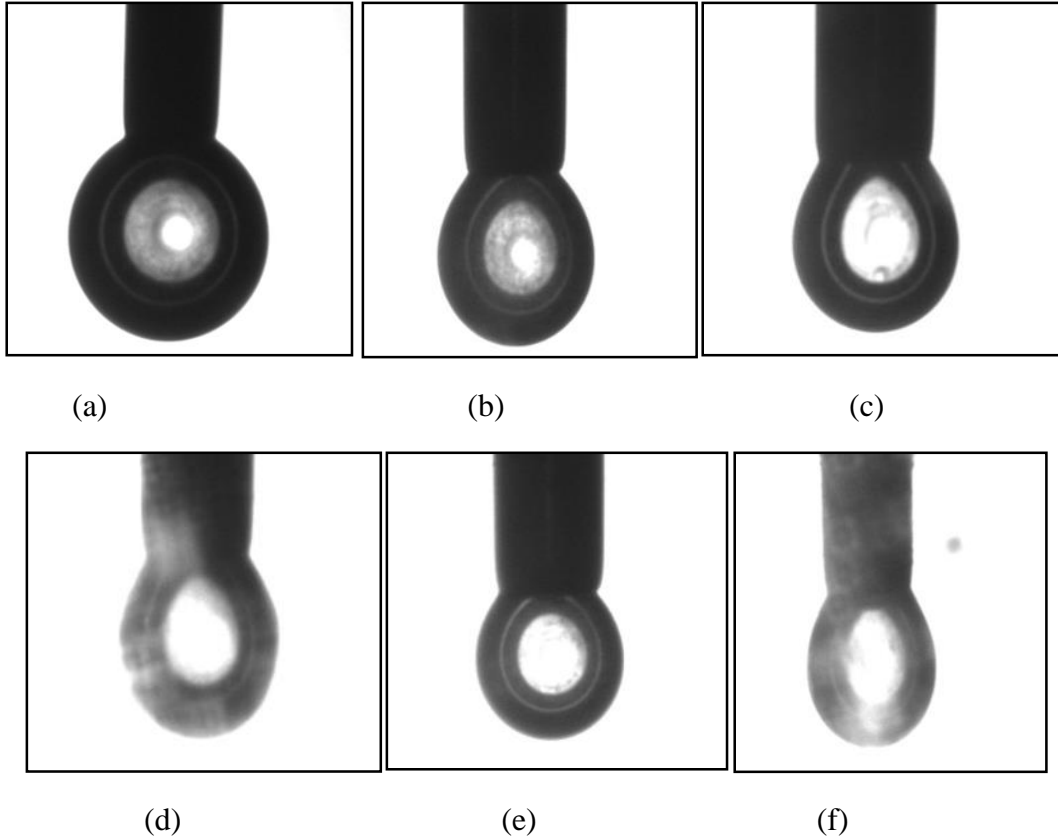


Figure 5.2: Shapes of drops of (a) 0 vol% (b) 0.05 vol% (c) 0.10 vol% (d) 0.15 vol% (e) 0.20 vol% and (f) 0.30 vol% fluorosurfactant in sc-CO<sub>2</sub> at 1500 psi and 50°C.

### 5.1.2 IFT Results and Discussion of Alpha-olefin-sulfonate (AOS)

Interfacial Tension (IFT) was measured between AOS surfactant solutions prepared in distilled water and CO<sub>2</sub> at 1500 psi and 50°C. It must be noted that 0% surfactant simply represents IFT between distilled water and CO<sub>2</sub>, i.e., no addition of surfactant into distilled water. Table A-2 (Appendix-A) shows the IFT measured for the respective surfactant concentrations and Figure 5.3 shows the behavior of IFT as a function of surfactant concentration.

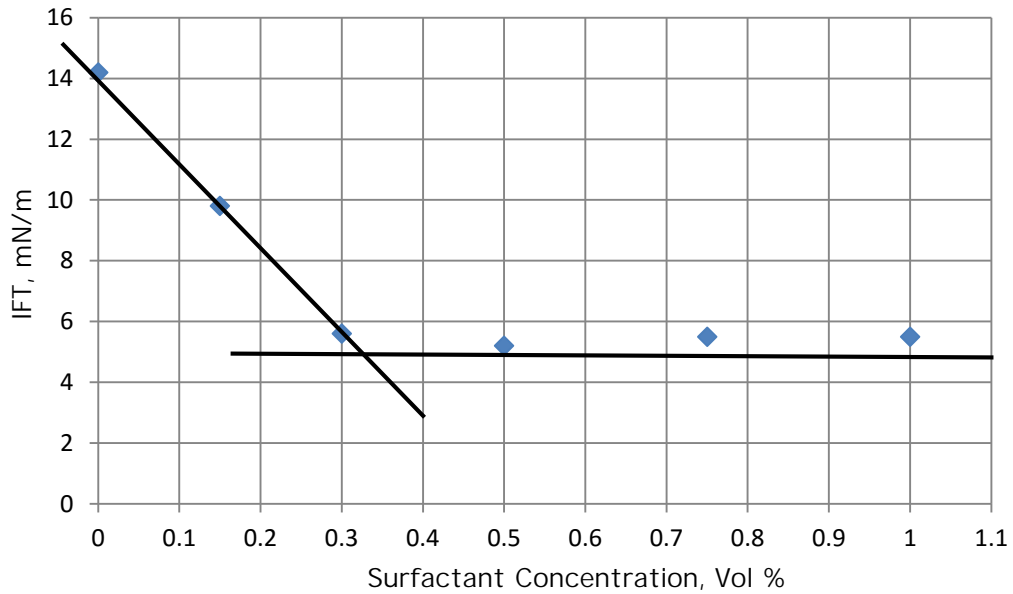


Figure 5.3: IFT vs. AOS surfactant concentration

The critical micelle concentration (CMC) for AOS was found to be around 0.3 vol% as above this concentration the IFT becomes stable and does not decrease further. For foam-flooding experiments 0.5 vol% surfactant solution was prepared in distilled water which is above the CMC of AOS.

The shapes of drops of surfactant solutions at various concentrations are shown below in the Figure 5.4. Enlarged images are presented in Appendix B.

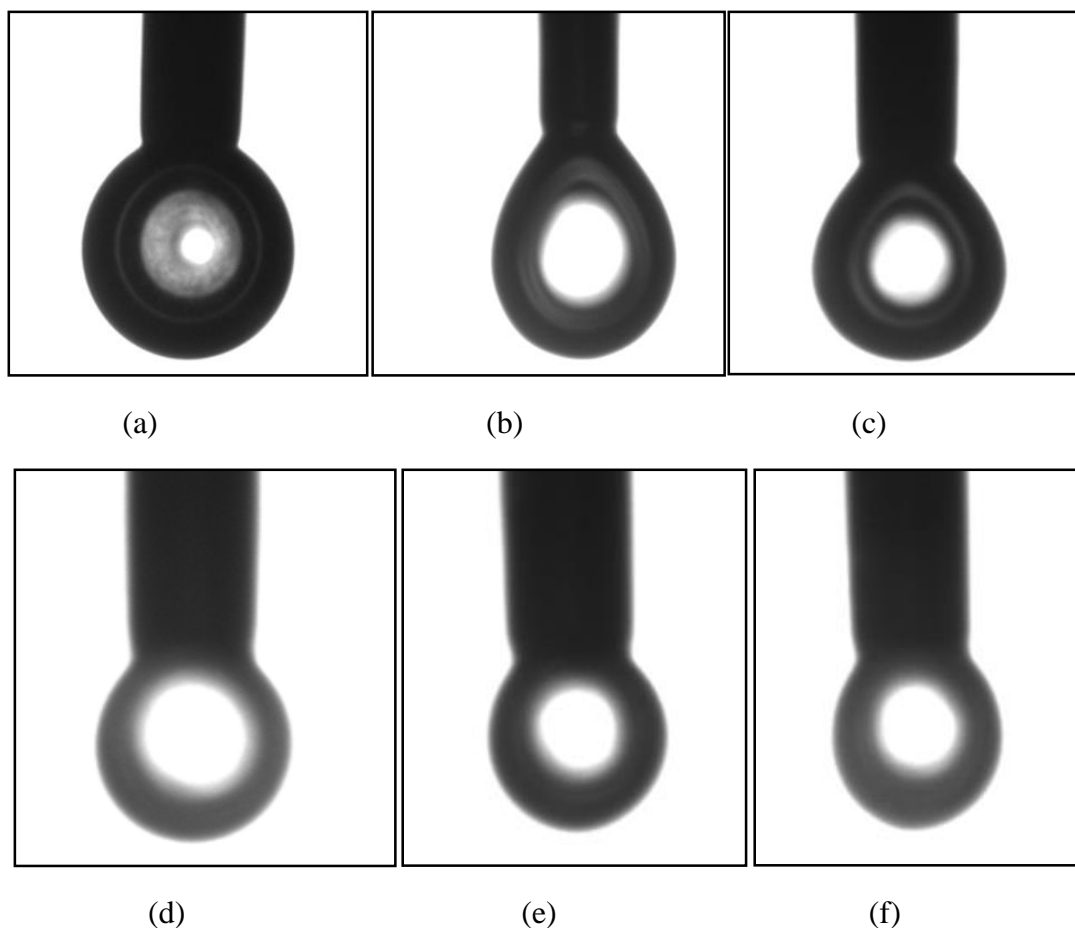


Figure 5.4: Shapes of drops of (a) 0 vol% (b) 0.15 vol% (c) 0.30 vol% (d) 0.50 vol% (e) 0.75 vol% and (f) 1.0 vol% AOS in sc-CO<sub>2</sub> at 1500 psi and 50°C.

### 5.1.3 IFT Results and Discussion of Witcolate Surfactant

Similar to the previous two surfactants, interfacial tension (IFT) was also measured between Witcolate surfactant solutions prepared in distilled water and CO<sub>2</sub> at 1500 psi and 50°C. It must be noted that, like in the case of previous surfactants, 0% surfactant simply represents IFT between distilled water and CO<sub>2</sub>, i.e., no addition of surfactant into distilled water. Table A-3 (Appendix-A) shows the IFT measured for the respective surfactant concentrations and figure 5.5 shows the plot of IFT vs. surfactant concentration.

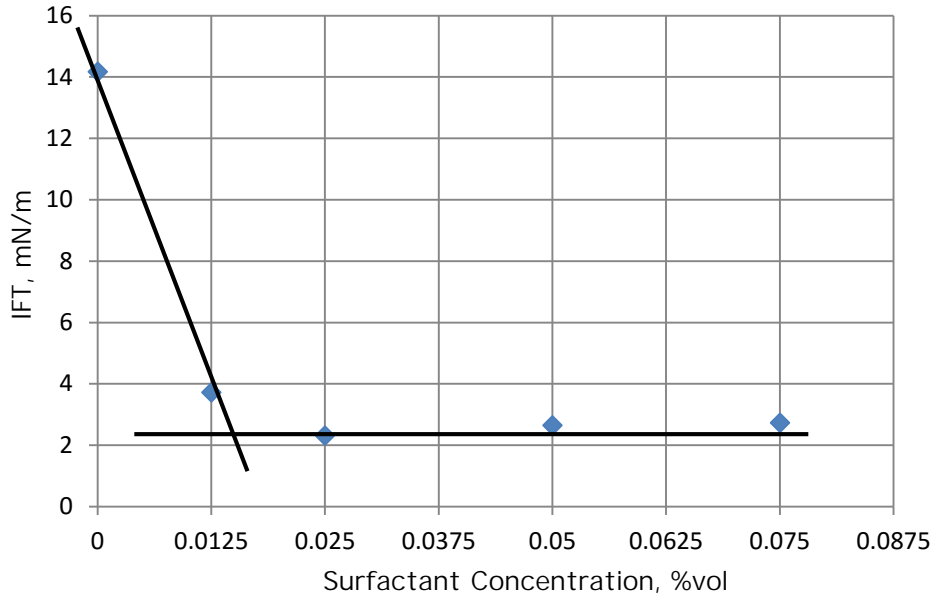


Figure 5.5: IFT vs. witcolate surfactant concentration

The critical micelle concentration (CMC) for Witcolate was found to be around 0.015 vol% as above this concentration the IFT becomes stable and does not decrease further. For foam-flooding experiments 0.05 vol% surfactant solution was prepared in distilled water which is above the CMC of Witcolate.

The shapes of drops of surfactant solutions at various concentrations are shown below in Figure 5.6. Enlarged images are presented in Appendix B.

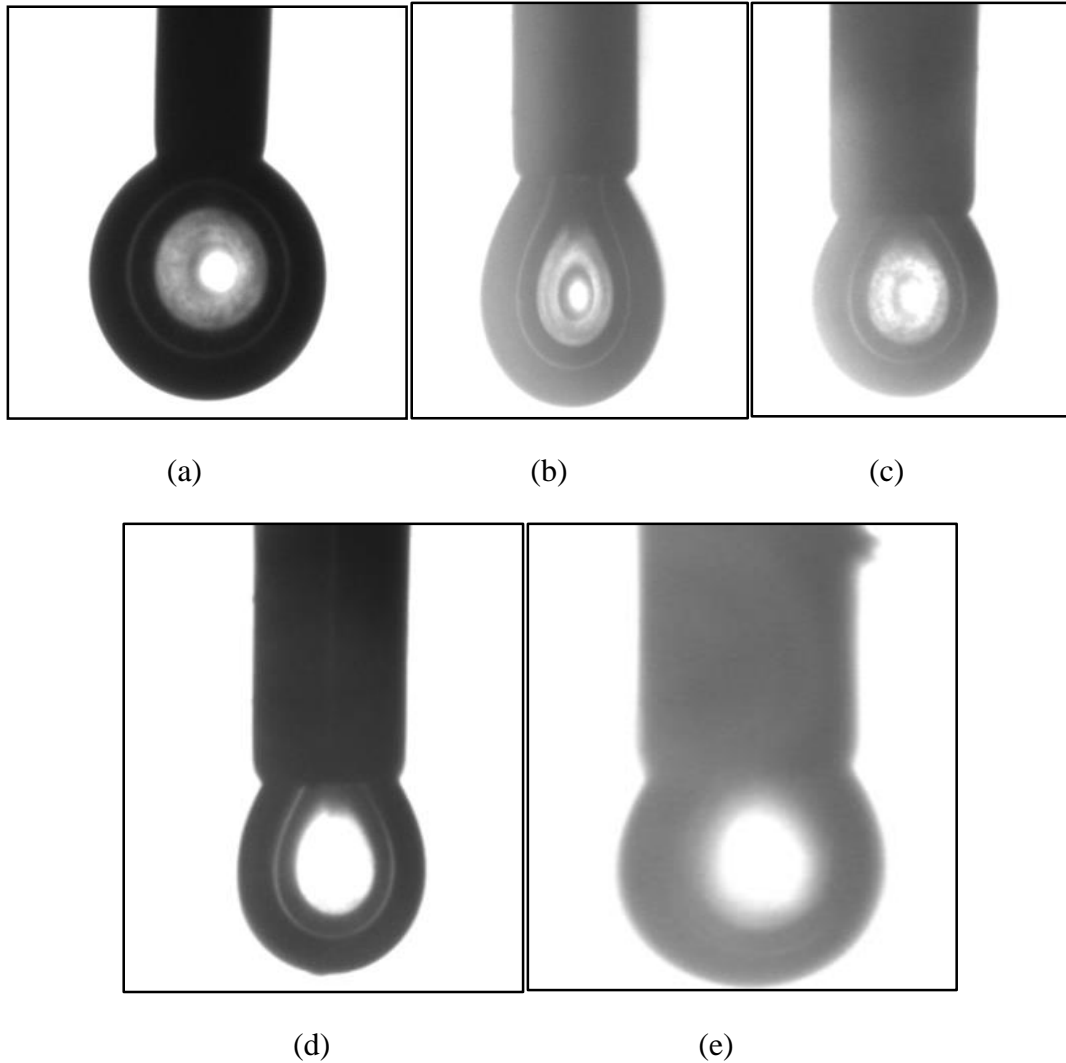


Figure 5.6: Shapes of drops of (a) 0 vol% (b) 0.0125 vol% (c) 0.025 vol% (d) 0.05 vol% and (e) 0.075 vol% witcolate in  $sc\text{-CO}_2$  at 1500 psi and 50°C.

## 5.2 Measurement of Core Properties

The dimensions of the core were measured before starting the foam flooding experiments. The core diameter, length and weight were measured to calculate the bulk volume of the cylindrical core. The core weight was again measured after surfactant saturation. The difference in weight between the wet and the dry core was divided by the surfactant density to get the pore volume of

the core. Porosity was then calculated using the pore and bulk volumes for each core. The data is tabulated in Table 5-1.

Table 5-1 Measured core properties

<b>Length</b>	<b>Diameter</b>	<b>Dry Weight</b>	<b>Wet Weight</b>	<b>Bulk Volume</b>	<b>Pore Volume</b>	<b>Porosity (<math>\Phi</math>)</b>
<b>cm</b>	<b>cm</b>	<b>g</b>	<b>g</b>	<b>cm<sup>3</sup></b>	<b>cm<sup>3</sup></b>	<b>%</b>
30.48	3.81	720.003	788.624	347.5	68.6	19.7

The core permeability was measured after the 100% surfactant saturated core was fixed in the system. Fluorosurfactant FS-51 was flowed through the core at different flow rates and pressure drop ( $\Delta P$ ) was recorded. Then, using Darcy’s Law permeability was calculated. After performing foam-flooding experiments, Witcolate surfactant was injected at different flow rates and respective  $\Delta P$  was recorded to calculate the permeability after all flooding experiments had been completed to see if the surfactants used caused any permeability alteration during the experiments.

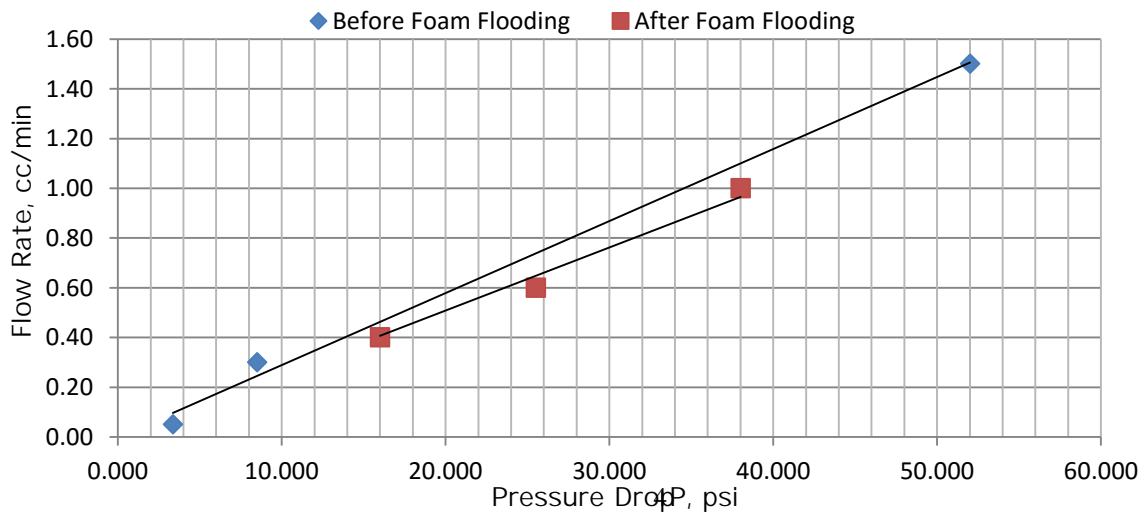


Figure 5.7: Flow rate vs. pressure drop to calculate permeability (before and after foam flooding)



It was observed that there was no significant change in permeability before and after foam flooding implying that surfactants did not cause any permeability alteration to the sandstone core. Before foam flooding the measured permeability was around 19 mD and after foam flooding it was around 18 mD.

### **5.3 Foam-flooding Experiment Results and Discussion**

After determining the critical micelle concentrations (CMC) of each surfactant, the next step was to use these surfactants for foam-flooding above their determined CMC's. When the sandstone core was fully saturated with surfactant solution at 1800 psi, it was placed in the core holder and fixed inside the system and foam-flooding was performed based on the injection strategies described earlier.

As described earlier (Table 4.1), foam-flooding with each surfactant involves four different experiments each for a foam quality of 0.70, 0.80, 0.90 and 0.95. Each experiment consists of five different sets of individual gas/liquid injection flow rates representing N<sub>2</sub>/CO<sub>2</sub> ratios of 0%, 5%, 10%, 15% and 20% respectively. N<sub>2</sub>/CO<sub>2</sub> ratio of 0% represents the base case of sc-CO<sub>2</sub>-surfactant flooding and subsequent sets of flow rates represent the replacement of CO<sub>2</sub> in base-case by N<sub>2</sub> in different proportions. Each set of flow rate was maintained until steady state conditions prevailed and pressure drop ( $\Delta P$ ) across the core was stable for about 30 minutes. The average pressure drop of the values stable for 30 minutes was calculated and then the next set of flow rate was initiated.

### **5.3.1 Foam-flooding Experiment Results and Discussion for Fluorosurfactant FS-51**

Co-injection of 0.15 vol% fluorosurfactant, sc-CO<sub>2</sub> and N<sub>2</sub> into the sandstone core was performed. The three fluids first passed through a porous filter medium which served as a foam generator. The generated foam then passed through the visual cell and then into the core. The foam visible in the visual cell was captured by camera and analyzed for foam texture the results of which are discussed in Section 5.4.

Total injection rate of 1 cc/min was maintained. Only the individual surfactant, sc-CO<sub>2</sub> and N<sub>2</sub> injection rates were varied in such a way that respective foam qualities and N<sub>2</sub>/CO<sub>2</sub> ratios were obtained yet total flow rate of 1 cc/min is maintained (as discussed in Section 4.3.2.6, Table 4.1).

Foam-flooding with each surfactant consists of four experiments. Each of this experiment represents a specific foam quality. Each experiment further consists of five sets of flow rates in which the first set served as the base case (with 0% N<sub>2</sub>). The subsequent steps represent different N<sub>2</sub>/CO<sub>2</sub> ratios. The injection of the three fluids at a particular set of flow rate was maintained until steady-state was achieved. Steady-state was assumed to be reached when  $\Delta P$  across the core was stable for about 30 minutes.

Table 4-1 shows the injection plan for experiments 1, 2, 3 and 4. Table A-4 shows the averaged steady-state  $\Delta P$  values for each of the four experiments. Figure 5.8 represents graphically the results of all four experiments. The results are discussed below.

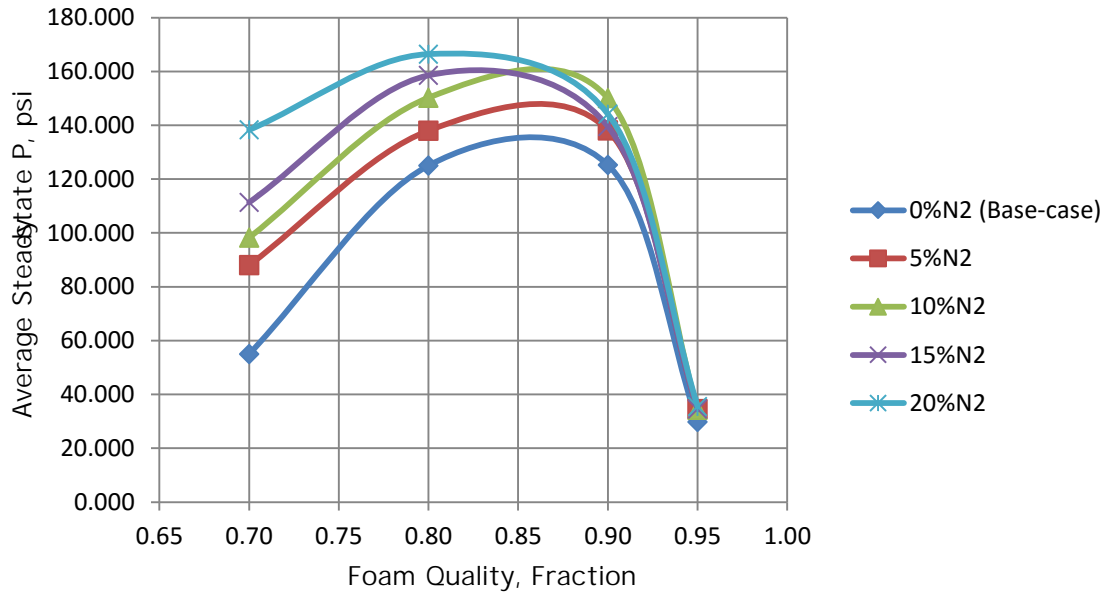


Figure 5.8: Average steady-state  $\Delta P$  vs. foam quality (fluorosurfactant FS-51)

It can be seen from Figure 5.8 that addition of  $N_2$  to  $sc\text{-CO}_2$  increases the  $\Delta P$  across the core for the same total flow rate (1 cc/min) at all foam qualities except 0.95.

Most profound effect of addition of  $N_2$  can be seen for foam quality of 0.70 where addition of just 5%  $N_2$  increases the  $\Delta P$  across the core by 33 psi. Further increase in  $N_2$  (10% - 20%) increases the  $\Delta P$  even more indicating foam became stronger with each additive proportion of  $N_2$ . This conclusion can be confidently made as the total flow rate of 1 cc/min is maintained for the same core i.e. core dimensions, porosity and permeability is the same for all experiments. This implies that any increase in  $\Delta P$  across the core is due to the increase in apparent viscosity of the injected foam. In other words, more viscous foam is more stable or strong, which is effective in improving the sweep. For foam quality of 0.70, maximum  $\Delta P$  was obtained for 20%  $N_2$  which was 138 psi compared to 55 psi with 0%  $N_2$ .

At foam quality of 0.80, similar observations were made i.e. with increase of  $N_2/CO_2$  ratio  $\Delta P$  across the core increased. All averaged  $\Delta P$  values for foam quality 0.80 were higher than those

for foam quality 0.70 for respective N<sub>2</sub>/CO<sub>2</sub> ratios. Average  $\Delta P$  for 0% N<sub>2</sub> was 125 psi whereas for 20% N<sub>2</sub> it was 166 psi.

For foam quality of 0.90, it was observed that  $\Delta P$  increased slightly from 125 psi at 0% N<sub>2</sub> to 138 psi at 5% N<sub>2</sub>. Further increase in proportion of N<sub>2</sub> did not increase  $\Delta P$  significantly implying that at this foam quality addition of N<sub>2</sub> beyond 5% did not increase the apparent foam viscosity i.e. did not improve the foam strength or stability.

At foam quality of 0.95, average  $\Delta P$  values for all N<sub>2</sub>/CO<sub>2</sub> ratios (0% - 20%) are identical implying that addition of N<sub>2</sub> did not have any effect on foam strength and stability. Also, all  $\Delta P$  values at foam quality 0.95 were the lowest compared to other foam qualities. This is because at such high foam quality where liquid injection rate is low compared to the gas injection rate, the foam becomes very dry and is weakened due to reduced number of lamellae.

It can be seen from Figure 5.8 that 0.90 is the critical foam quality ( $q_g^*$ ) above which foam weakens and  $\Delta P$  starts to drop. Also, optimum foam quality for foam created by fluorosurfactant FS-51 was 0.80 as highest  $\Delta P$  values (or apparent foam viscosities) were obtained at this foam quality with or without addition of N<sub>2</sub>. It was also observed that effect of addition of N<sub>2</sub> to CO<sub>2</sub> became less profound as the foam quality was increased. Effect of addition of N<sub>2</sub> was clearly profound at foam quality 0.70 and as the foam quality is increased effect of addition of N<sub>2</sub> decreases and at foam quality 0.95 becomes negligible.

### **5.3.2 Foam-flooding Experiment Results and Discussion for Alpha-olefin-sulfonate (AOS)**

After the four experiments for fluorosurfactant were completed, 2 pore volumes (PV) of AOS surfactant were flushed through the core to satisfy the adsorption of surfactant, if any, on the

rock and to displace the previous surfactant from the core. Then, co-injection of 0.50 vol% AOS, sc-CO<sub>2</sub> and N<sub>2</sub> into the sandstone core was performed. The three fluids first passed through a porous filter medium which served as a foam generator. The generated foam then passed through the visual cell and then into the core. The foam visible in the visual cell was captured by camera and analyzed for foam texture the results of which are discussed in Section 5.4.

Total injection rate of 1 cc/min was maintained. Only the individual surfactant, sc-CO<sub>2</sub> and N<sub>2</sub> injection rates were varied in such a way that respective foam qualities and N<sub>2</sub>/CO<sub>2</sub> ratios were obtained and yet the total flow rate of 1 cc/min is maintained (as discussed in Section 4.3.2.6, Table 4.1).

Foam-flooding with each surfactant consists of four experiments. Each of this experiment represents a specific foam quality. Each experiment further consists of five sets of flow rates in which the first set served as the base case (with 0% N<sub>2</sub>). The subsequent steps represent different N<sub>2</sub>/CO<sub>2</sub> ratios. The injection of the three fluids at a particular set of flow rate was maintained until steady-state was achieved. Steady-state was assumed to be reached when  $\Delta P$  across the core was stable for about 30 minutes.

Table 4-1 shows the injection plan for experiments 5, 6, 7 and 8. Table A-5 shows the averaged steady-state  $\Delta P$  values for each of the four experiments. Figure 5.9 represents graphically the results of all four experiments. The results are discussed below.

It can be seen in Figure 5.8 that, in general, addition of N<sub>2</sub> to sc-CO<sub>2</sub> increases the pressure drop  $\Delta P$  across the core. For a foam quality of 0.70, addition of 5% N<sub>2</sub> to sc-CO<sub>2</sub> increases the  $\Delta P$  from 120 psi at 0% N<sub>2</sub> to 143 psi. Further increase in proportion of N<sub>2</sub> also increases the  $\Delta P$  reaching a maximum of 180 psi at 20% N<sub>2</sub> for 0.70 foam quality. This increase in  $\Delta P$  signifies

strengthening of foam due to increase in its apparent viscosity. Other factors for this increase in  $\Delta P$  can be confidently ruled out due to the fact that total injection rate ( $q_t = 1$  cc/min) was maintained in all cases and also the same core was used. The increase in  $\Delta P$  is thus the sole effect of increase in apparent foam viscosity.

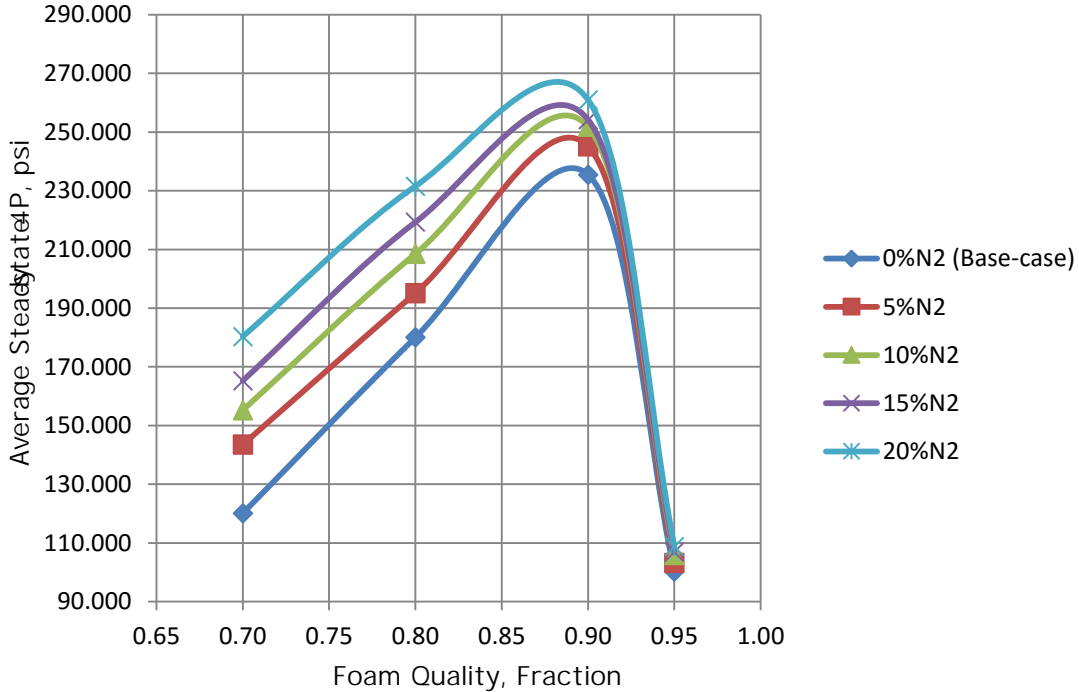


Figure 5.9: Average steady-state  $\Delta P$  vs. foam quality (AOS)

Similarly for foam quality of 0.80,  $\Delta P$  increases from 180 psi at 0%  $N_2$  to 231 psi at 20%  $N_2$ . The respective  $\Delta P$  values at all  $N_2/CO_2$  ratios were higher than those for foam quality of 0.70 implying that foam is stronger at foam quality of 0.80 than at 0.70.

At foam quality of 0.90, only marginal increase in  $\Delta P$  was observed with each additive proportion of  $N_2$ .  $\Delta P$  was 235 psi at 0%  $N_2$  and 260 psi at 20%  $N_2$ . However, all  $\Delta P$  values at foam quality of 0.90 were higher than those at foam qualities of 0.70 and 0.80. This implies that foam using AOS is strongest at foam quality of 0.90.

At foam quality of 0.95,  $\Delta P$  drops significantly to around 100 psi. Also, addition of  $N_2$  to sc- $CO_2$  does not have any apparent effect of foam strength. This is because at high foam qualities foam is very dry and is therefore weakened.

It was also observed that at foam qualities of 0.70 and 0.80 effect of addition of  $N_2$  to sc- $CO_2$  is equally visible and profound but at foam quality of 0.90 the effect is diminishing. At foam quality of 0.95, the effect of addition of  $N_2$  is completely negligible.

It can be seen from Figure 5.9 that 0.90 is the critical foam quality ( $f_g^*$ ) above which foam weakens and  $\Delta P$  starts to drop. Also, optimum foam quality for foam created by AOS was 0.90 as highest  $\Delta P$  values (or apparent foam viscosities) were obtained at this foam quality with or without addition of  $N_2$ . It was also observed that effect of addition of  $N_2$  to  $CO_2$  became less profound at this optimum foam quality and it was negligible beyond it at foam quality of 0.95.

### **5.3.3 Foam-flooding Experiment Results and Discussion for Witcolate Surfactant**

After the foam-flooding with AOS, 2 pore volumes (PV) of Witcolate surfactant were flushed through the core to replace the previous AOS surfactant from the core. Then, co-injection of 0.05 vol% Witcolate surfactant, sc- $CO_2$  and  $N_2$  into the sandstone core was performed. The three fluids first passed through a porous filter medium which served as a foam generator. The generated foam then passed through the visual cell and then into the core. The foam visible in the visual cell was captured by camera and analyzed for foam texture the results of which are discussed in Section 5.4.

Total injection rate of 1 cc/min was maintained. Only the individual surfactant, sc- $CO_2$  and  $N_2$  injection rates were varied in such a way that respective foam qualities and  $N_2/CO_2$  ratios were obtained yet total flow rate of 1 cc/min is maintained (as discussed in Section 4.3.2.6, Table 4.1).

Foam-flooding with each surfactant consists of four experiments. Each of this experiment represents a specific foam quality. Each experiment further consists of five sets of flow rates in which the first set served as the base case (with 0% N<sub>2</sub>). The subsequent steps represent different N<sub>2</sub>/CO<sub>2</sub> ratios. The injection of the three fluids at a particular set of flow rate was maintained until steady-state was achieved. Steady-state was assumed to be reached when  $\Delta P$  across the core was stable for about 30 minutes.

Table 4-1 shows the injection plan for experiments 9, 10, 11 and 12. Table A-6 shows the averaged steady-state  $\Delta P$  values for each of the four experiments. Figure 5.10 represents graphically the results of all four experiments. The results are discussed below.

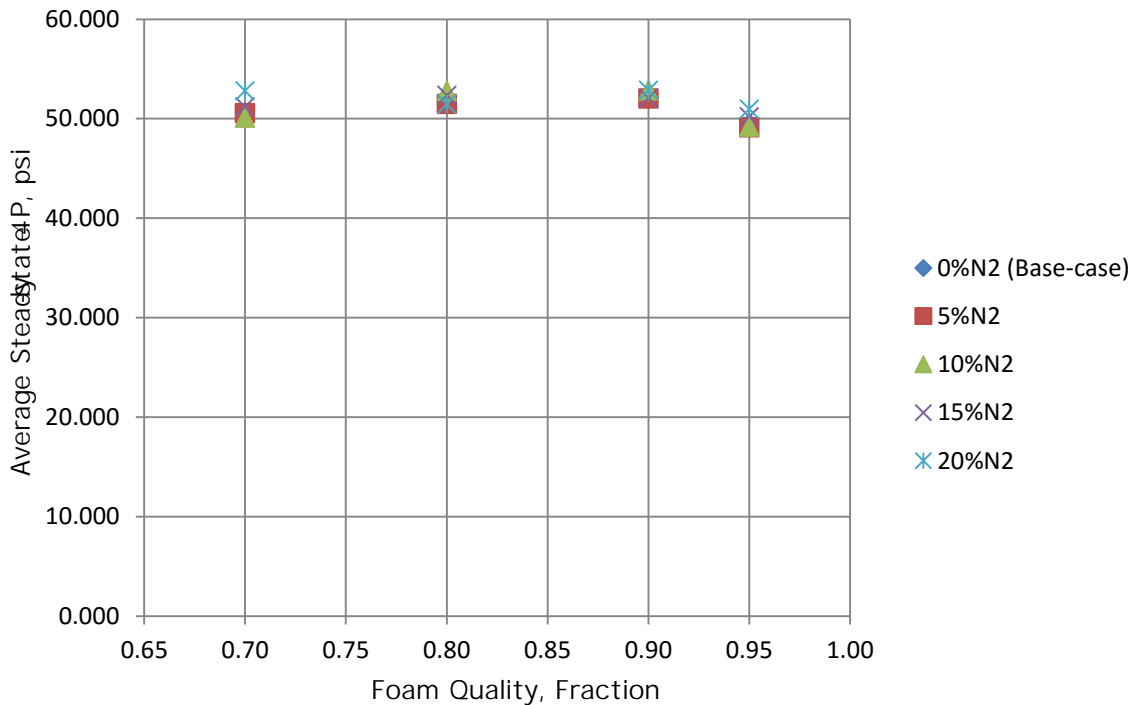


Figure 5.10: Average steady-state  $\Delta P$  vs. foam quality (Witcolate)



The third surfactant Witcolate was found to be a very poor foaming agent. It did not generate any foam whatsoever with CO<sub>2</sub> or N<sub>2</sub> or their mixture. This was supported by the visualization evidence obtained through the visual cell where no foam was seen during co-injection of the three fluids. Also, pressure drop  $\Delta P$  across the core was stable at an average value of ~50 psi for a total flow rate of 1 cc/min at all foam qualities and N<sub>2</sub>/CO<sub>2</sub> ratios. No increase in  $\Delta P$  was observed with increase in foam quality or increase in N<sub>2</sub>/CO<sub>2</sub> ratio at each of these foam qualities.

#### **5.4 Foam Texture Analysis Results and Discussion**

Foam images were captured through the visual cell and were analyzed using 'ImageJ' image analysis program. The procedure to use the program was described briefly in Section 4.3.4. The results of the analysis will be shown and discussed in this section. Foam image analysis was done for fluorosurfactant FS-51 and alpha-olefin-sulfonate (AOS). Since the third surfactant, Witcolate, did not form any foam so no image analysis was possible whatsoever.

### 5.4.1 Image Analysis Results and Discussion for Fluorosurfactant FS-51

Foam images (8-bit analyzed images) captured during experiments 1, 2, 3 and 4 involving co-injection of 0.15 vol% fluorosurfactant, sc-CO<sub>2</sub> and N<sub>2</sub> are shown below and discussion is followed.

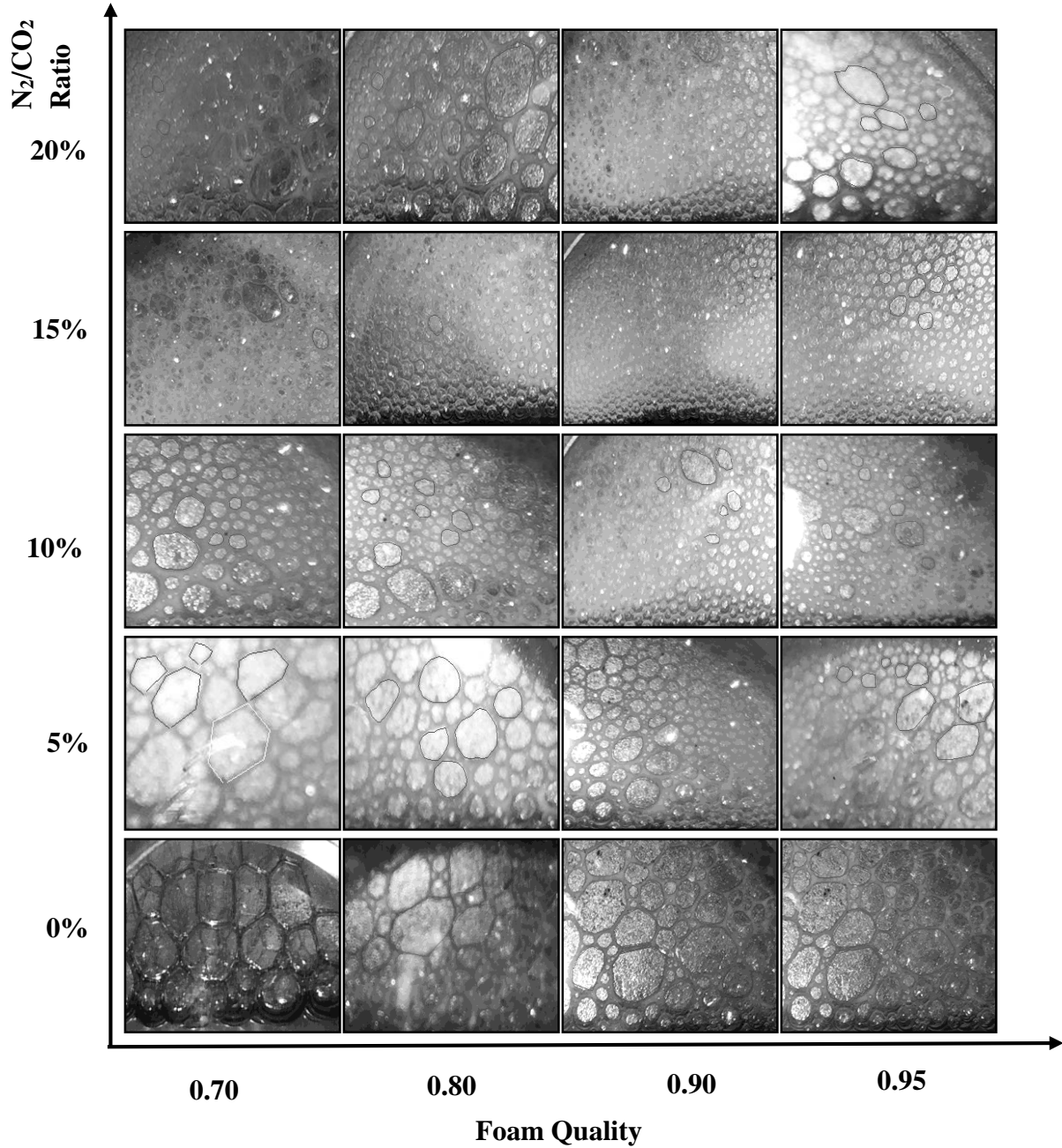


Figure 5.11: 8-bit Analyzed Foam Images for Fluorosurfactant FS-51

First, a qualitative analysis of captured foam images is done based on the fact that coarse-textured foam with polyhedral bubble shapes is weaker with a wide bubble size distribution whereas strong foam is fine-textured and bubbles are more spherical with a narrow bubble size distribution. A qualitative analysis of the captured foam images using fluorosurfactant FS-51 shows that for foam qualities of 0.70, 0.80 and 0.90, in general, with the addition of N<sub>2</sub> (from 0% to 20%) foam bubbles tend to become smaller and finer. Also, the difference between the sizes of bubbles becomes less with the addition of N<sub>2</sub> or in other words the bubble size distribution becomes narrower. This analysis acts as a support to the pressure drop ( $\Delta P$ ) data obtained at these foam qualities for different N<sub>2</sub>/CO<sub>2</sub> ratios based on which conclusions were made that foam had become stronger (its viscosity had increased) with the addition of N<sub>2</sub> since stronger foam has finer bubbles and narrow bubble size distribution. Foam for these foam qualities also could be seen getting denser (higher bubble intensity) signifying foam strength had improved. For a foam quality of 0.95, it can be seen that bubble sizes are large and more polyhedral in shape for 0% N<sub>2</sub> and with the addition of N<sub>2</sub> bubbles tend to become spherical but no visible proof of bubble density increasing was observed. This supports the lower pressure drop ( $\Delta P$ ) at 0.95 foam quality and also the negligible effect in  $\Delta P$  with addition of N<sub>2</sub>.

It was also observed visually that bubble sizes become smaller with the addition of N<sub>2</sub>. At foam qualities of 0.70, 0.80 and 0.90 foam bubbles at 15% and 20% N<sub>2</sub> are very small which made it difficult to analyze in the 'ImageJ' program. At 0.95 foam quality it was observed that foam bubble sizes became comparatively larger to those at previous foam qualities.

However, a quantitative analysis was also done to determine the circularity of the foam bubbles. The results of this analysis are shown below and discussion is followed.

Average circularity values of foam bubbles with fluorosurfactant FS-51 are tabulated in Table A-7. The same results are presented in a graphical format in Figure 5.12 below:

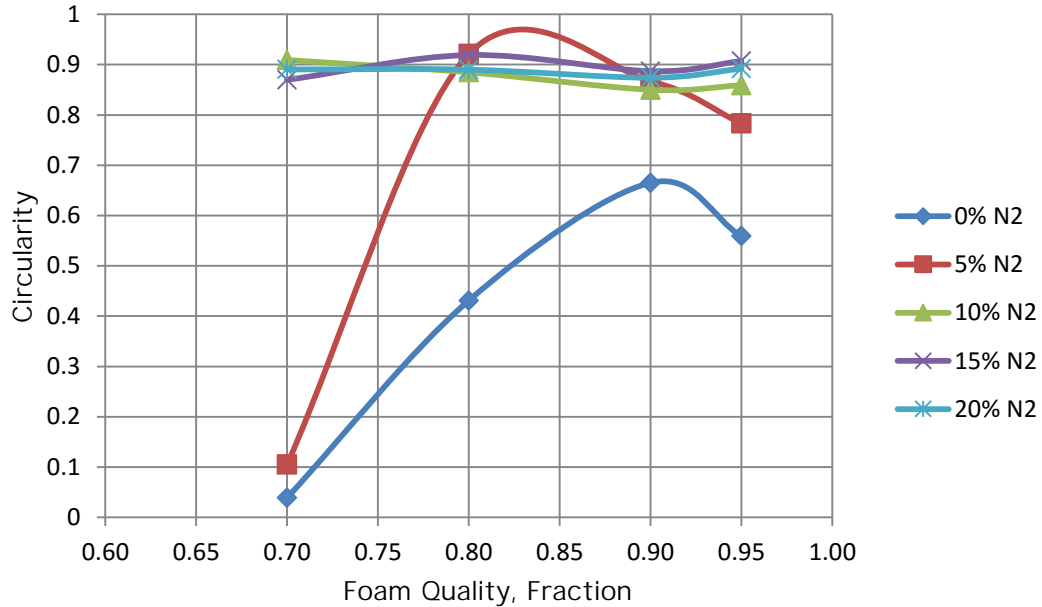


Figure 5.12: Average circularity vs. foam quality for fluorosurfactant FS-51

From Figure 5.12, it was observed that the circularity of foam bubbles increases significantly at all foam qualities when N<sub>2</sub> is added to sc-CO<sub>2</sub>. It was also observed for sc-CO<sub>2</sub>-foam (0% N<sub>2</sub>) that circularity increases till foam quality of 0.90 and then decreases. Similar observation was made for foam with 5% N<sub>2</sub>. But for foam with higher proportions of N<sub>2</sub> (10% - 20%) circularity is around 0.9 at all foam qualities signifying that addition of N<sub>2</sub> had made the foam texture finer and more spherical.

### 5.4.2 Image Analysis Results and Discussion for Alpha-olefin-sulfonate (AOS)

Foam images (8-bit analyzed images) captured during experiments 5, 6, 7 and 8 involving co-injection of 0.5 vol% AOS, sc-CO<sub>2</sub> and N<sub>2</sub> are shown below and discussion is followed.

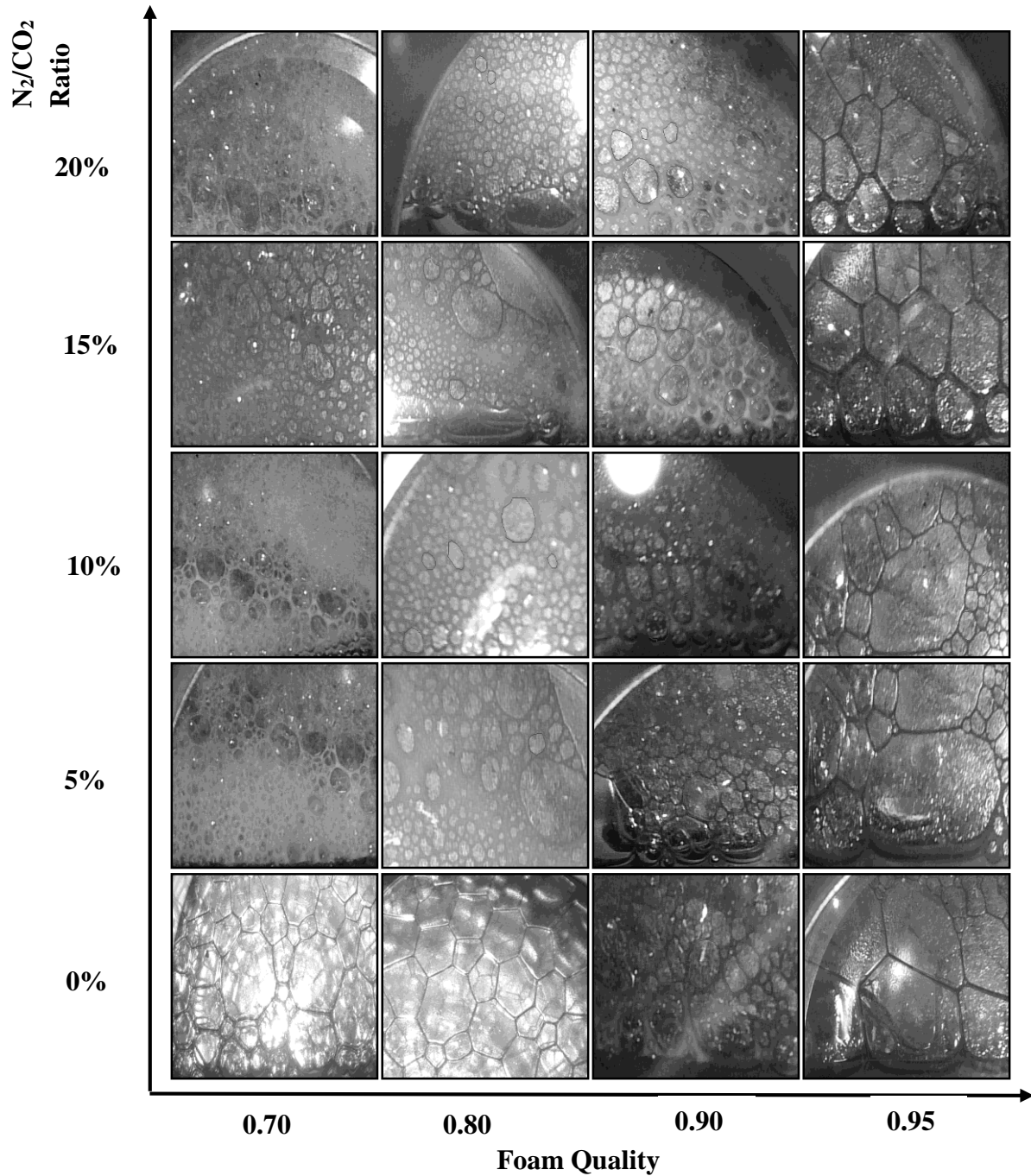


Figure 5.13: 8-bit Analyzed Foam Images for AOS

A qualitative analysis of the captured foam images using AOS shows that for foam qualities of 0.70, 0.80 and 0.90, in general, with the addition of N<sub>2</sub> (from 0% to 20%) foam bubbles tend to become smaller and finer. Also, the difference between the sizes of bubbles becomes less with the addition of N<sub>2</sub> or in other words the bubble size distribution becomes narrower. This analysis also acts as a support to the pressure drop ( $\Delta P$ ) data obtained at these foam qualities for different N<sub>2</sub>/CO<sub>2</sub> ratios based on which conclusions were made that foam had become stronger (its viscosity had increased) with the addition of N<sub>2</sub> since stronger foam has finer bubbles and narrow bubble size distribution. But for a foam quality of 0.95, it can be seen that bubble sizes are large and with the addition of N<sub>2</sub> no significant visible effects are seen, either in the bubble shapes or their size distributions, which could point towards strengthening of the foam.

It was observed visually that at foam qualities of 0.70 and 0.80, there was significant change in bubble sizes when N<sub>2</sub> was introduced. Just 5% addition of N<sub>2</sub> made the bubbles smaller in size and spherical in shape. At foam quality of 0.90, a clear change in bubble sizes was seen after addition of 15% and 20% N<sub>2</sub>. At 0.95 foam quality, no visible effects were seen after addition of N<sub>2</sub>. The shapes and sizes of bubbles were similar at all proportions of N<sub>2</sub>.

However, a quantitative analysis was also done to determine the circularity of the foam bubbles. The results of this analysis are shown below and discussion is followed.

Average circularity values of foam bubbles with AOS are tabulated in Table A-8. The same results are presented in a graphical format in Figure 5.14 below.

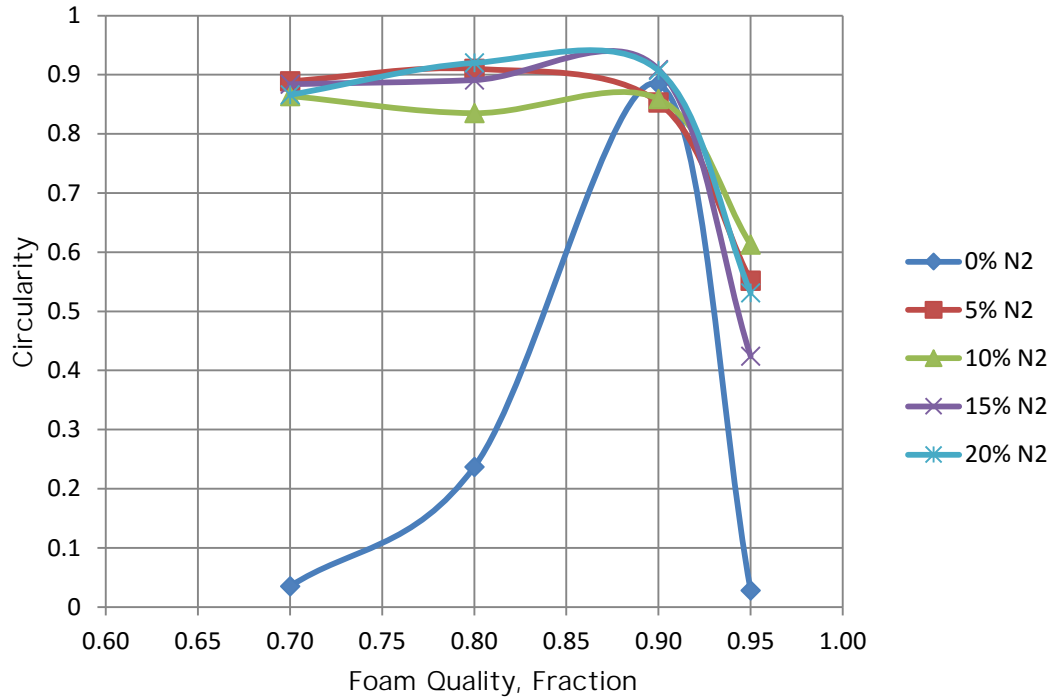


Figure 5.14: Average circularity vs. foam quality for AOS

It was observed from Figure 5.14 that the average circularity of foam bubbles with AOS improved at all foam qualities with the addition of N<sub>2</sub> to sc-CO<sub>2</sub>. With the addition of N<sub>2</sub> average circularity of foam bubbles increased significantly to around 0.9. The circularity of foam bubbles decreased above 0.90 foam quality for all proportions of N<sub>2</sub>. This supports the pressure drop ( $\Delta P$ ) data as a drop in  $\Delta P$  was observed at 0.95 foam quality signifying foam became weaker thus meaning its texture had become coarse and shape polyhedral. Qualitative analysis of foam images at 0.95 foam quality showed the polyhedral shapes of the bubbles and also this quantitative analysis also shows the decrease in circularity supporting the pressure drop data.

## CHAPTER 6

### CONCLUSIONS AND RECOMMENDATIONS

This research was conducted specifically to find a better and viable solution to the problem of CO<sub>2</sub> not being able to generate strong foam above its supercritical conditions making the foam EOR process inefficient and economically unprofitable due to lowering of sweep efficiencies and the trapped oil not being recovered. Based on the comparisons between CO<sub>2</sub>-foam and N<sub>2</sub>-foam and the potential benefits of adding N<sub>2</sub> to CO<sub>2</sub>-foam in bulk media as discussed in the Chapter 2 were tested in sandstone porous media by designing and performing several foam flooding experiments using three different surfactants as described in Chapter 4. Although, no direct mathematical correlation exists between foam strength and foam texture, both qualitative and quantitative analysis was done to support, interpret and justify the pressure drop ( $\Delta P$ ) data obtained during the foam flooding experiments. This analysis was based on the theory that strong foam is fine-textured with spherical bubbles and weak foam is coarse-textured with polyhedral bubble shapes.

From the results and analysis of the different foam flooding experiments, following conclusions are made:

1. For both FS-51 and AOS, addition of any proportion of N<sub>2</sub> to sc-CO<sub>2</sub> made the foam stronger as evident from the increased steady-state pressure drop  $\Delta P$  across the core (or equivalently increased apparent foam viscosity) at all foam qualities except 0.95.



2. The improved foam strength was supported by foam texture analysis where addition of N<sub>2</sub> made foam bubbles smaller in size and more spherical. Also, average circularity of bubbles improved significantly with addition of just 5% N<sub>2</sub>. Circularity did not change much with further addition of N<sub>2</sub>. Only, the bubble intensity increased making the foam denser.
3. For both FS-51 and AOS, effect of addition of N<sub>2</sub> diminishes as foam quality is increased. The effect is clearly visible at foam qualities of 0.70 and 0.80 and becomes less significant at 0.90 foam quality. At foam quality of 0.95, foam with 0% N<sub>2</sub> and 20% N<sub>2</sub> exhibit the same pressure drop ( $\Delta P$ ) i.e. addition of N<sub>2</sub> had no effect on foam viscosity whatsoever.
4. Critical foam quality ( $f_g^*$ ) for foam with fluorosurfactant FS-51 and alpha-olefin sulfonate (AOS) was 0.90 and with Witcolate no foam was formed with CO<sub>2</sub>, N<sub>2</sub> or their mixture.
5. Optimum foam quality without addition of N<sub>2</sub> at which foam was strongest was 0.90 for both FS-51 and AOS.
6. Optimum foam quality with addition of N<sub>2</sub> was 0.80 at which 20% N<sub>2</sub> gave the strongest foam.
7. Foam with AOS was stronger than that with FS-51 based on the steady-state pressure drop ( $\Delta P$ ) values recorded.
8. The three surfactants did not alter the permeability of the sandstone core. Since fluorosurfactant FS-51 and AOS formed strong foam, they are good options for foam EOR applications in sandstone reservoirs.

Based on the observations and conclusions of this research, the following recommendations are suggested for future work in this area:

1. Core-flooding experiments should be performed at optimum foam quality and  $N_2/CO_2$  ratio to determine if the apparent increase in foam strength has any effect on oil recovery before and after addition of  $N_2$ .
2. Visual core-flood experiments should be performed to better scan the propagation of mixed  $CO_2/N_2$  foam in porous media.
3. Effects of temperature and pressure should be studied on the properties of mixed  $CO_2/N_2$ -foam.

## REFERENCES

- [1] Ali, J., Burley, R. W., & Nutt, C. W. (1985). Foam Enhanced Oil Recovery from Sand Packs. *Chemical Engineering Research and Design*, 63(2), 101-111.
- [2] Aarra, M. G., Skauge, A., & Solbakken, J. S. (2013). Supercritical CO<sub>2</sub> Foam - The Importance of CO<sub>2</sub> Density on Foams Performance. *SPE Enhanced Oil Recovery Conference*, 2(2012). <http://doi.org/10.2118/165296-MS>
- [3] Apaydin, O. G., & Kovscek, A. R. (2000). Surfactant Concentration and End Effects on Foam Flow in Porous Media. *Doe*, (TR — 120 Report).
- [4] Bernard, G., and Holm, L. (1967). Method for Recovering Oil from Subterranean Formations, U.S. Patent 3,342,256.
- [5] Blauer, R.E. and Kohlhaas, C.A. (1974). Formation Fracturing with Foam. Paper SPE 5003 presented at the *Fall Meeting of the Society of Petroleum Engineers* of AIME. Houston, Texas, USA, October 6-9.
- [6] Bullen, R. S., & Bratrud, T. F. (1976). Fracturing With Foam. *Journal of Canadian Petroleum Technology*, 15(2), 27-32.
- [7] Chambers, K.T. and Radke, C. J. (1991) 'Capillary Phenomena in Foam Flow Through Porous Media', in Morrow, N. R. (ed.) *Interfacial Phenomena in Petroleum Recovery*. New York: Marcel Dekker, pp. 191-255 (Chapter 6).
- [8] Chang, S.-H., & Grigg, R. B. (1994). Laboratory Flow Tests Used To Determine Reservoir Simulator Foam Parameters for EVGSAU CO<sub>2</sub> Foam Pilot. *Proceedings of Permian Basin Oil and Gas Recovery Conference*, 483-492. <http://doi.org/10.2118/27675-MS>
- [9] Chang, S.-H., & Grigg, R. (1999). Effects of Foam Quality and Flow Rate on CO<sub>2</sub>-Foam Behavior at Reservoir Temperature and Pressure. *SPE Reservoir Evaluation & Engineering*, 2(May 1998), 19-22. <http://doi.org/10.2118/56856-PA>
- [10] Du, D. X., Beni, A. N., Farajzadeh, R., & Zitha, P. L. J. (2008). Effect of Water Solubility on Carbon Dioxide Foam Flow in Porous Media: An X-ray Computed Tomography Study. *Industrial & Engineering Chemistry Research*, 47(16), 6298-6306. <http://doi.org/10.1021/ie701688j>
- [11] Ettinger, R. A., & Radke, C. J. (1992). Influence of Texture on Steady Foam Flow in Berea Sandstone. *SPE Reservoir Engineering*, 7(February), 83-90. <http://doi.org/10.2118/19688-PA>

- [12] Falls, A., Lawson, J., & Hirasaki, G. (1988). The Role of Noncondensable Gas in Steam Foams. *Journal of Petroleum Technology*, 40(1), 95–104. <http://doi.org/10.2118/15053-PA>
- [13] Farajzadeh, R., Andrianov, A., Bruining, H., & Zitha, P. L. J. (2009). Comparative study of CO<sub>2</sub> and N<sub>2</sub> foams in porous media at low and high pressure-temperatures. *Industrial and Engineering Chemistry Research*, 48(9), 4542–4552. <http://doi.org/10.1021/ie801760u>
- [14] Friedmann, F., & Jensen, J.A. (1986). Some Parameters Influencing Formation and Propagation of Foams in Porous Media, Paper SPE 15087. *SPE California Regional Meeting*, Oakland, USA, April 2-4.
- [15] Gauglitz, P. A, Friedmann, F., Kam, S. I., & Rossen, W. R. (2002). Foam Generation in Porous Media. *SPE/DOE Improved Oil Recovery Symposium*. Tulsa, Oklahoma. <http://doi.org/10.2118/75177-MS>
- [16] Gauglitz, P.A., Friedmann, F., Kam, S.I., and Rossen, W.R. (2002) 'Foam Generation in Homogeneous Porous Media', *Chemical Engineering Science*, 57(19), pp. 4037-4052.
- [17] Harris, P. C. (1995). N<sub>2</sub> And CO<sub>2</sub> Foam Fracturing Fluids On A Flow-Loop Viscometer. *SPE Production & Facilities*, 10(3), 197–203. Retrieved from <Go to ISI>://A1995RN22600010
- [18] Hirasaki, G. J., van Domselaar, H. R., & Nelson, R. C. (1983). Evaluation of the Salinity Gradient Concept in Surfactant Flooding. *Society of Petroleum Engineers Journal*, 23(3), 486–500. <http://doi.org/10.2118/8825-PA>
- [19] Holt, T., & Vassenden, F. (1996). Effects of Pressure on Foam Stability; Implications for Foam Screening. *Society of Petroleum Engineers*, 543–552.
- [20] Holm, L. W. (1968). The Mechanism of Gas and Liquid Flow Through Porous Media in the Presence of Foam. *Society of Petroleum Engineers Journal*, 8(4), 359–369. <http://doi.org/10.2118/1848-PA>
- [21] Hutchins, R., & Miller, M. (2005). A Circulating-Foam Loop for Evaluating Foam at Conditions of Use. *SPE Production & Facilities*, 20(April), 5–8. <http://doi.org/10.2118/80242-PA>
- [22] Isaacs, E., McCarthy, F., & Maunder, J. (1988). Investigation of Foam Stability in Porous Media at Elevated Temperatures. *SPE Reservoir Engineering*, 3(May), 565–572. <http://doi.org/10.2118/15647-PA>
- [23] ImageJ (2016) *ImageJ*, Available at: <http://rsb.info.nih.gov/ij/index.html> (Accessed: 1st January 2015).

- [24] Liu, D., Castanier, L. M., & Brigham, W. E. (1992). Displacement by Foam in Porous Media. *SPE Annual Technical Conference and Exhibition, 4-7 October, Washington, D.C.*
- [25] Liu, Y., Grigg, R., & Svec, R. (2006). Foam Mobility and Adsorption in Carbonate Core. *SPE Journal*, (April), 1–8.
- [26] Mitchell, B.J. Viscosity of Foam, Ph.D. Thesis, University of Oklahoma, 1970.
- [27] Nguyen, T. A., & Ali, S. M. F. Effect of Nitrogen On the Solubility And Diffusivity of Carbon Dioxide Into Oil And Oil Recovery By the Immiscible WAG Process, (1). <http://doi.org/10.2118/95-64>
- [28] Osterloh, W.T., & Jante, M.J. (1992). Effects of Gas and Liquid Velocity on Steady-State Foam Flow. *SPE/DOE Eighth Symposium on Enhanced Oil Recovery, Tulsa.*
- [29] Owete, O., & Brigham, W. (1987). Flow Behavior of Foam: A Porous Micromodel Study. *SPE Reservoir Engineering*, 2(3), 315–323. <http://doi.org/10.2118/11349-PA>
- [30] Patzek, T. W. (1996). Field Applications of Steam Foam for Mobility Improvement and Profile Control. *SPE Reservoir Engineering*, 11(02), 79–85. <http://doi.org/10.2118/29612-PA>
- [31] Rossen, W.R. (1996) 'Foams in Enhanced Oil Recovery', in Prudhomme R.K., and Khan S. (ed.) *Foams: Theory, Measurement, and Applications*. New York: Marcel Dekker.
- [32] Schramm, L.L. (1994) *Foams: Fundamentals and Applications in the Petroleum Industry*, Washington, DC: American Chemical Society.
- [33] Suffridge, F., Raterman, K., & Russell, G. (1989). Foam performance under reservoir conditions. *SPE Annual Technical ...*. Retrieved from <http://www.onepetro.org/mslib/servlet/onepetroreview?id=00019691>
- [34] Tanzil, D. (2001). Foam Generation and Propagation in Heterogeneous Porous Media. PhD Dissertation, Rice University, Houston, Texas, USA.
- [35] Tsau, Jyun-Syung, & Grigg, R. B. (1997). Assessment of Foam Properties and Effectiveness in Mobility Reduction for CO<sub>2</sub>-Foam Floods. *SPE International Symposium on Oilfield Chemistry*. <http://doi.org/10.2118/37221-MS>
- [36] Turta, A., & Singhal, A. (2002). Field Foam Applications in Enhanced Oil Recovery Projects: Screening and Design Aspects. *Journal of Canadian Petroleum Technology*, 41(10). <http://doi.org/10.2118/02-10-14>

[37] Yan, W. (2006). Foam for Mobility Control on Alkaline/Surfactant/ Enhanced Oil Recovery Process. PhD Dissertation, Rice University, Houston, Texas, USA.

[38] Zhdanov, S., Amiyani, A., Surguchev, L. M., Castanier, L. M., & Hanssen, J. E. (1996). Application of foam for gas and water shut-off: review of field experience. *SPE European Petroleum Conference*, (SPE 36914), 377–388. Retrieved from <http://www.onepetro.org/mslib/servlet/onepetroreview?id=00036914>

## APPENDIX-A

Table A-1 Fluorosurfactant FS-51 concentration and corresponding measured IFT

<b>Surfactant Concentration</b>	<b>IFT</b>
<b>Vol %</b>	<b>mN/m</b>
0.00	14.17
0.05	3.00
0.10	2.00
0.15	2.07
0.20	2.30
0.30	2.00

Table A-2 AOS surfactant concentration and corresponding measured IFT

<b>Surfactant Concentration</b>	<b>IFT</b>
<b>Vol %</b>	<b>mN/m</b>
0	14.2
0.15	9.8
0.3	5.6
0.5	5.2
0.75	5.5
1	5.5

Table A-3 Witcolate surfactant concentration and corresponding measured IFT

<b>Surfactant Concentration</b>	<b>IFT</b>
<b>Vol %</b>	<b>mN/m</b>
0.0000	14.2
0.0125	3.7
0.0250	2.3
0.0500	2.6
0.0750	2.7

Table A-4 Average steady-state  $\Delta P$  values (in psi) for foam-flooding of fluorosurfactant FS-51

Experiment #	Foam Quality	Proportion of N <sub>2</sub>				
		0% N <sub>2</sub>	5% N <sub>2</sub>	10% N <sub>2</sub>	15% N <sub>2</sub>	20% N <sub>2</sub>
<b>1</b>	<b>0.70</b>	55.016	88.001	98.255	111.354	138.275
<b>2</b>	<b>0.80</b>	125.031	138.015	150.254	158.543	166.442
<b>3</b>	<b>0.90</b>	125.251	138.095	150.046	139.545	144.145
<b>4</b>	<b>0.95</b>	29.780	34.564	34.345	34.502	35.549

Table A-5 Average steady-state  $\Delta P$  values (in psi) for foam-flooding of AOS

Experiment #	Foam Quality	Proportion of N <sub>2</sub>				
		0% N <sub>2</sub>	5% N <sub>2</sub>	10% N <sub>2</sub>	15% N <sub>2</sub>	20% N <sub>2</sub>
<b>1</b>	<b>0.70</b>	120.101	143.514	155.245	165.288	180.348
<b>2</b>	<b>0.80</b>	180.031	195.124	208.501	219.312	231.558
<b>3</b>	<b>0.90</b>	235.484	245.148	251.798	254.227	260.989
<b>4</b>	<b>0.95</b>	100.247	103.177	105.897	106.878	108.774

Table A-6 Average steady-state  $\Delta P$  values (in psi) for foam-flooding of witcolate

Foam Quality	Proportion of N <sub>2</sub>				
	0% N <sub>2</sub>	5% N <sub>2</sub>	10% N <sub>2</sub>	15% N <sub>2</sub>	20% N <sub>2</sub>
<b>0.70</b>	50.010	50.544	50.104	51.188	52.812
<b>0.80</b>	51.848	51.487	52.778	52.354	51.467
<b>0.90</b>	52.115	52.055	52.845	52.074	52.871
<b>0.95</b>	49.484	49.149	49.197	50.211	50.978



Table A-7 Average circularity of foam bubbles with fluorosurfactant FS-51

Foam Quality	Proportion of N <sub>2</sub>				
	0% N <sub>2</sub>	5% N <sub>2</sub>	10% N <sub>2</sub>	15% N <sub>2</sub>	20% N <sub>2</sub>
<b>0.70</b>	0.039	0.105	0.909	0.870	0.890
<b>0.80</b>	0.431	0.921	0.885	0.919	0.89
<b>0.90</b>	0.665	0.867	0.85	0.887	0.874
<b>0.95</b>	0.559	0.783	0.859	0.907	0.892

Table A-8 Average circularity of foam bubbles with AOS

Foam Quality	Proportion of N <sub>2</sub>				
	0% N <sub>2</sub>	5% N <sub>2</sub>	10% N <sub>2</sub>	15% N <sub>2</sub>	20% N <sub>2</sub>
<b>0.70</b>	0.035	0.889	0.864	0.884	0.866
<b>0.80</b>	0.237	0.91	0.835	0.891	0.92
<b>0.90</b>	0.884	0.853	0.859	0.909	0.907
<b>0.95</b>	0.028	0.552	0.613	0.424	0.531

## APPENDIX-B

The enlarged shapes of drops of fluorosurfactant FS-51 solutions at various concentrations are shown below in the following figures:



Figure B.1: Shape of distilled water drop in CO<sub>2</sub> (0% surfactant) at 1500 psi and 50°C



Figure B.2: Shape of 0.05 vol% fluorosurfactant FS-51 in CO<sub>2</sub> at 1500 psi and 50°C



Figure B.3: Shape of 0.10 vol% fluorosurfactant FS-51 in CO<sub>2</sub> at 1500 psi and 50°C



Figure B.4: Shape of 0.15 vol% fluorosurfactant FS-51 in CO<sub>2</sub> at 1500 psi and 50°C



Figure B.5: Shape of 0.20 vol% fluorosurfactant FS-51 in CO<sub>2</sub> at 1500 psi and 50°C



Figure B.6: Shape of 0.30 vol% fluorosurfactant FS-51 in CO<sub>2</sub> at 1500 psi and 50°C

The enlarged shapes of drops of AOS surfactant solutions at various concentrations are shown below in the following figures:

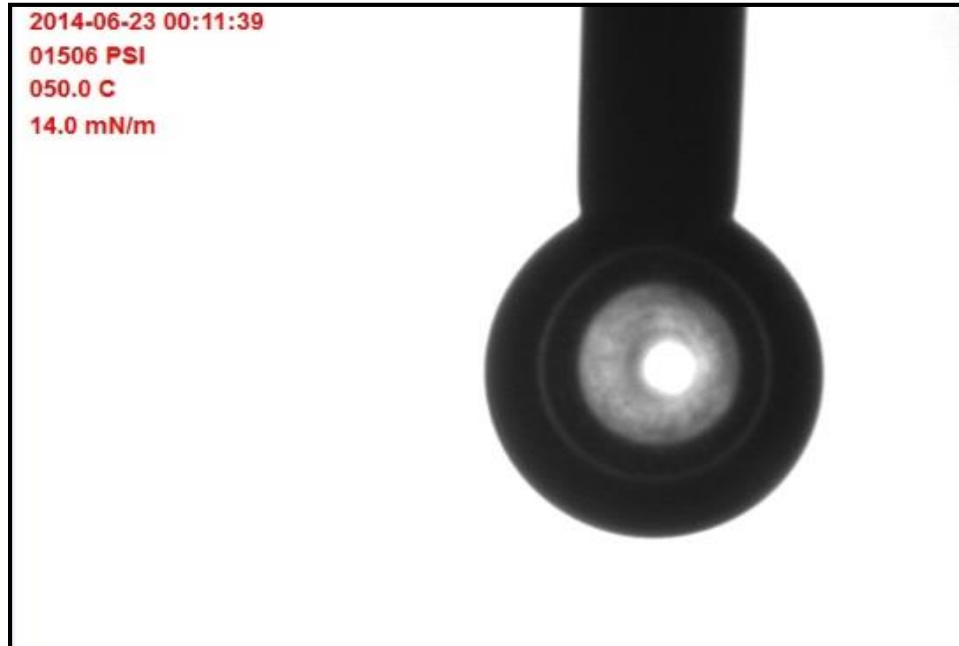


Figure B.7: Shape of distilled water drop in CO<sub>2</sub> (0% surfactant) at 1500 psi and 50°C



Figure B.8: Shape of 0.15 vol% AOS in CO<sub>2</sub> at 1500 psi and 50°C

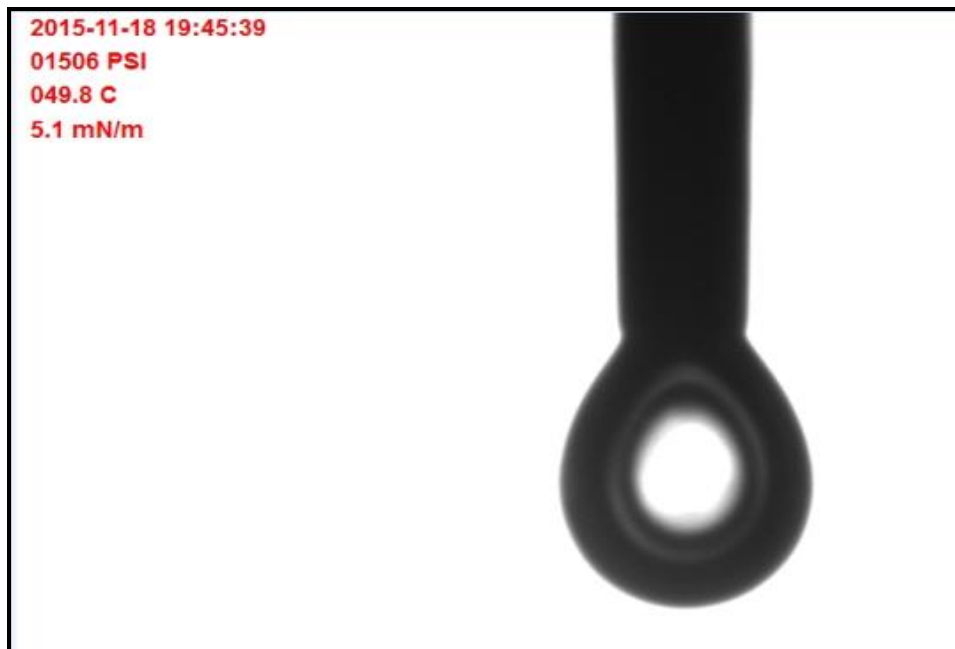


Figure B.9: Shape of 0.30 vol% AOS in CO<sub>2</sub> at 1500 psi and 50°C



Figure B.10: Shape of 0.50 vol% AOS in CO<sub>2</sub> at 1500 psi and 50°C



Figure B.11: Shape of 0.75 vol% AOS in CO<sub>2</sub> at 1500 psi and 50°C

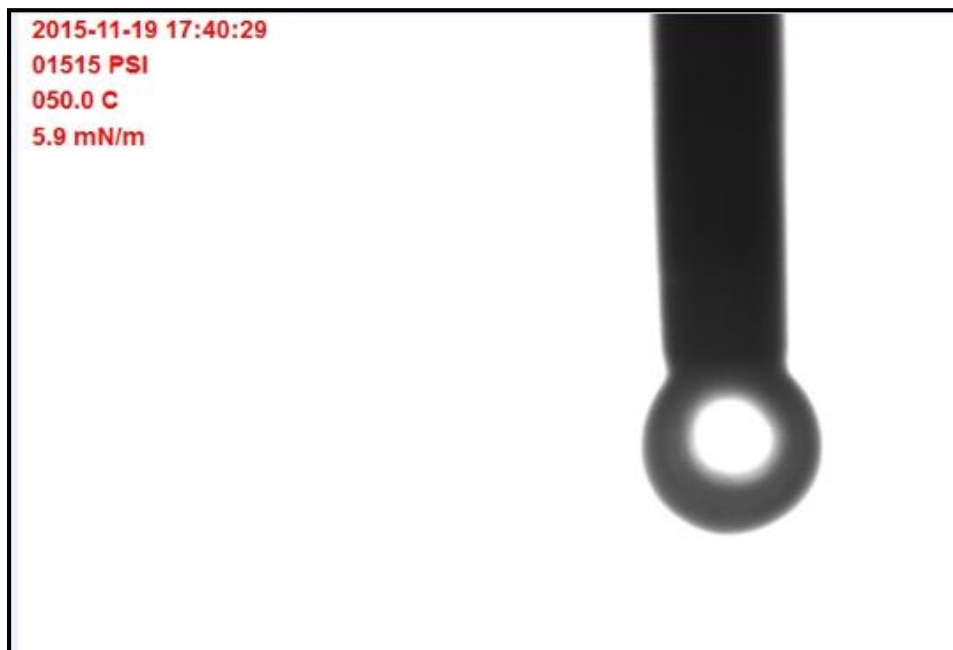


Figure B.12: Shape of 1.0 vol% AOS in CO<sub>2</sub> at 1500 psi and 50°C

The enlarged shapes of drops of witcolate surfactant solutions at various concentrations are shown below in the following figures:



Figure B.13: Shape of distilled water drop in CO<sub>2</sub> (0% surfactant) at 1500 psi and 50°C



Figure B.14: Shape of 0.0125 vol% witcolate in CO<sub>2</sub> at 1500 psi and 50°C



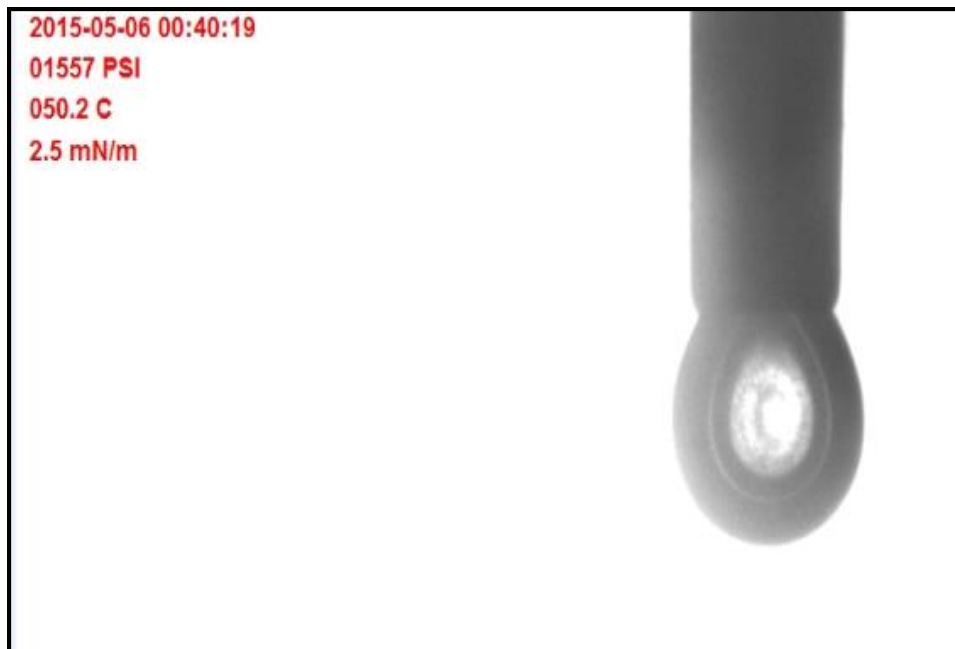


Figure B.15: Shape of 0.025 vol% witcolate in CO<sub>2</sub> at 1500 psi and 50°C



Figure B.16: Shape of 0.05 vol% witcolate in CO<sub>2</sub> at 1500 psi and 50°C

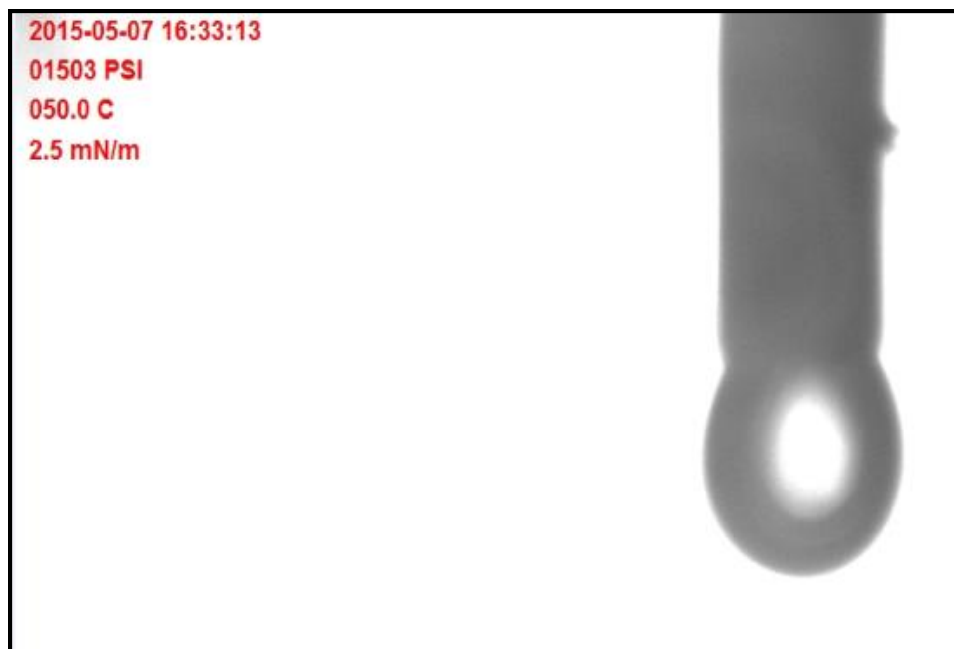


Figure B.17: Shape of 0.075 vol% witcolate in CO<sub>2</sub> at 1500 psi and 50°C

Enlarged foam images (8-bit analyzed images) captured during experiments 1, 2, 3 and 4 involving co-injection of 0.15 vol% fluorosurfactant, sc-CO<sub>2</sub> and N<sub>2</sub> are shown below:

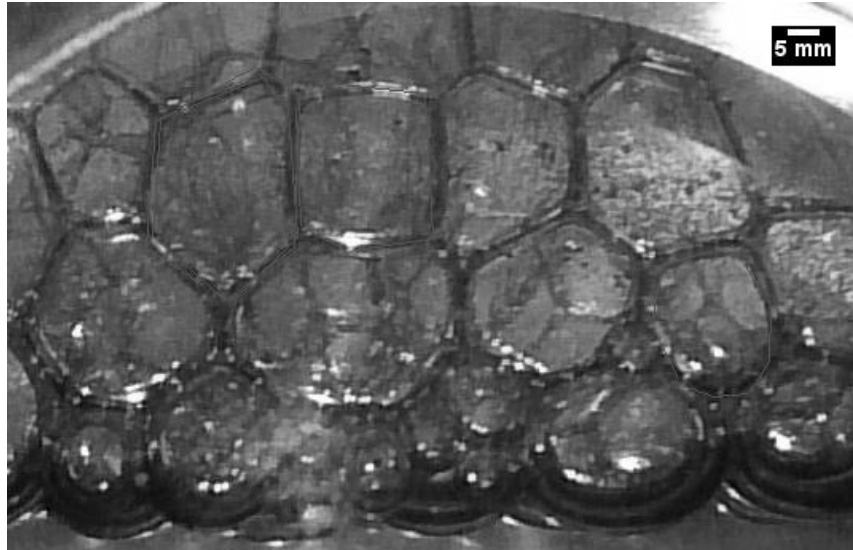


Figure B.18: 8-bit analyzed foam image using fluorosurfactant FS-51 for foam quality 0.70 and 0% N<sub>2</sub>

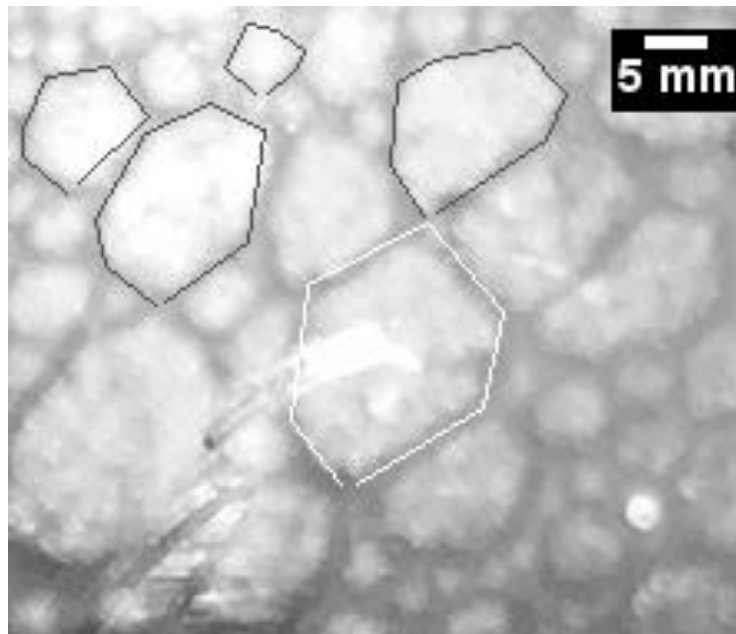


Figure B.19: 8-bit analyzed foam image using fluorosurfactant FS-51 for foam quality 0.70 and 5% N<sub>2</sub>

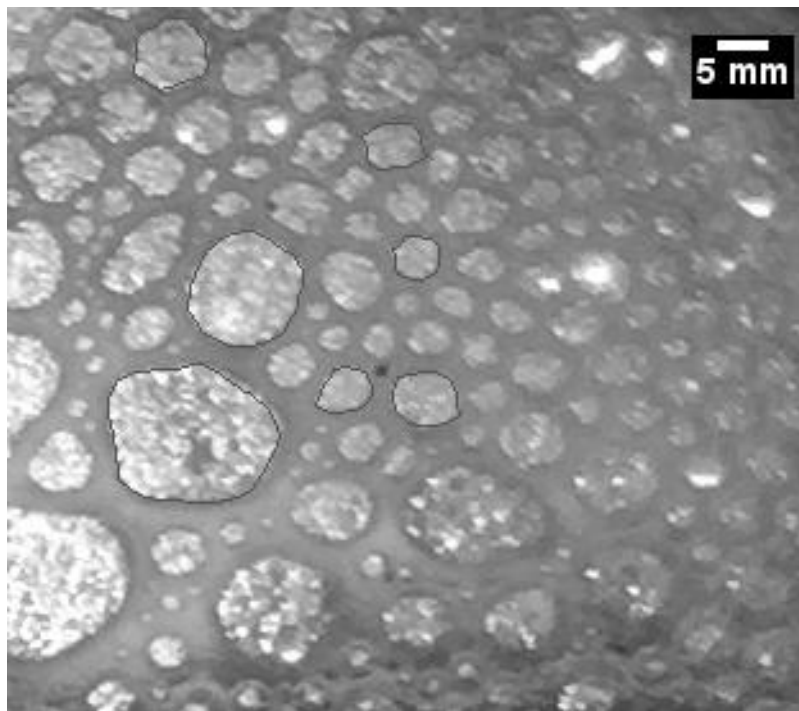


Figure B.20: 8-bit analyzed foam image using fluorosurfactant FS-51 for foam quality 0.70 and 10% N<sub>2</sub>

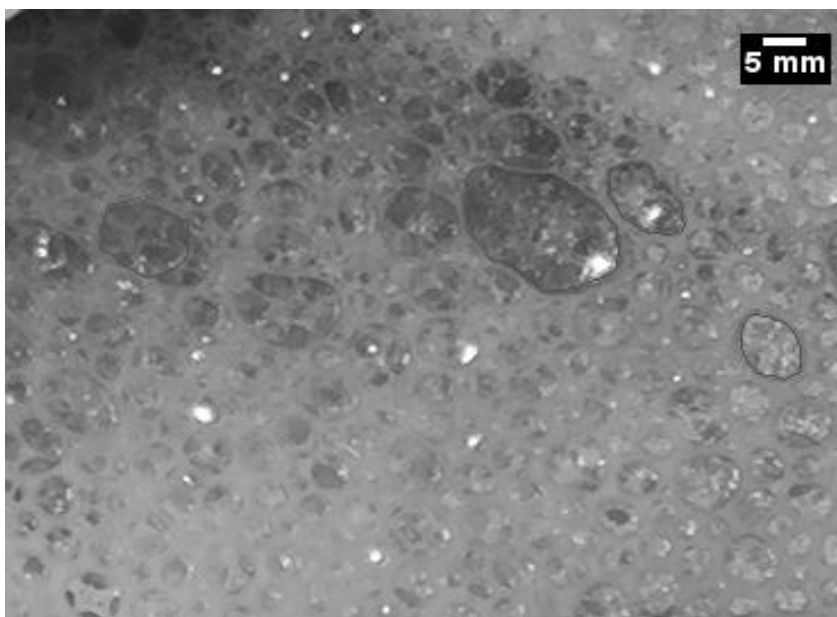


Figure B.21: 8-bit analyzed foam image using fluorosurfactant FS-51 for foam quality 0.70 and 15% N<sub>2</sub>

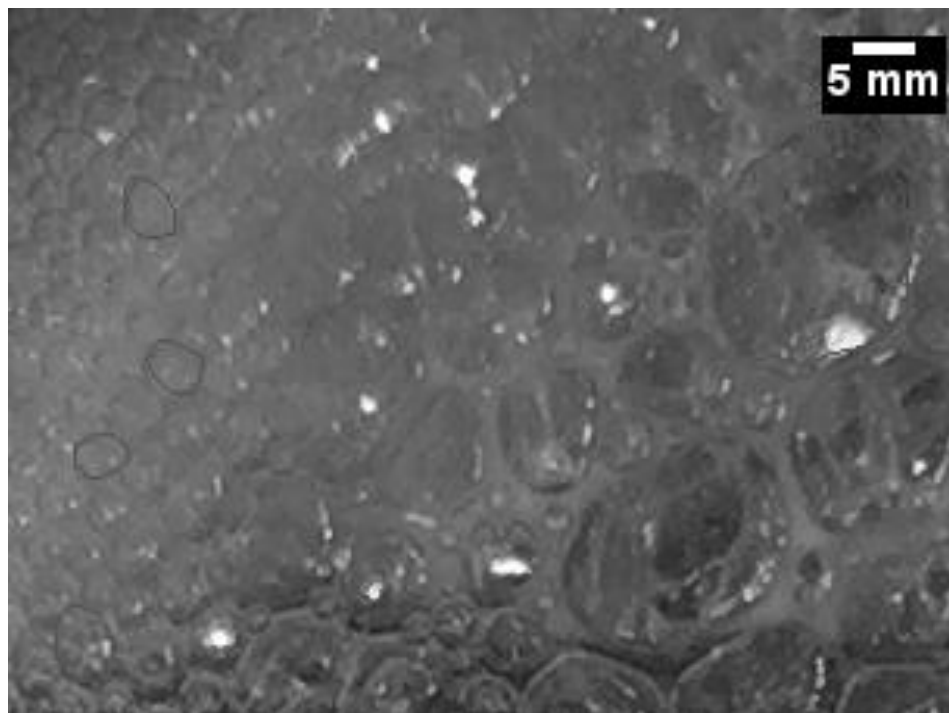


Figure B.22: 8-bit analyzed foam image using fluorosurfactant FS-51 for foam quality  
0.70 and 20% N<sub>2</sub>

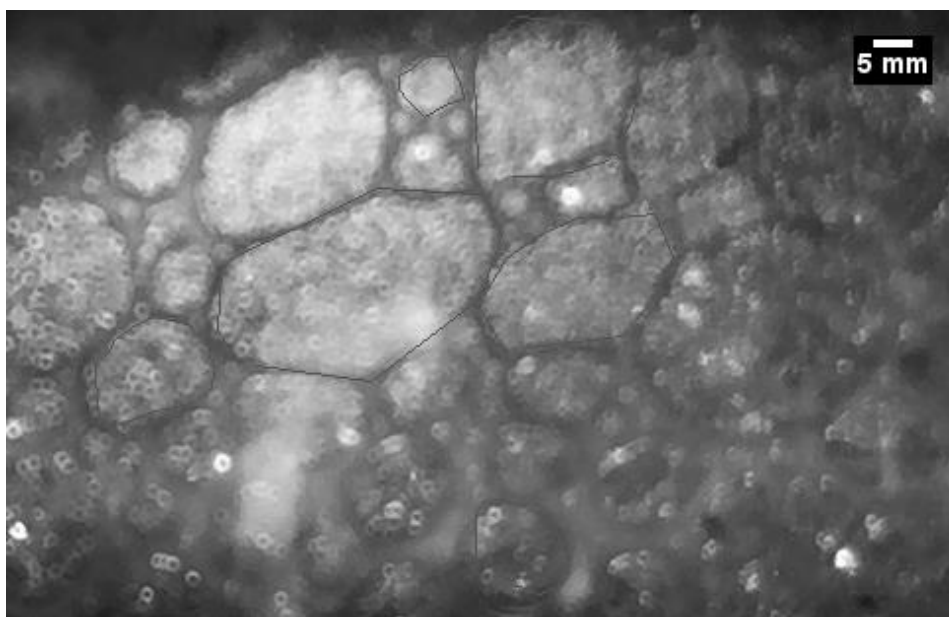


Figure B.23: 8-bit analyzed foam image using fluorosurfactant FS-51 for foam quality  
0.80 and 0% N<sub>2</sub>

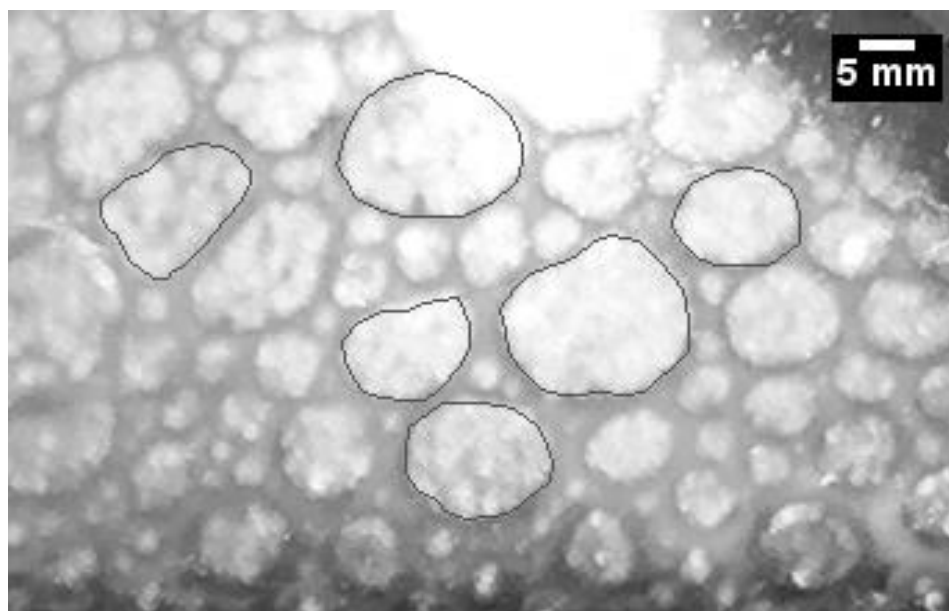


Figure B.24: 8-bit analyzed foam image using fluorosurfactant FS-51 for foam quality 0.80 and 5% N<sub>2</sub>

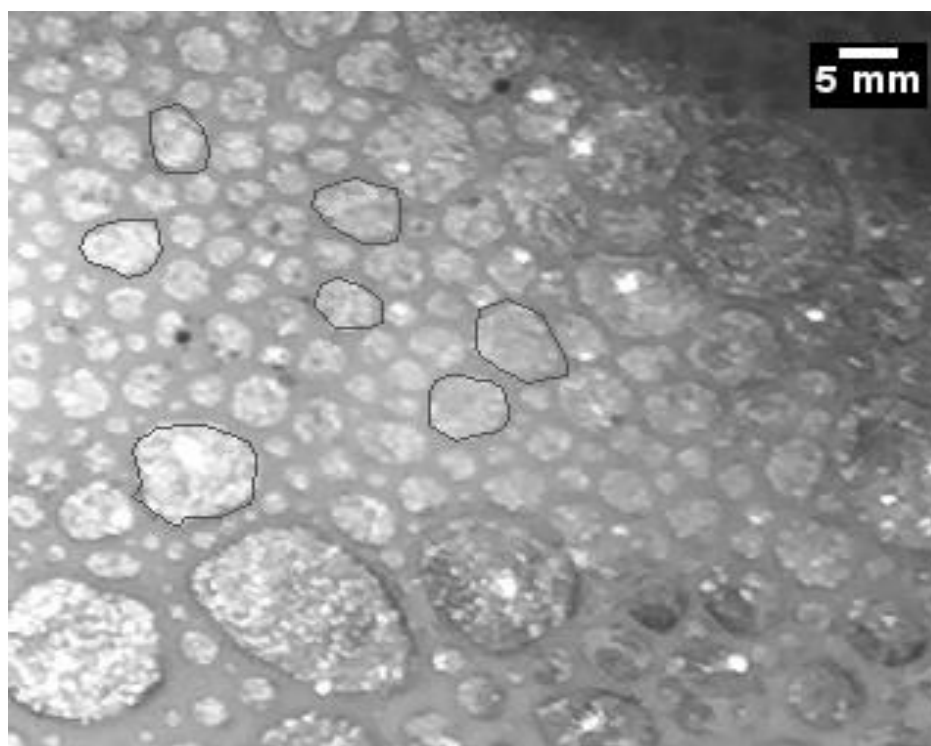


Figure B.25: 8-bit analyzed foam image using fluorosurfactant FS-51 for foam quality 0.80 and 10% N<sub>2</sub>

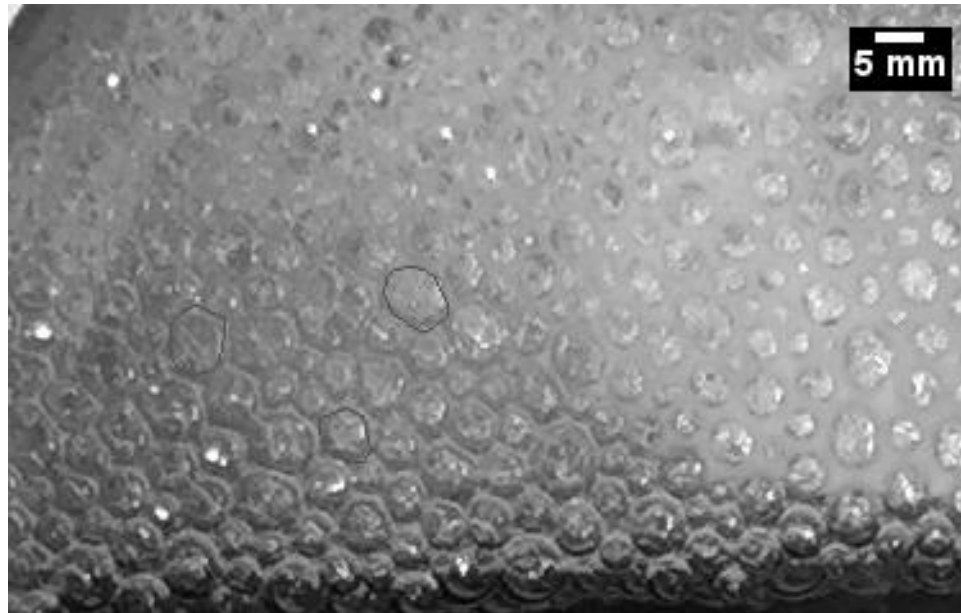


Figure B.26: 8-bit analyzed foam image using fluorosurfactant FS-51 for foam quality  
0.80 and 15% N<sub>2</sub>

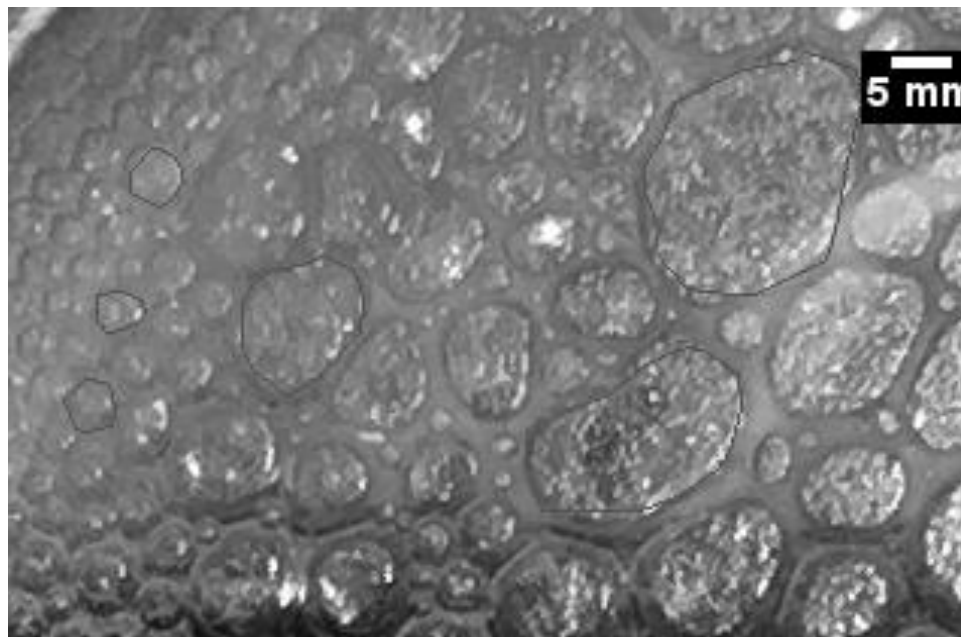


Figure B.27: 8-bit analyzed foam image using fluorosurfactant FS-51 for foam quality  
0.80 and 20% N<sub>2</sub>

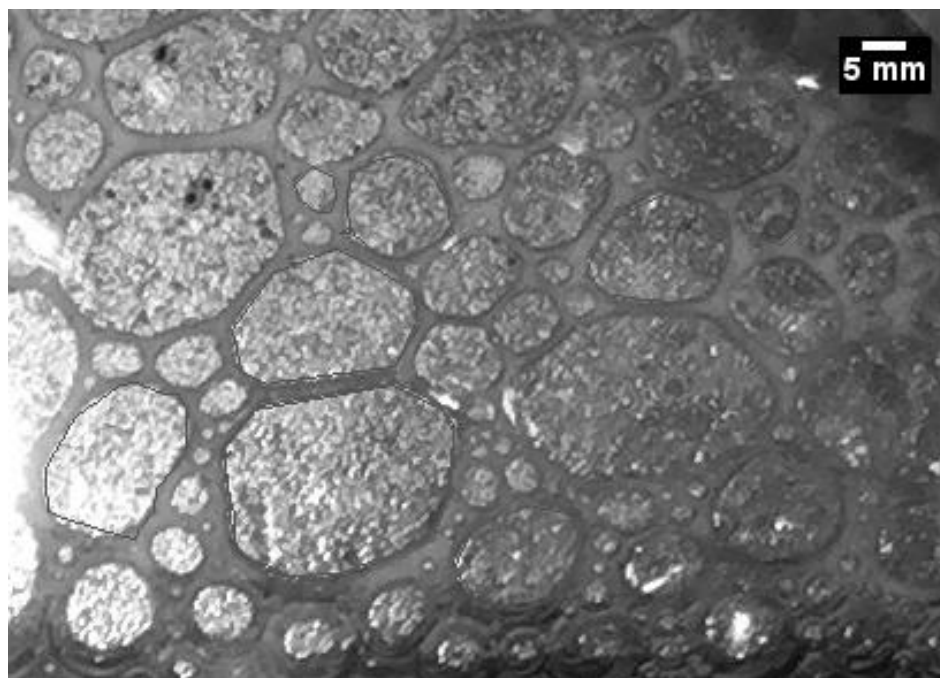


Figure B.28: 8-bit analyzed foam image using fluorosurfactant FS-51 for foam quality  
0.90 and 0% N<sub>2</sub>

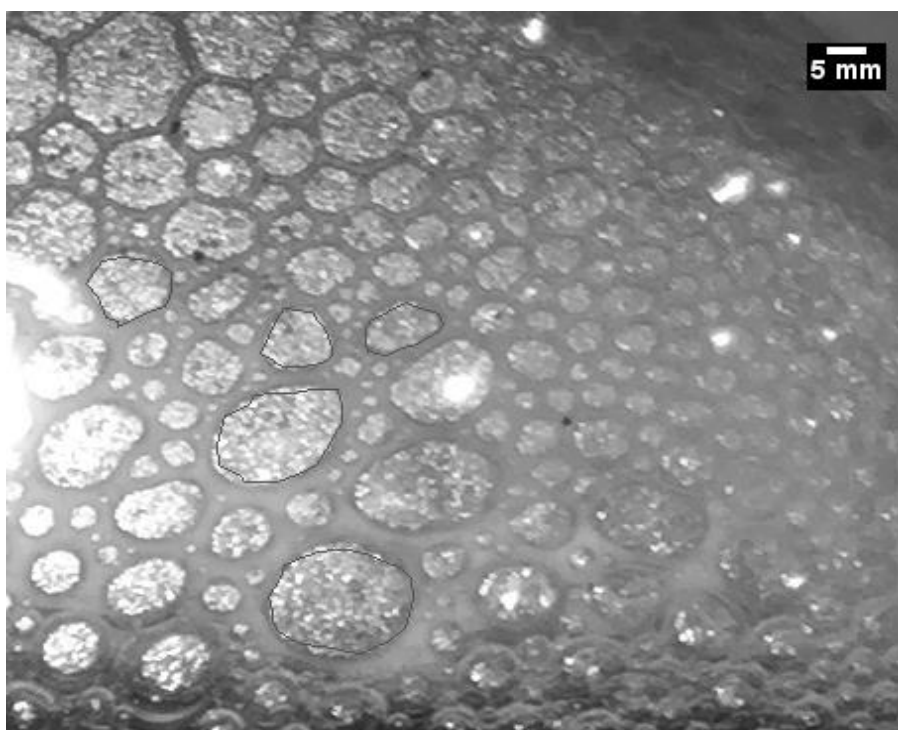


Figure B.29: 8-bit analyzed foam image using fluorosurfactant FS-51 for foam quality  
0.90 and 5% N<sub>2</sub>



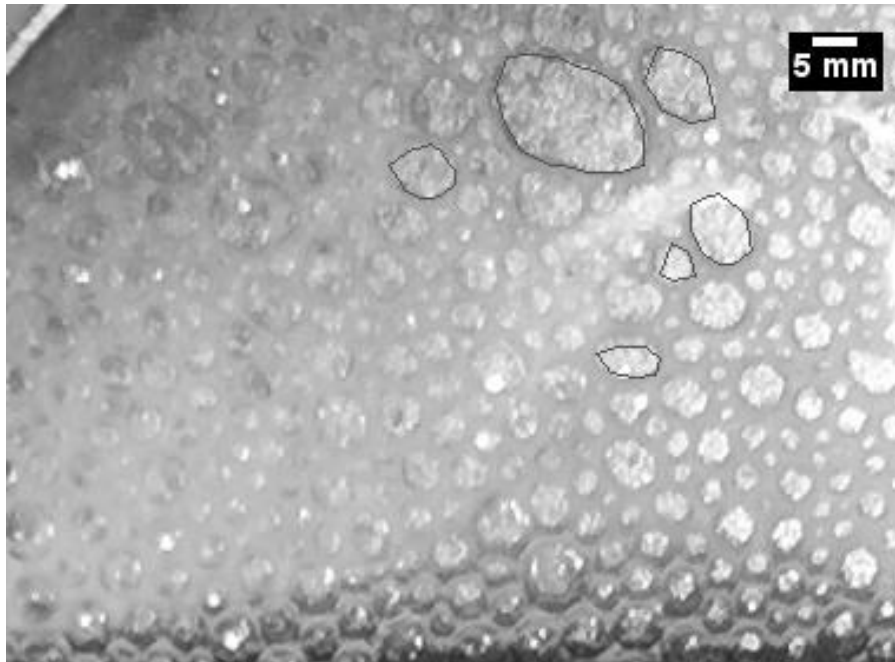


Figure B.30: 8-bit analyzed foam image using fluorosurfactant FS-51 for foam quality  
0.90 and 10% N<sub>2</sub>

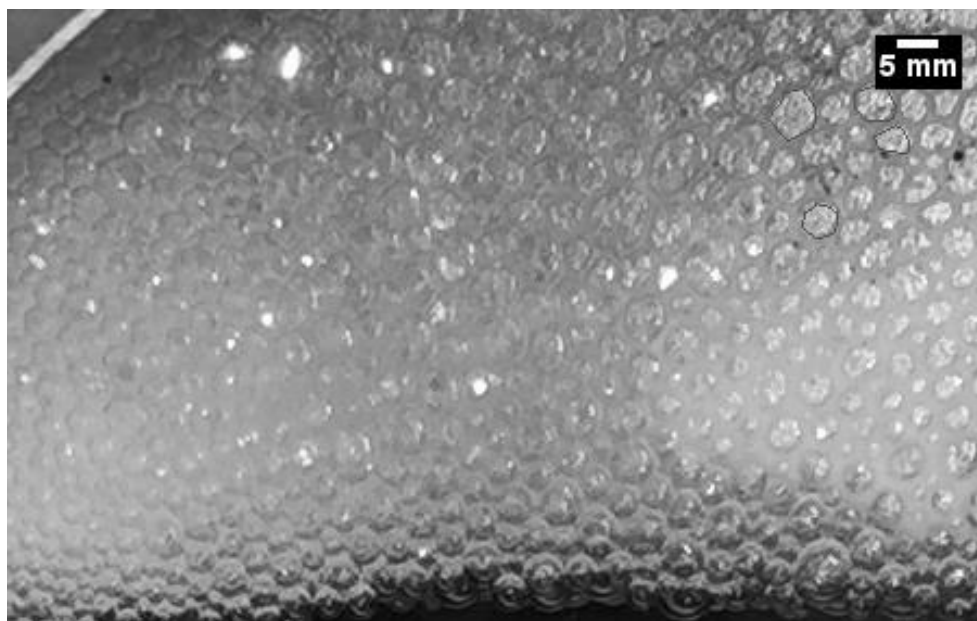


Figure B.31: 8-bit analyzed foam image using fluorosurfactant FS-51 for foam quality  
0.90 and 15% N<sub>2</sub>

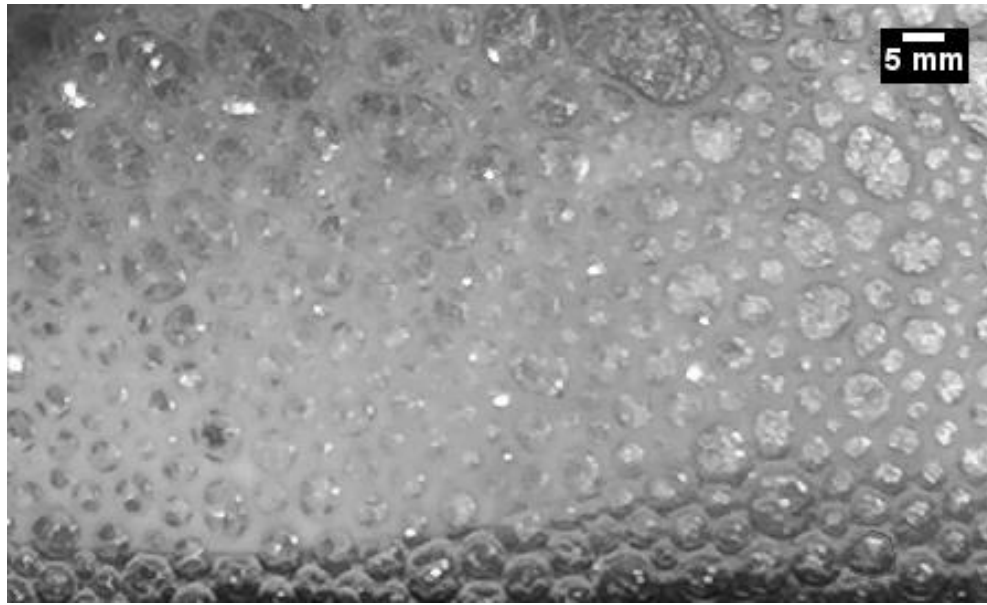


Figure B.32: 8-bit analyzed foam image using fluorosurfactant FS-51 for foam quality 0.90 and 20% N<sub>2</sub>

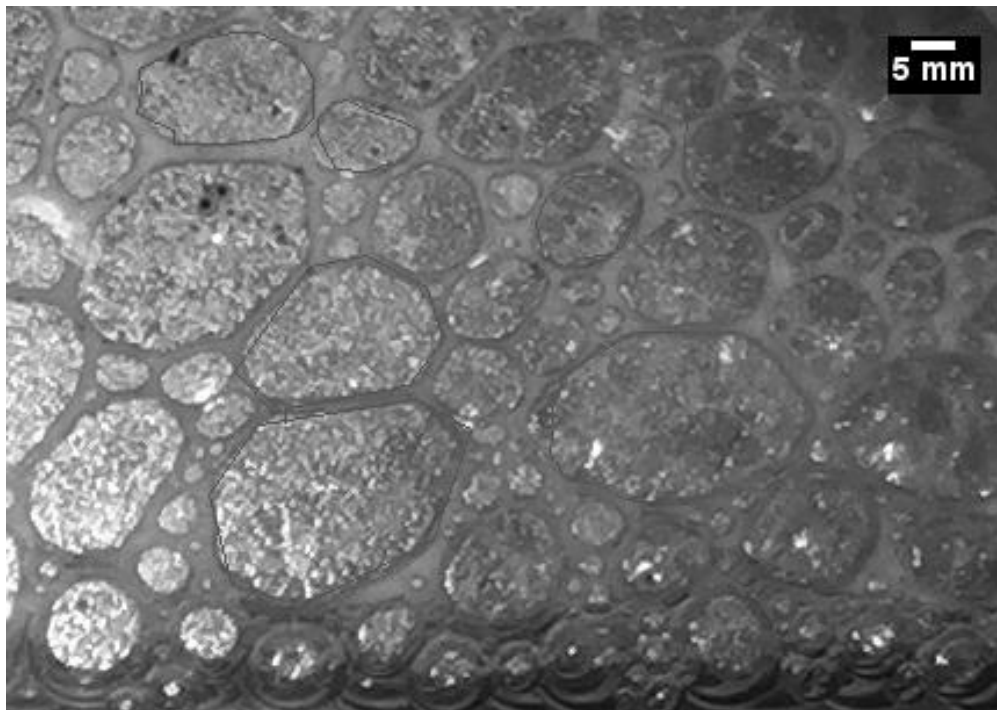


Figure B.33: 8-bit analyzed foam image using fluorosurfactant FS-51 for foam quality 0.95 and 0% N<sub>2</sub>

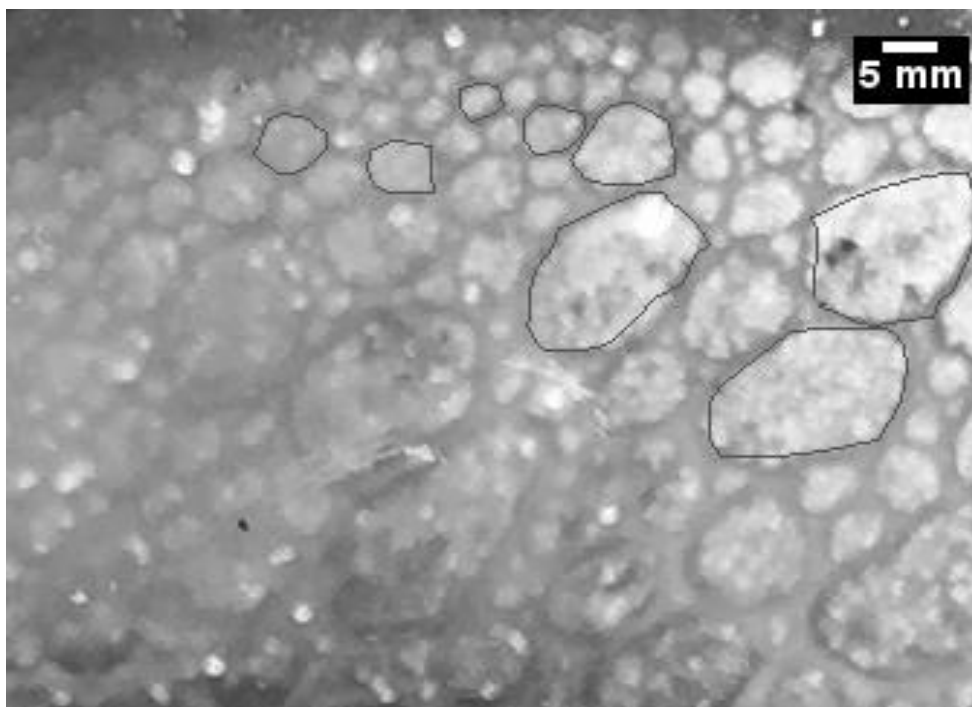


Figure B.34: 8-bit analyzed foam image using fluorosurfactant FS-51 for foam quality 0.95 and 5% N<sub>2</sub>

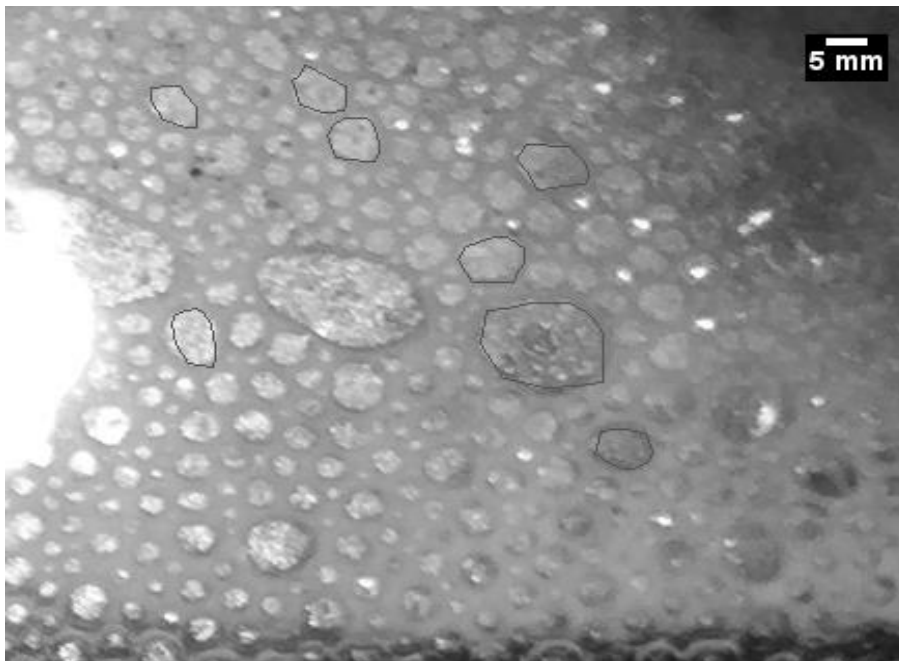


Figure B.35: 8-bit analyzed foam image using fluorosurfactant FS-51 for foam quality 0.95 and 10% N<sub>2</sub>

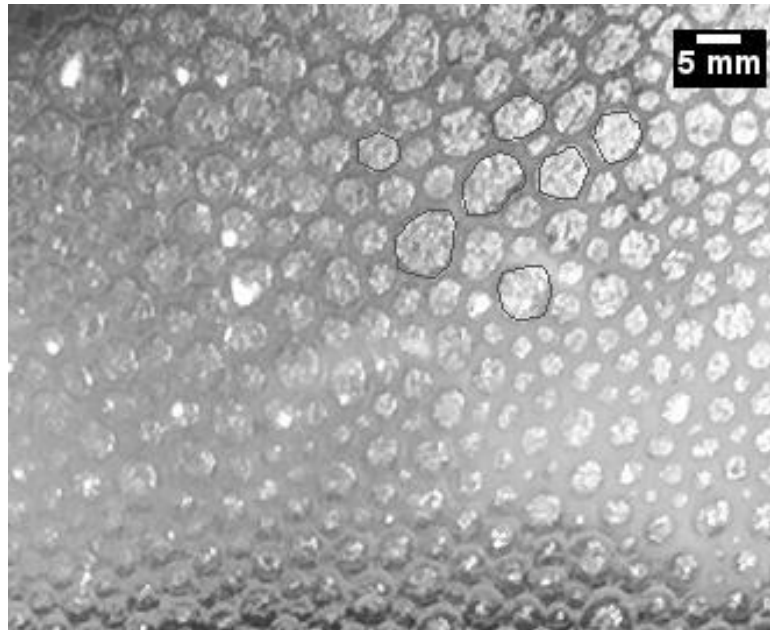


Figure B.36: 8-bit analyzed foam image using fluorosurfactant FS-51 for foam quality  
0.95 and 15% N<sub>2</sub>

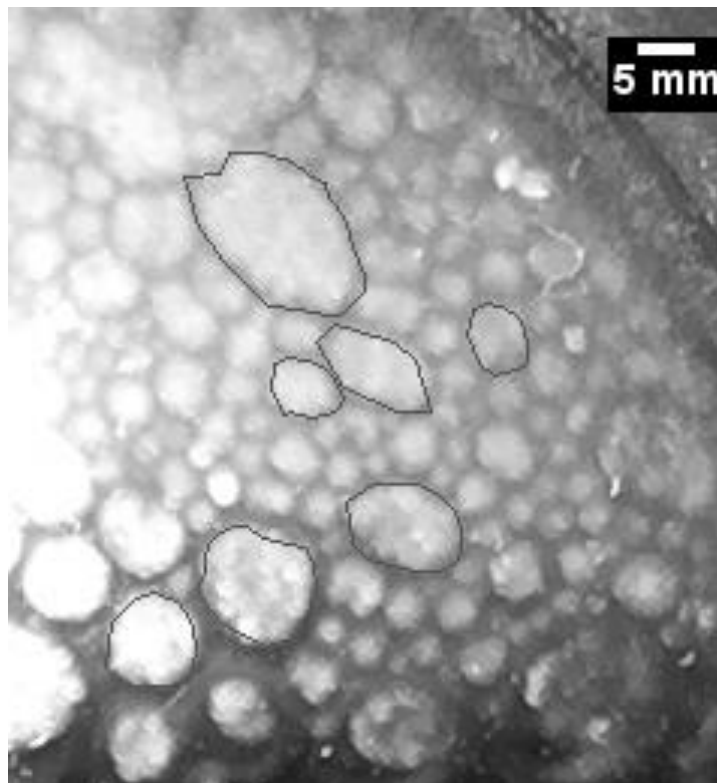


Figure B.37: 8-bit analyzed foam image using fluorosurfactant FS-51 for foam quality  
0.95 and 20% N<sub>2</sub>

Enlarged foam images (8-bit analyzed images) captured during experiments 5, 6, 7 and 8 involving co-injection of 0.5 vol% AOS, sc-CO<sub>2</sub> and N<sub>2</sub> are shown below:

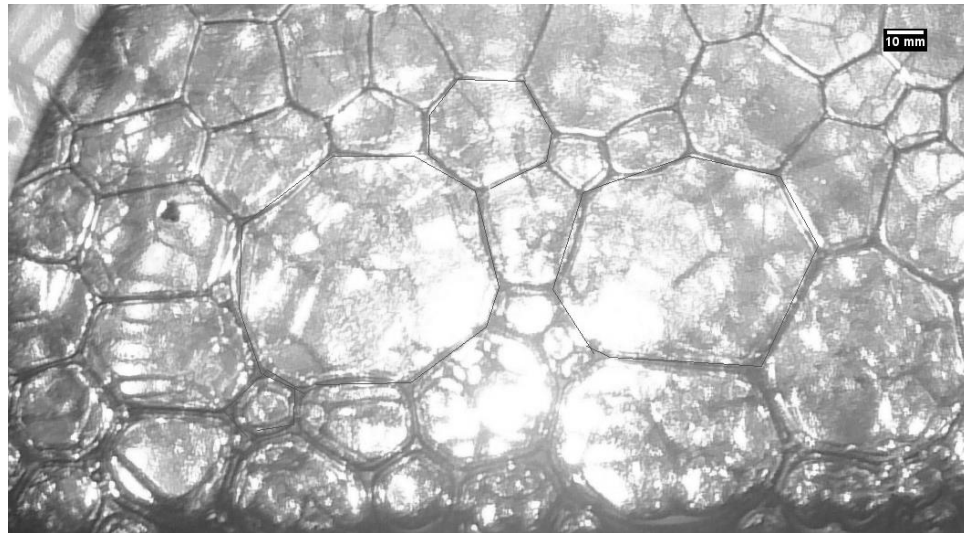


Figure B.38: 8-bit analyzed foam image using AOS surfactant for foam quality 0.70 and 0% N<sub>2</sub>

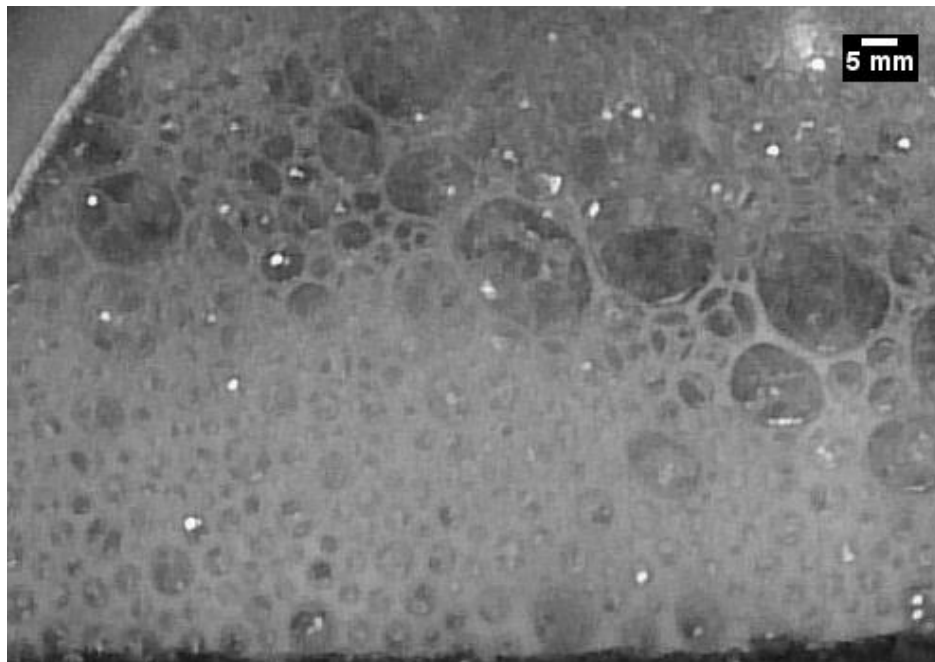


Figure B.39: 8-bit analyzed foam image using AOS surfactant for foam quality 0.70 and 5% N<sub>2</sub>

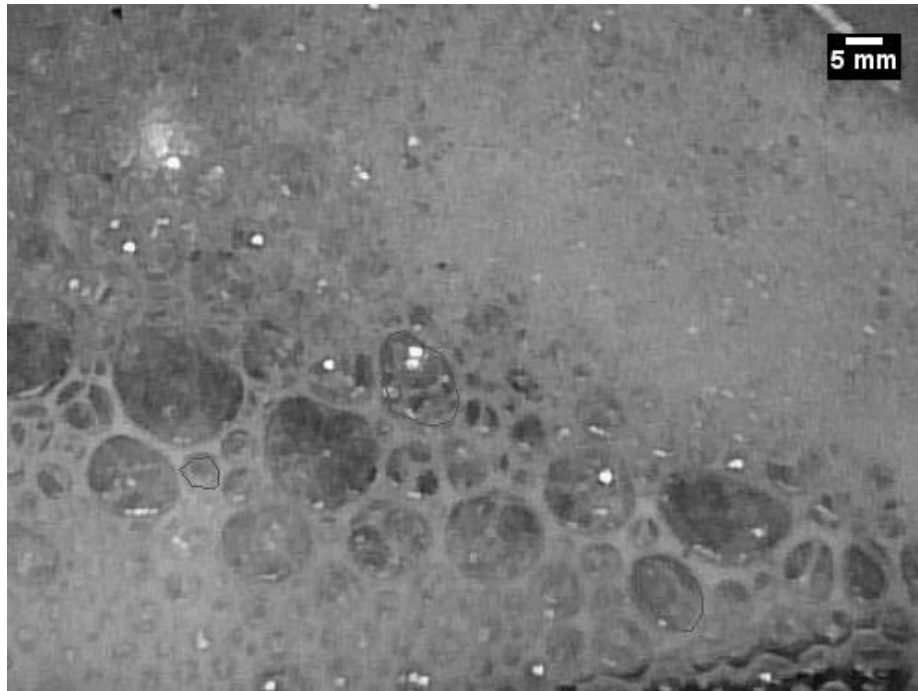


Figure B.40: 8-bit analyzed foam image using AOS surfactant for foam quality 0.70 and 10% N<sub>2</sub>

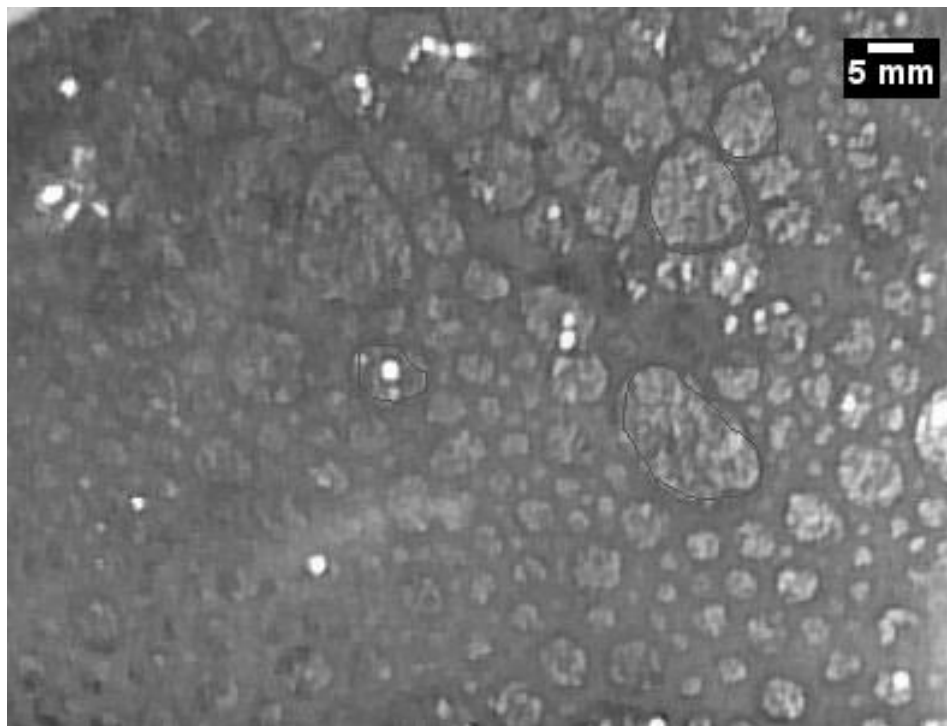


Figure B.41: 8-bit analyzed foam image using AOS surfactant for foam quality 0.70 and 15% N<sub>2</sub>

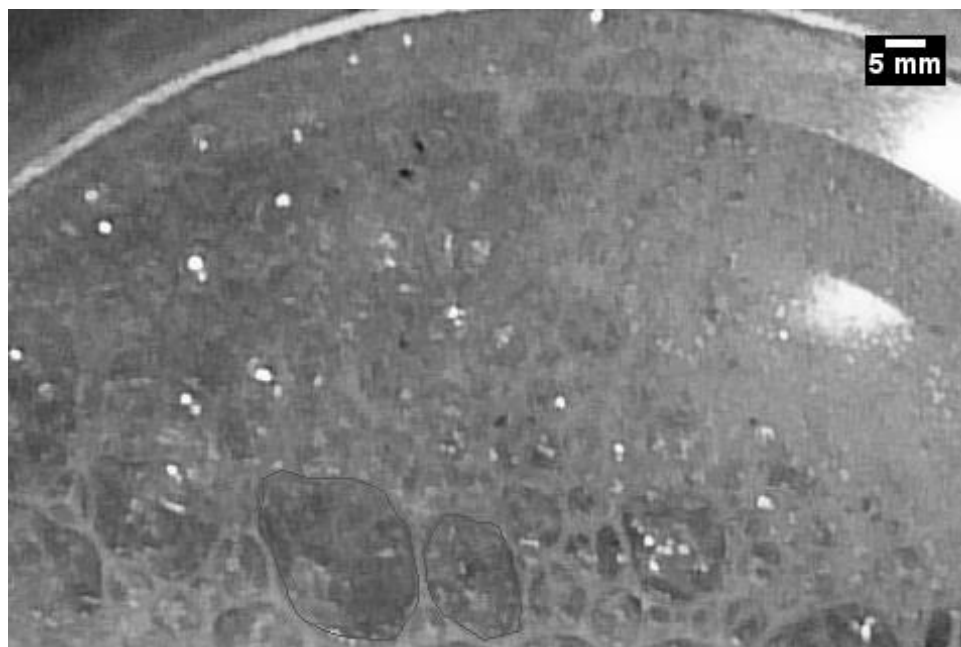


Figure B.42: 8-bit analyzed foam image using AOS surfactant for foam quality 0.70 and 20% N<sub>2</sub>

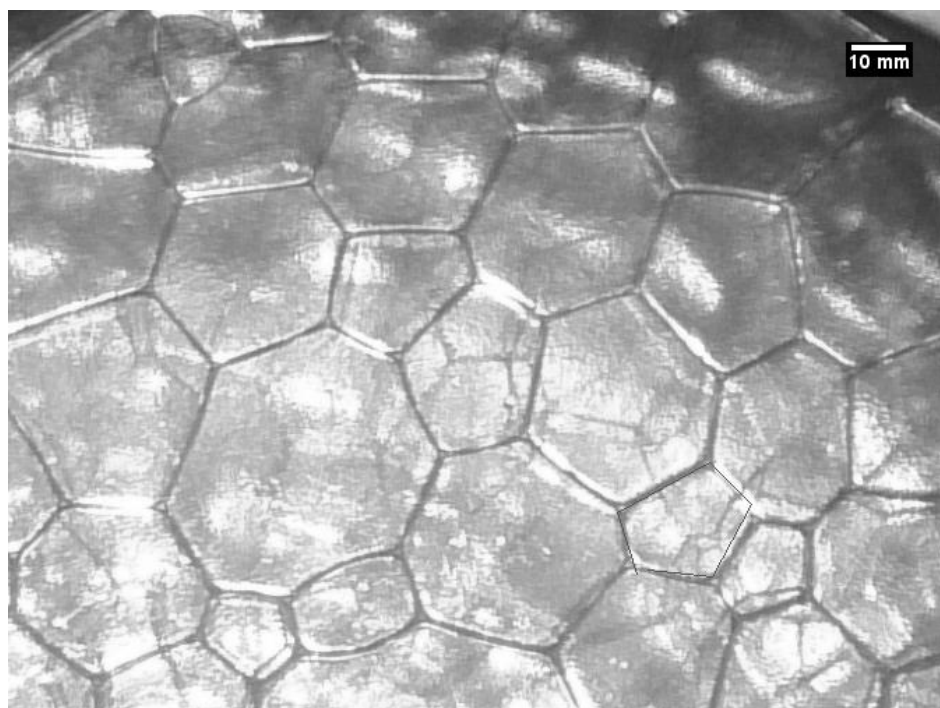


Figure B.43: 8-bit analyzed foam image using AOS surfactant for foam quality 0.80 and 0% N<sub>2</sub>

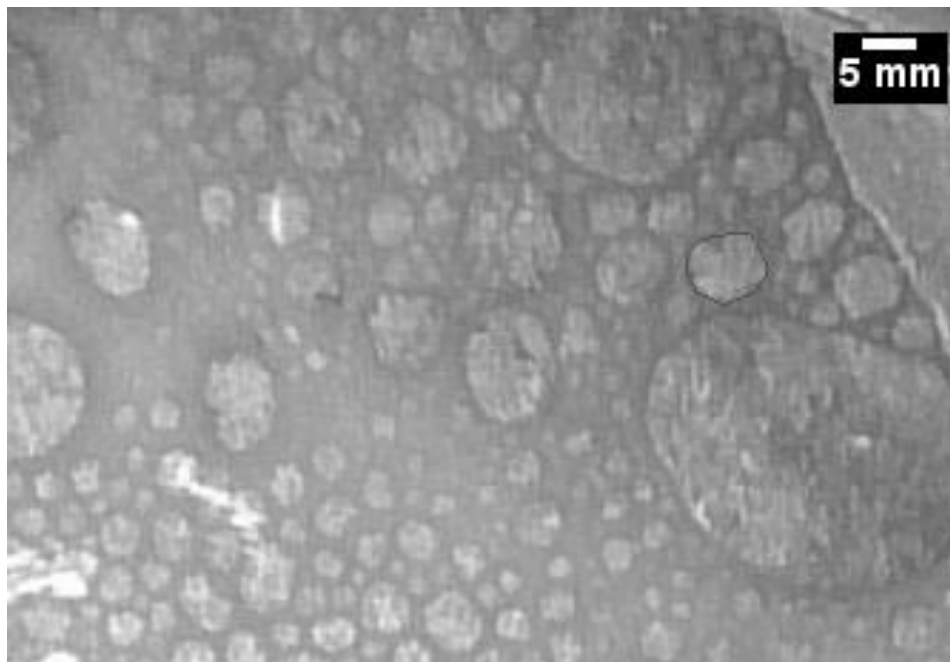


Figure B.44: 8-bit analyzed foam image using AOS surfactant for foam quality 0.80 and 5% N<sub>2</sub>

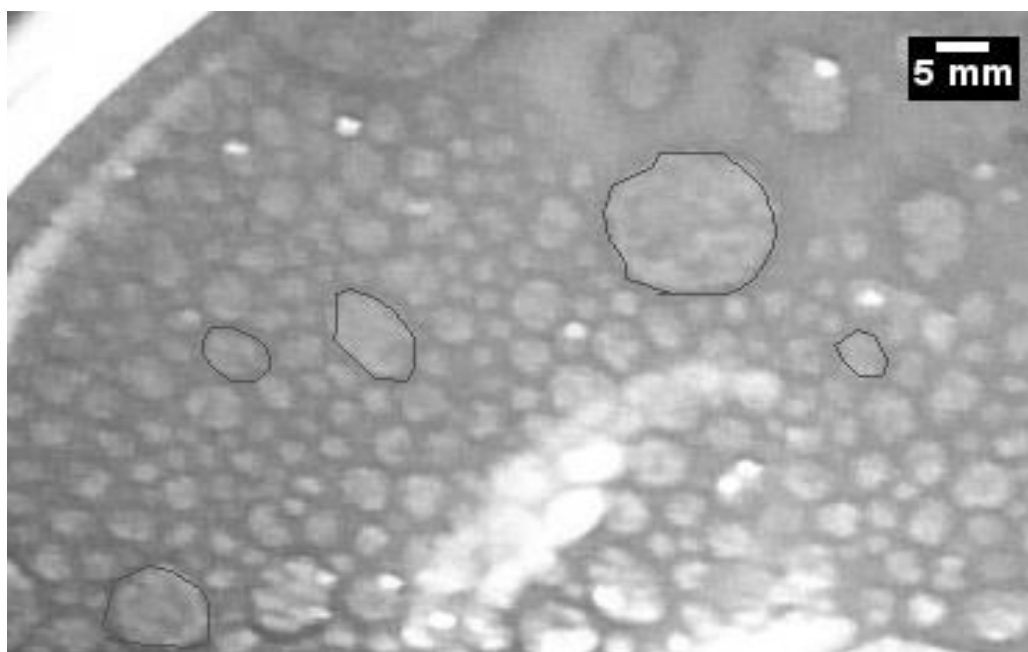


Figure B.45: 8-bit analyzed foam image using AOS surfactant for foam quality 0.80 and 10% N<sub>2</sub>



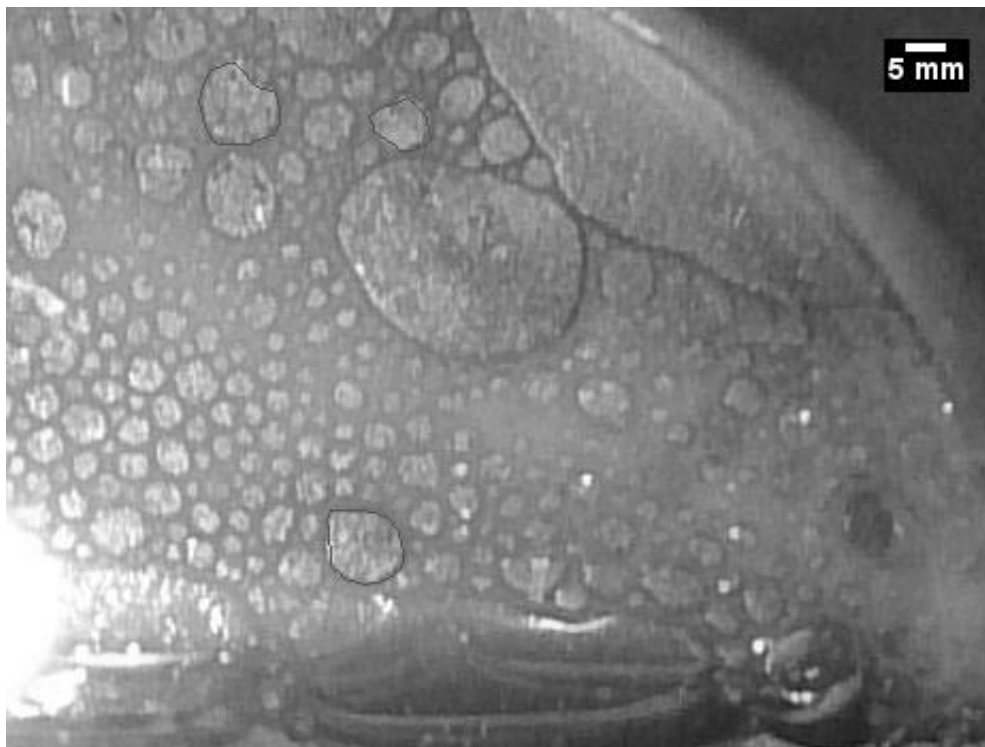


Figure B.46: 8-bit analyzed foam image using AOS surfactant for foam quality 0.80 and 15% N<sub>2</sub>

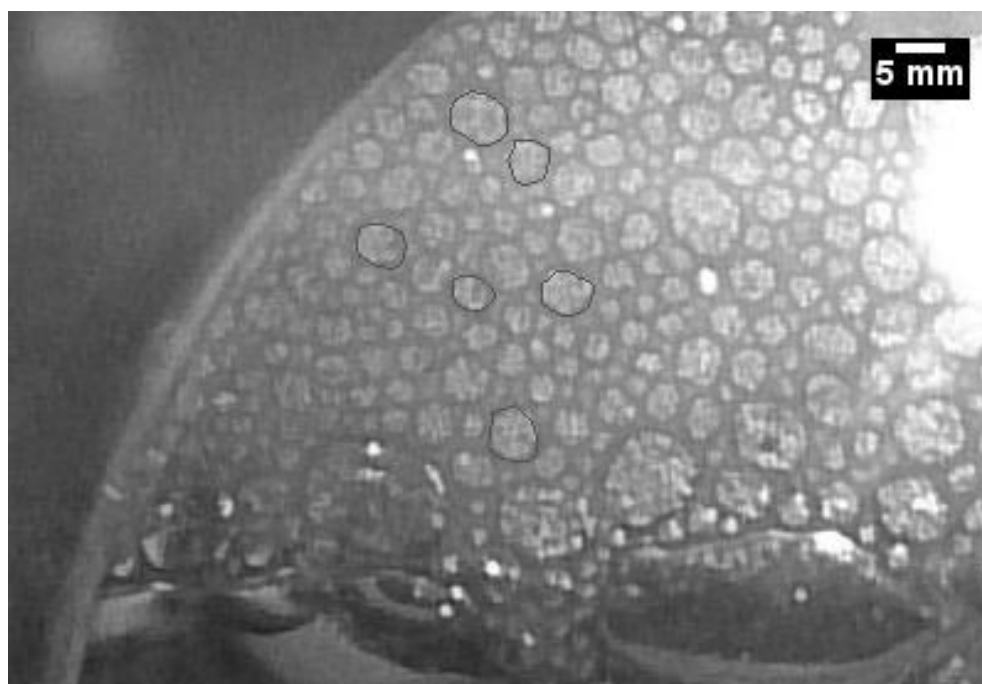


Figure B.47: 8-bit analyzed foam image using AOS surfactant for foam quality 0.80 and 20% N<sub>2</sub>

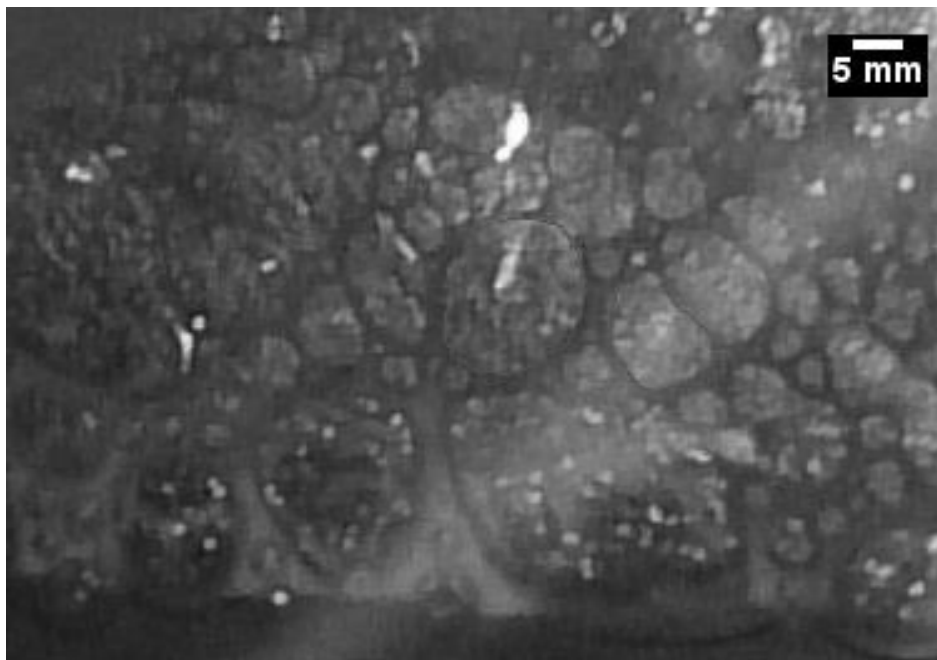


Figure B.48: 8-bit analyzed foam image using AOS surfactant for foam quality 0.90 and 0% N<sub>2</sub>

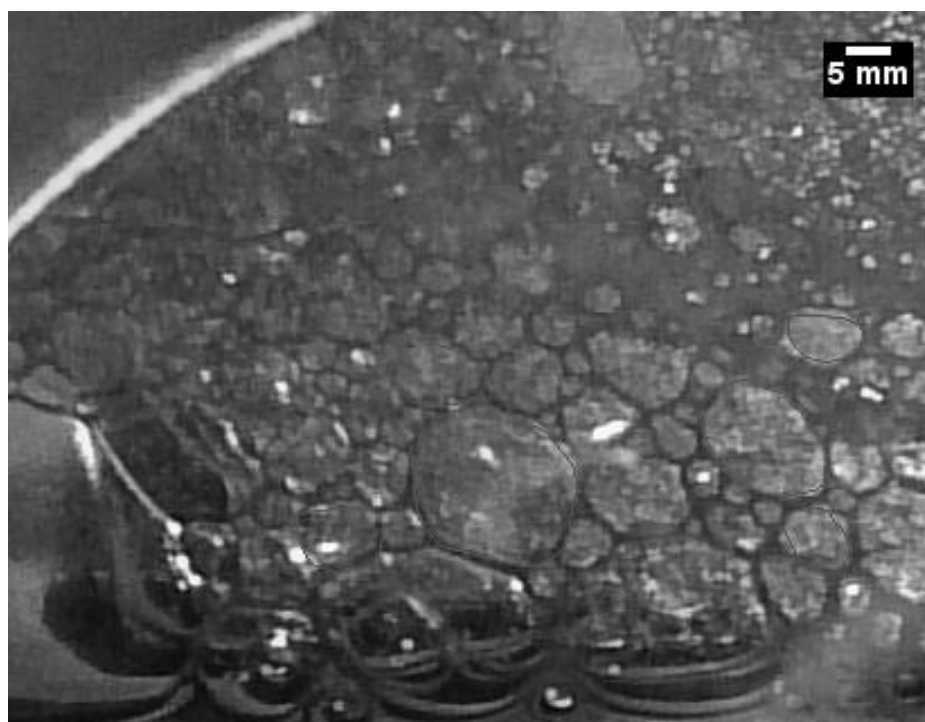


Figure B.49: 8-bit analyzed foam image using AOS surfactant for foam quality 0.90 and 5% N<sub>2</sub>



Figure B.50: 8-bit analyzed foam image using AOS surfactant for foam quality 0.90 and 10% N<sub>2</sub>



Figure B.51: 8-bit analyzed foam image using AOS surfactant for foam quality 0.90 and 15% N<sub>2</sub>

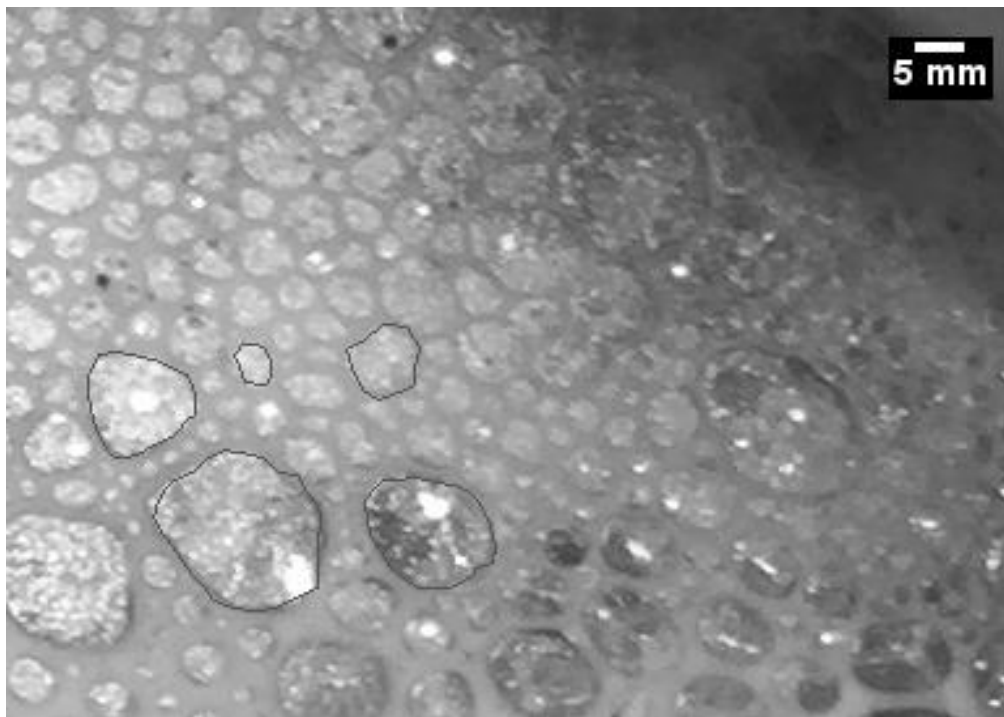


Figure B.52: 8-bit analyzed foam image using AOS surfactant for foam quality 0.90 and 20% N<sub>2</sub>

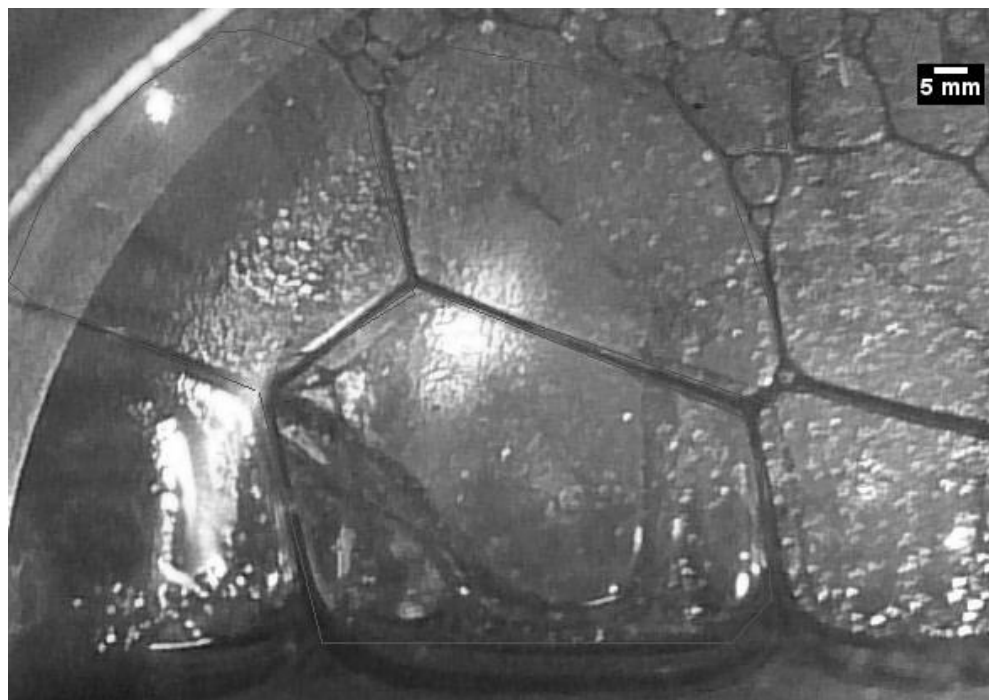


Figure B.53: 8-bit analyzed foam image using AOS surfactant for foam quality 0.95 and 0% N<sub>2</sub>

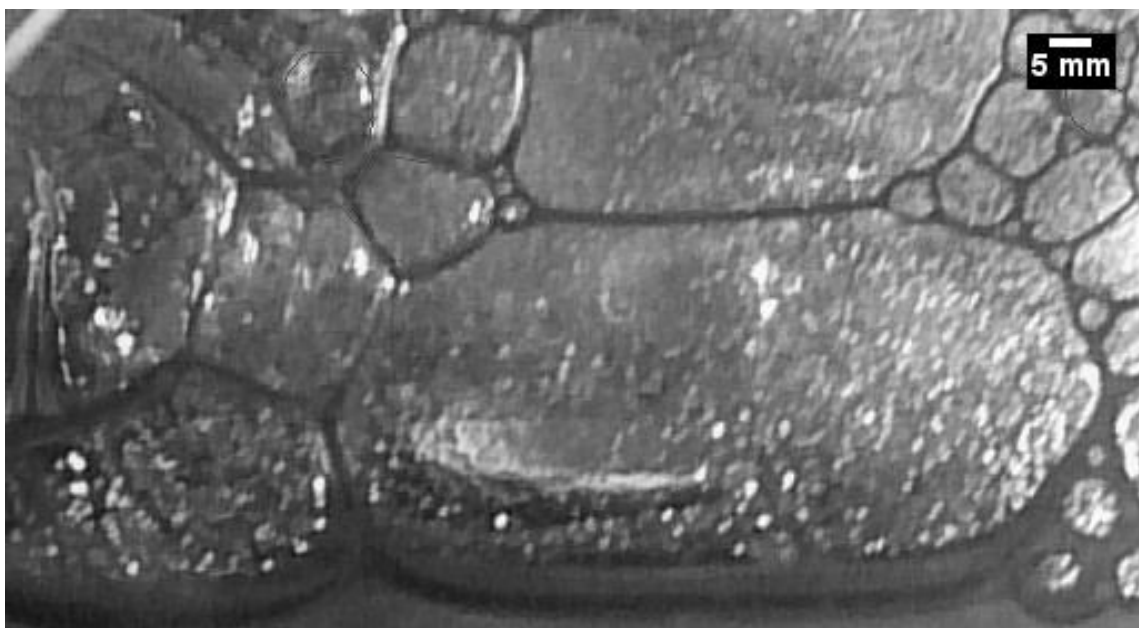


Figure B.54: 8-bit analyzed foam image using AOS surfactant for foam quality 0.95 and 5% N<sub>2</sub>

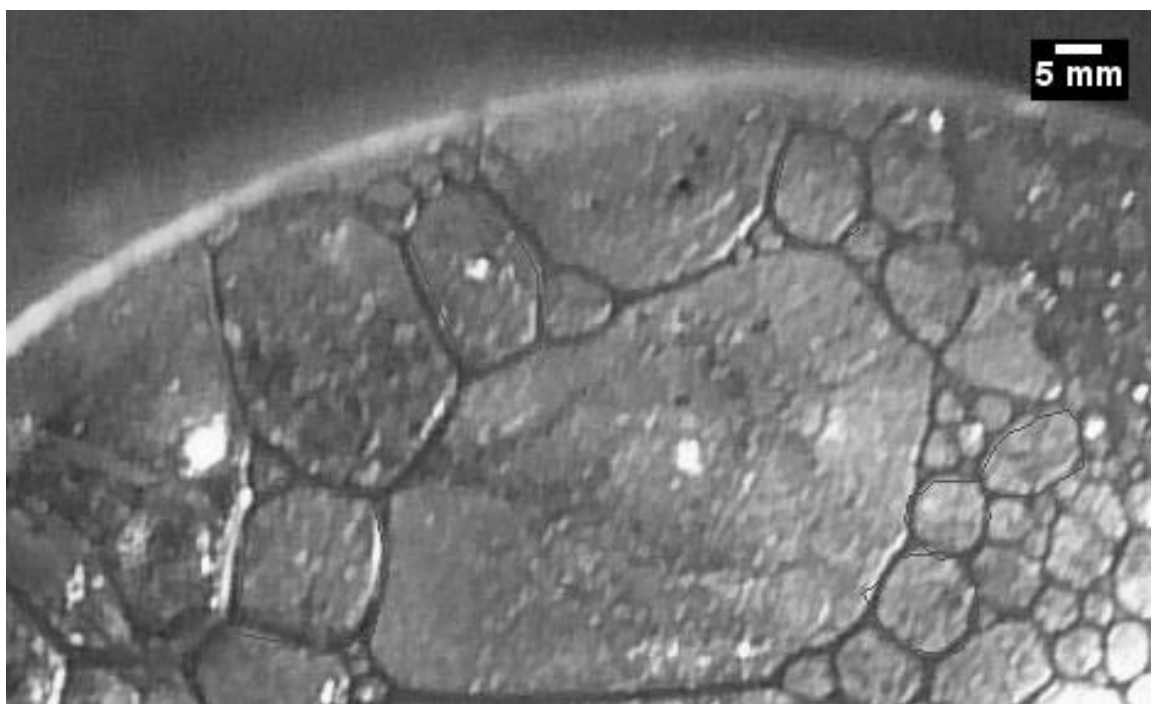


Figure B.55: 8-bit analyzed foam image using AOS surfactant for foam quality 0.95 and 10% N<sub>2</sub>

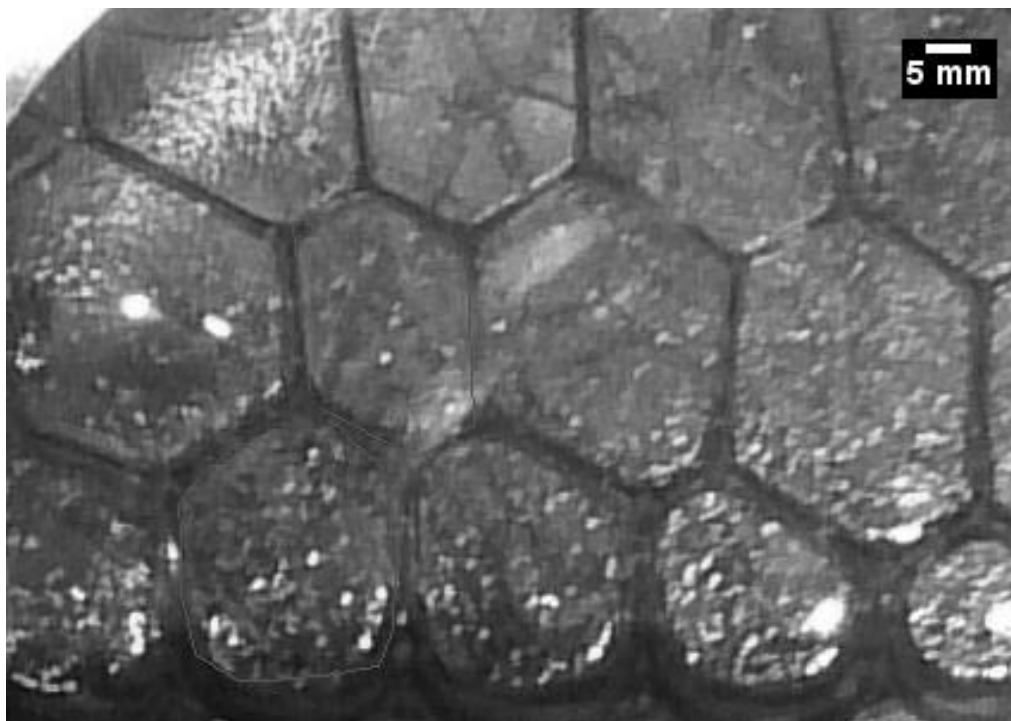


Figure B.56: 8-bit analyzed foam image using AOS surfactant for foam quality 0.95 and 15% N<sub>2</sub>

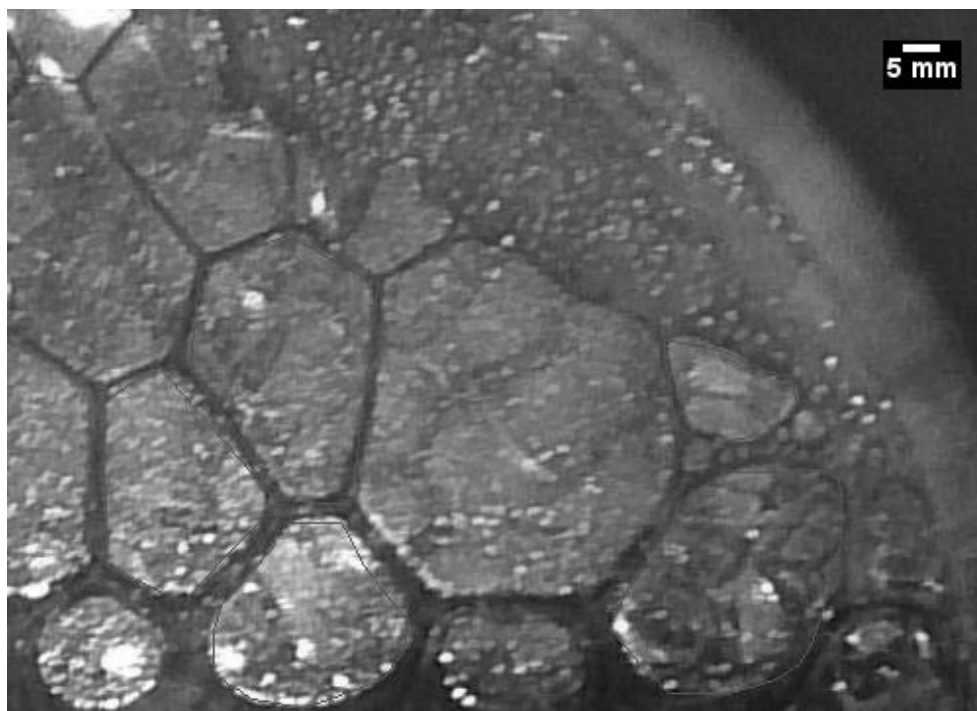


Figure B.57: 8-bit analyzed foam image using AOS surfactant for foam quality 0.95 and 20% N<sub>2</sub>

## VITAE

Name : Mohammed Abdul Qadeer Siddiqui

Nationality : Indian

Date of Birth : 1/26/1992

Email : siddiqui.maqadeer@gmail.com

Address : 2304, Riyadh Street, Rabea Terraces, KFUPM, Dhahran

Native Address : Mehdiapatnam, Hyderabad, Telangana, India

Educational Qualification : M.Sc. (Petroleum Engineering)

February, 2016

King Fahd University of Petroleum & Minerals (KFUPM)

Dhahran, Saudi Arabia

B.Sc. (Petroleum Engineering)

September, 2013

King Fahd University of Petroleum & Minerals (KFUPM)

Dhahran, Saudi Arabia